TECHNISCHE UNIVERSITÄT MÜNCHEN

Lehrstuhl für genomorientierte Bioinformatik

Comparative Omics Analysis in Mice and Men for Diabetes Research

Jörn Leonhardt

Vollständiger Abdruck der von der Fakultät Wissenschaftszentrum Weihenstephan für Ernährung, Landnutzung und Umwelt der Technischen Universität München zur Erlangung des akademischen Grades eines

Doktors der Naturwissenschaften

genehmigten Dissertation.

Vorsitzender:	Prof. Dr. Martin Hrabě de Angelis
Prüfer der Dissertation:	1. Prof. Dr. Hans-Werner Mewes
	2. apl. Prof. Dr. Johannes Beckers

Die Dissertation wurde am 21.12.2016 bei der Technischen Universität München eingereicht und durch die Fakultät Wissenschaftszentrum Weihenstephan für Ernährung, Landnutzung und Umwelt am 05.04.2017 angenommen.

Abstract

Type 2 Diabetes Mellitus (T2DM) is one of the most prevalent metabolic diseases world wide with its clinical complications imposing major human and financial burden on societies. The etiology of T2DM is rather complex, involving interactions between various genetic and environmental factors. The underlying pathogenic mechanisms are not fully understood. Until today, there is no cure for T2DM. Functional studies aiming at the investigation of the disease's underlying causes are primarily done in animal models, in particular in mouse models. While the clinical phenotypes of such models are usually well characterized, it is often not known how well they actually mimic the disease's physiology on the molecular level. This gap of knowledge clearly complicates the replication of results among different models as well as the transfer of findings from animal models to human settings.

The objective of this thesis was to assess the comparability of findings in mouse models for diabetes research on the basis of results from large scale screening methods (›omics‹). To this end, I address the within-species comparison of gene-expression changes in liver in response to Non-Alcoholic Fatty-Liver Disease (NAFLD) – a condition often found in people with T2DM – within four different mouse models of diet induced NAFLD in the first part of my thesis. Using whole genome mRNA profiling in 72 murine liver samples, the changes of 22,030 genes across the four models were compared. Although heterogenous genetically, the models display considerable overlap among their genetic responses to the NAFLD phenotypes. I discuss how such universal adaptions to NAFLD progression in all four models might be relevant for the disease progression in human. In the second part of my work, I investigated the cross-species translatability of metabolic changes as observed in the genetic db/db mouse model of obesity linked T2DM to humans. To this end, targeted and untargeted metabolomics were applied to 666 human serum and 40 murine plasma samples, measuring 319 metabolites that are present in the blood of both species. Comparing the metabolic changes linked to T2DM in humans with those observed in the db/db mouse model, we found consistent changes both in the carbohydrate and the amino acid metabolism. In contrast, the changes of lipids were mainly uncorrelated. Potential reasons for these similarities and dissimilarities

are discussed in the context of the db/db mouse model, providing the basis for a reliable transfer of metabolomics data from the db/db mouse model to the human system.

Both studies demonstrate the value of system-wide characterizations of animal models on the molecular level employing omics technologies. In particular, using molecular traits, i.e. changes in gene-expression or metabolite levels in response to disease phenotypes, instead of their clinical phenotypes alone, these models can be described in much more detail. Taken together, the comparison of molecular alterations across models or between models and humans provides valuable information about common and distinct molecular features. This is crucial for the interpretation of findings from different studies that use the same models and, more importantly, for the transfer of findings obtained in models to humans. Moreover, knowing which molecular features of human diseases can be adequately mimicked by a model and which can not is a potential reference point both for the systematic improvement of current models, and for the design of new and maybe better ones.

Zusammenfassung

Als eine der häufigsten metabolischen Erkrankungen weltweit stellt Typ 2 Diabetes Mellitus (T2DM) mit seinen klinischen Komplikationen eine immensen sozialen und finanziellen Belastung für die heutige Gesellschaft dar. Die Etiologie von T2DM ist komplex und umfasst das Zusammenspiel zahlreicher genetischer und Umweltfaktoren. Die der Erkrankung zu Grunde liegende Mechanismen sind nach wie vor nicht vollständig verstanden und bis heute gibt es kein Heilmittel für T2DM.

Funktionale Studien mit dem Ziel, die Krankheit und ihre Ursachen zu erforschen werden hauptsächlich in Tiermodellen, primär in Mausmodellen, unternommen. Während die klinischen Phänotypen dieser Modelle in der Regel sehr gut beschrieben sind, herrscht häufig Unklarheit darüber, wie gut diese Modelle die Krankheitsphysiologie auf molekularer Ebene widerspiegeln. Diese Wissenslücke erschwert die Einordnung der in solchen Modellen erworbenden Erkenntnisse und lässt verlässliche Aussagen über die Bedeutung der Ergebnisse für den Menschen häufig nicht zu.

Ziel dieser Dissertation war es die Vergleichbarkeit und Übertragbarkeit von wissenschaftlichen Ergebnissen aus Mausmodellen in der Diabetesforschung anhand von Messdaten aus Hochdurchsatzmethoden (›omics‹) auf molekularer Ebene zu untersuchen. Dazu betrachte ich im ersten Teil meiner Arbeit Änderungen der Genexpression in der Leber als Antwort auf das Krankheitsbild der Nicht-alkoholische Fettleber (NAFLD) – einer häufigen Komplikation in Menschen mit T2DM – in vier verschiedenen Maumodellen. Anhand genomweiter mRNA Expressionsdaten aus 72 Lebergewebeproben konnten Änderungen in der Expression von 22,030 Genen zwischen allen vier Mausmodellen verglichen werden. Trotz ihrer genetischen Unterschiede zeigen alle vier Mausmodellen ähnliche Genexpressionsmuster als Antwort auf den NAFLD Phänotypen.

Im zweiten Teil meiner Arbeit untersuche ich die Veränderungen im Blutmetabolismus in Menschen mit T2DM und Tieren des db/db Mausmodells mit dem Ziel, die Übertragbarkeit von Ergebnissen aus dem Modell in den Menschen zu analysieren. Hierfür wurden Metabolomics Messungen in 666 menschlichen Serumproben und

40 murinen Plasmaproben unternommen, wodurch 319 Metaboliten identifiziert werden konnten die im Blut beider Spezies zu finden sind. Der Vergleich der relativen Änderungen der Metabolitenkonzentrationen zwischen Menschen mit T2DM und Tieren des db/db Mausmodells offenbart ähnliche Muster in Kohlenhydrat und Aminosäurestoffwechsel, und größere Differenzen im Lipidstoffwechsel. Erkenntnisse über die stoffwechselspezifischen Ähnlichkeiten und Unterschiede zwischen Modell und Mensch schaffen eine Basis für einen verlässlicheren Ergebnistransfer von Metabolomics Messungen.

Beide Studien verdeutlichen das Potential systemweiter Charakterisierungen der Krankheitsphysiologie von Tiermodellen auf molekularer Ebene, in diesem Fall mit Hilfe von omics Messmethoden. Molekularer Merkmale wie zum Beispiel spezifische Änderungen der Genexpression oder relative Änderungen von Metabolitenkonzentrationen beschreiben Modelle deutlich detaillierter als ihre phänotypischen Merkmale. Der Vergleich solcher Mermale zwischen Modellen oder zwischen Modell und Mensch liefern wertvolle Hinweise über modell- oder spezies-spezifische Gemeinsamkeiten und Unterschiede in der Krankheitsphysiologie. Erkenntnisse darüber, welche Aspekte der Krankheitsphysiologie tatsächlich von einem Modell simuliert werden und welche nicht, ermöglichen neben einer verlässlichen Interpretation von Ergebnissen die gezielte Verbesserung existierender und die Schaffung neuer Tiermodelle.

Danksagung

Meine Arbeit entstand im Rahmen des Deutschen Zentrums für Diabetesforschung (DZD) und dem Helmholtz Diabetes Center (HDC) unter der Betreuung von Hans-Werner Mewes und Gabi Kastenmüller.

Zuerst möchte ich mich bei meinem Doktorvater Hans-Werner Mewes bedanken, der mir die Möglichkeit zu dieser Arbeit über ein spannendes und relevantes Thema in einem einzigartigen und interdisziplinären Forschungsumfeld gegeben hat.

Besonderer Dank gebührt Gabi. Sie war entscheidend in der Planung, Umsetzung und Ausarbeitung meiner Arbeit beteiligt. Vor allem aber ihre stete Unterstützung und Zuversicht waren über die Jahre von unschätzbarem Wert für mich.

An dieser Stelle möchte ich außerdem Johannes Beckers für das zweite Gutachten meiner Arbeit danken.

Ebenso geht mein Dank an die vielen langjährigen Kooperationspartner, vor allem aber Susanne, Melanie, Barbara, Martin und Peter. Ohne ihren Einsatz und ihre Hilfsbereitschaft wären wesentliche Aspekte meiner Arbeit nicht umsetzbar gewesen.

Weiterhin möchte ich meinen Kollegen am IBIS und ICB für die freundschaftliche Zusammenarbeit und schöne gemeinsame Zeit danken. Mein Dank gilt dabei im Besonderen meinen Zimmerkollegen Daniel, Matthias und Johannes. Unsere zahlreichen Diskussionen und ihre vielen klugen Ratschläge waren ein wertvoller Beitrag zu meiner Arbeit.

Ich danke außerdem meinen Eltern und meinen Schwestern für ihre Unterstützung und ihr Vertrauen in mich.

Schließlich möchte ich noch meine kleine Familie, Claudia und Thea erwähnen, die den langen Weg mit mir gegangen sind und während dieser Zeit immer für mich da waren. Dafür bin ich euch sehr dankbar.

Scientific contributions

The scientific contributions of this thesis have been published in scientific journals and presented at conferences as listed below.

Chapter 3

- Kahle M, Schäfer A, Seelig A, Schultheiß J, Wu M, Aichler M, **Leonhardt J**, Rathkolb B, Rozman J, Sarioglu H, Hauck SM, Ueffing M, Wolf E, Kastenmüller G, Adamski J, Walch A, Hrabé de Angelis M, Neschen S. High fat diet-induced modifications in membrane lipid and mitochondrial-membrane protein signatures preced the development of hepatic insulin resistance in mice.
  Molecular Metabolism, 4(1):39-50, 2014.

- Kahle M, Horsch M, Fridrich B, Seelig A, Schultheiß J, **Leonhardt J**, Irmler M, Beckers J, Rathkolb B, Wolf E, Franke N, Gailus-Durner V, Fuchs H, Hrabé de Angelis M, Neschen S. Phenotypic comparison of common mouse strains developing high-fat diet-induced hepatosteatosis.
  Molecular Metabolism, 2(4):435-46, 2013.

Chapter 4

- **Leonhardt J**, Neschen S, Scheerer M, Zukunft S, Stückler F, Krumsiek J, Illig T, Gieger C, Meisinger C, Rathmann W, Adamski J, Peters A, Hrabé de Angelis M, Suhre K, Kastenmüller G. Similarities and differences in the blood metabolomes between diabetic mice and men: How well does the db/db model mimic human type 2 diabetes?
  International Conference on Systems Biology, Melbourne, Australia, 2014.

- Adam J, Brandmaier S, **Leonhardt J**, Scheerer MF, Mohney RP, Xu T, Bi J, Rotter M, Troll M, Chi S, Heier M, Herder C, Rathmann W, Giani G, Adamski J, Illig T, Strauch K, Li Y, Gieger C, Peters A, Suhre K, Ankerst D, Meitinger T, Hrabe de Angelis M, Roden M, Neschen S, Kastenmüller G, Wang-Sattler

R. Metformin Effect on Non-Targeted Metabolite Profiles in Patients with Type 2 Diabetes and Multiple Murine Tissues.
Diabetes, Epub ahead of print, 2016.

- **Leonhardt J**, Neschen S, Scheerer M, ..., Illig T, Gieger C, Meisinger C, Rathmann W, Adamski J, Peters A, Hrabé de Angelis M, Suhre K, Kastenmüller G. Similarities and differences in the blood metabolomes ...
Diabetes/Diabetologia, in preparation, 2016.

Further contributions

- Ellwanger DC, **Leonhardt J**, and Mewes HW. Large-scale modeling of condition-specific gene regulatory networks by information integration and inference.
Nucleic Acid Research, 42(21), 2014.

- Bartel J, Kahle M, **Leonhardt J**, Neschen S and Stümpflen V. A systems-biological perspective of non-alcoholic fatty liver disease in mice.
German conference on Bioinformatics, Freising, Germany, 2011.

- Quell J, Altmaier E, Wenninger S, **Leonhardt J**, Römisch-Margl W, Kastenmüller G, Mewes HW and Schoser B. Metabolic characteristics of lipid-myopathies revealed by quantitative targeted metabolomics.
International Conference on Systems Biology, Mannheim, Germany, 2011.

Contents

Chapter 1

Introduction

Diabetes (from the Greek verb ›diabaínein‹, meaning ›to pass through‹) is as old as written history. The first records about it date back to 1500 BC, when ancient Egyptian physicians described conditions of excessive thirst, continuous urination and heavy weight loss. In 1675, English physician Thomas Willis wrote in ›Pharmaceutice Rationalis‹ about a case study of a man who, within twenty four hours, has voided almost a gallon and a half of limpid, clear, and wonderful sweet water, that has tasted as if it had been mixed with honey [1]. In his description, Willis coined the term ›mellitus‹ (Latin: ›honey sweet‹), and subsequently the term ›diabetes mellitus‹ was used to differentiate the disease from unrelated conditions with similar symptoms such as diabetes insipidus (from the Latin noun ›insidipus‹, meaning ›without taste‹).

Diabetes mellitus (abbreviated ›diabetes‹ in the following) summarizes a group of chronic metabolic disorders that are characterized by high blood glucose (›hyperglycemia‹), which is, according to the latest report of the World Health Organization (WHO) and the International Diabetes Foundation (IDF) consultation in 2006, defined as fasting glucose levels in blood or plasma $\geq 7\,\mathrm{mmol\,l^{-1}}$ [2]. Based on the underlying etiology and the clinical stages reflecting the various degrees of hyperglycemia, different types of diabetes are distinguished. The two most common forms of diabetes are Type 1 Diabetes Mellitus (T1DM) and T2DM. While T1DM is an autoimmune disease where the body's immune system attacks and destroys the pancreatic

beta cells, resulting in a lack of insulin (›absolute insulin deficiency‹), T2DM is caused by a combination of factors including deficient insulin secretion (›relative insulin deficiency‹ or ›insulin insufficiency‹) and impaired insulin action (›insulin resistance‹). In addition to these two main types, there are some less common forms of diabetes. Gestational diabetes, for instance, is a transient form of diabetes with similar symptoms like those of T2DM, emerging during pregnancy and in most cases disappearing shortly after delivery [3].

Although they are essential for the assessment and diagnosis of the disease, such classifications may conceal known and unknown varieties of the disease. Hence, it is important to note that diabetes comes in diverse forms with sometimes very different underlying causes [3].

1.1 Diabetes: an epidemic of the 21st century

In its status report on noncommunicable diseases from 2014 [4], the WHO estimated the global prevalence of diabetes among adults (> 18 years) to 9%. At the same time, the IDF came to a similar conclusion stating that worldwide, approximately 387 million adults between 20 and 79 years lived with diabetes, corresponding to a prevalence of 8.3% in this age group (Figure 1.1) [3]. More importantly these these numbers are expected to continue growing. From the 1980s until today, the global prevalence of diabetes in adults almost doubled [5]. Assuming a similar development for the next years, the IDF projects the number of diabetes to increase by 55% until 2035, rising beyond 592 million people affected worldwide. Note that these numbers include an estimate of 46.3% undiagnosed diabetes cases [3].

Although diabetes has traditionally been viewed as a disease of the rich countries, the current estimates suggest that with 77%, the greater part of people suffering from diabetes lives in low- to middle-income countries [3].

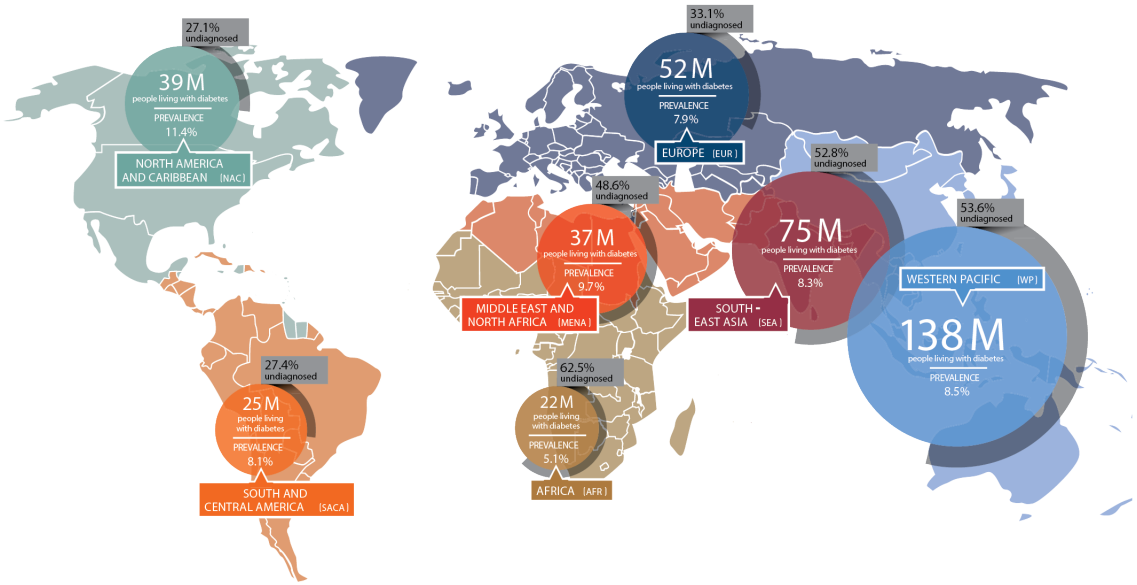

Figure 1.1 – Worldwide diabetes prevalence; status as of 2014. Adopted from the IDF Diabetes Atlas 6th edition (2014 update) [3].

Diabetes imposes a major human burden on societies. In 2014, approximately 4.9 million people died from the consequences of various macro- or micro-vascular complications of diabetes [3]. Diabetics have a two to four times higher risk for coronary artery disease than the rest of the population, making cardiovascular diseases the main causes of death (75-80%) in these people [6]. Other disabling and sometimes life-threatening complications that accompany diabetes include microvascular defects such as retinopathy (eye disease), nephropathy (kidney disease), and neuropathy (nerve damage) [7, 8].

Apart from the obvious human burden, diabetes imposes also significant costs on public budgets. Given the increasing diabetes rates worldwide, the spendings for medical treatment will further rise in the next years. In 2014, the global annual costs for direct medical spendings and reduced productivity were estimated to reach almost 612 billion US dollars. Note that from this sum, as much as 144.3 billion US dollars were allocated to Europe [3].

Today, the WHO estimates that worldwide, approximately 90-95% of people suffering from diabetes have T2DM [9].

1.2 Etiology and pathogenesis of T2DM

Hyperglycemia resulting from impaired insulin-mediated regulation of glucose homeostasis is the ultimate and most striking manifestation of T2DM – and maybe the easiest one to measure [10]. Insulin is a hormone which is produced in pancreatic β-cells. Together with its counterpart hormone glucagon, insulin regulates glucose homeostasis (Figure 1.2). Glucose that circulates for instance in response to a carbohydrate containing diet is the main stimulus for insulin release from the pancreas. Insulin promotes glucose uptake from the blood into the body's cells, where it is stored or converted to energy. In addition to this feedback loop between insulin and glucagon, glucose homeostasis is likely to be influenced by other hormons such as the very recently discovered glucogenic hormone asprosin [11].

The clinical appearance of T2DM is diffuse and ranges from predominant insulin resistance with relative insulin insufficiency to severe defects of insulin secretion with or without missing insulin action [12]. However, when T2DM is diagnosed for the first time, almost always both relative insulin insufficiency and insulin resistance are present. The underlying etiology that causes the defects in insulin action and insulin secretion is complex and not fully understood. Since the rates of T2DM increased very fast in the last decades worldwide, it is unlikely that changes in the gene pool alone are responsible for the explosion of T2DM prevalence. Instead, it is generally believed that the interplay between genetic, epigenetic, and environmental factors are responsible for the onset of T2DM.

T2DM pathogenesis is a slow and silent process. Many people live for years with intermediate states of hyperglycemia, which are characterized by Impaired Fasting Glucose (IFG) or Impaired Glucose Tolerance (IGT). In IFG, fasting blood glucose is higher than normal ($\geq 6.1\,\mathrm{mmol\,l^{-1}}$) but not high enough to be diagnosed as diabetes ($< 7\,\mathrm{mmol\,l^{-1}}$) [2]. Similarly, in IGT, blood glucose 2 h after a 75 g glucose drink, for instance as part of an Oral Glucose Tolerance Test (OGTT) [13], is higher than normal ($\geq 7.8\,\mathrm{mmol\,l^{-1}}$) but below the diagnostic cut-off for diabetes ($< 11.1\,\mathrm{mmol\,l^{-1}}$) [2].

This early stage of T2DM, which is often referred to as ›prediabetes‹, usually comes without symptoms.

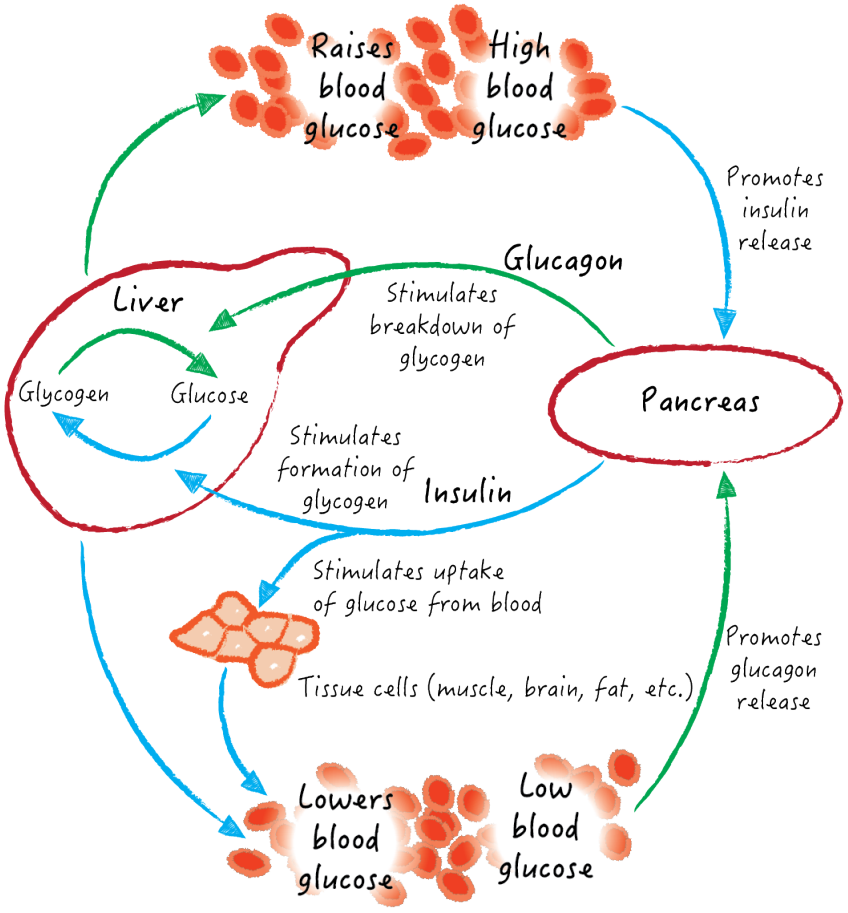

Figure 1.2 – Glucose homeostasis. Glucose homeostasis is mainly regulated by insulin and glucagon, two hormones that are released from the pancreas. Figure adapted from [3].

The cause for IFG and IGT in prediabetes are mainly defects in the response to insulin action. In prediabetes, waning insulin action is balanced by an increased insulin secretion of pancreatic β-cells, which thereby maintain glucose homeostasis. Only when insulin resistance becomes more pronounced and increased insulin secretion is not longer able to compensate for missing insulin action the concentrations of circulating glucose start to rise and hyperglycemia emerges. In the past it was thought that insulin resistance is the primary dysfunction in T2DM. Today, however, it is believed that T2DM pathogenesis is mainly driven by the perturbation of

the feedback loop between insulin-secreting pancreatic β-cells and insulin sensitive tissues (Figure 1.2) [14].

1.2.1 Environmental and non-genetic risk factors

Several studies have shown that obesity is the most important single predictor of T2DM incidence [15–17]. In line with that, the rates of T2DM cases are highest in countries where prospering wealth leads to an oversupply of food and people indulge in a sedentary lifestyle. In 2014, approximately 1.9 billion adults were overweight (BMI $\geq 25\,\mathrm{kg\,m^{-2}}$) worldwide, of which 600 million were obese (BMI $\geq 30\,\mathrm{kg\,m^{-2}}$) [3]. In many countries, the prevalence for obesity raises in parallel with the prevalence for T2DM (Table 1.1). Besides the total body weight, the way the body stores fat seems to be crucial for the individual T2DM risk, as well. People who store fat primarily in the abdomen seem to be at higher risk for T2DM than people who store fat in their thighs or hips [18].

Physical inactivity is considered as an independent risk factor for T2DM, although it is closely related to overweight and obesity. For instance, in a cross-sectional study in adults without a history of diabetes, physical activity ($\geq 2.5\,\mathrm{h}$ per week) significantly reduced the risk for IFG, IGT, and T2DM in both sexes, irrespective of the body weight [19].

The prevalence of T2DM increases with age. People older than 45 years have a significantly higher risk of getting the disease than younger people, most likely because they tend to exercise less, to loose muscle mass, and to gain body weight. Chen et al. have suggested that increased T2DM risk in older people may be diet related [20]. The authors have shown that the differences in glucose tolerance and relative insulin resistance between old (65-82 years) and young (18-36 years) nonobese men (body weight within 15% of desirable values according to the 1959 Metropolitan Life Insurance Co. tables) disappear under a carbohydrate rich diet [20]. However, we watch the onset of T2DM moving more and more down to young adults and adolescents lately.

Table 1.1 – Prevalence of T2DM and overweight or obesity in adults in selected countries for the years 2010 and 2014

	T2DM * (%)			Overweight† (%)		
Country	**2010**	**2014**	**Change**	**2010**	**2014**	**Change**
Australia	7.6	8.1	+0.5%	63.8	66.4	+2.6%
Brazil	7.0	7.6	+0.6%	50.4	54.2	+3.8%
Canada	8.3	9.1	+0.8%	65.6	67.7	+2.1%
China	8.1	10.1	+2.0%	30.5	35.4	+4.9%
France	7.9	8.6	+0.7%	62.0	64.1	+2.1%
Germany	8.3	9.0	+0.7%	57.6	59.7	+2.1%
India	7.8	8.5	+0.7%	18.9	21.4	+2.5%
Italy	8.8	9.5	+0.7%	61.9	64.0	+2.1%
Japan	10.6	11.2	+0.6%	25.3	26.5	+1.2%
Republic of Korea	8.4	9.4	+1.0%	31.1	35.5	+4.4%
Spain	9.3	9.9	+0.6%	62.9	65.6	+2.7%
United Kingdom	9.2	10.1	+0.9%	64.3	66.7	+2.4%
United States of America	9.4	10.5	+1.1%	67.7	69.6	+1.9%

*People with fasting glucose $\geq 7\,\mathrm{mmol\,l^{-1}}$ or on medication for raised blood glucose or with a history of diagnosis of diabetes; †BMI $\geq 25\,\mathrm{kg\,m^{-2}}$; Data according to the WHO [4].

Although glucose tolerance usually returns to normal after pregnancy, women with a history of gestational diabetes were shown to have increased risk of developing T2DM in the future [21].

It is estimated that 20-30% of the western population lives with a condition in which fat is accumulating in the liver, commonly referred to as NAFLD or ›hepatosteatosis‹ [22]. NAFLD appears to be linked to T2DM and people with NAFLD have increased risk to develop T2DM [22, 23]. The prevalence of NAFLD is particularly high among the obese (57%) [24] or in people with T2DM irrespective of their body weight (70%) [25]. Along with obesity and IFG, NAFLD constitutes a cluster of diabetes risk factors which is commonly referred to as ›metabolic syndrome‹. Sometimes, NAFLD is referred to as an early (prediabetic) manifestation of T2DM in the liver.

Various nutritional factors such as a poor diet (i.e. unfavorable nutrient compositions) have also been shown to increase T2DM risk. In particular, while diets containing high proportions of saturated fats appear to promote insulin resistance and T2DM, diets rich in nutrients with a low glycemic index (e.g. fibers, minimally processed whole grain) seem to lower the risk for T2DM [26, 27].

It has been shown that certain chemicals which are present in consumer products such as children's toys, packing materials or detergents, but also food, interfere with the endocrine system and are related to T2DM risk [28, 29]. For instance, several studies have shown that the hormonal active chemical Bisphenol A (BPA), which is one of the highest volume chemicals in the worldwide production of plastic, has various effects that are linked to obesity and T2DM. In rats, low doses of BPA altered adipogenesis, leading to a decreased number of adipocytes with in turn increased cell volumes, resulting in a gain of body weight [28]. Data from other studies have shown that BPA exposure during the prenatal period results in an increased body weight in adulthood [29]. One potential mechanism which may explain the manifold effects of BPA, especially during development, is that it permanently alters gene transcription by decreasing DNA methylation [29].

Epigenetic factors (e.g. DeoxyriboNucleic Acid (DNA) methylation patterns influencing gene expression), which are invidually achieved, are also suggested to affect diabetes risk. For example, it has been shown that both the mother's weight and her history of gestational diabetes increase the diabetes risk of the offspring [30]. Another study done by Ziegler et al. has shown that women with gestational diabetes who breast fed their children over a period of more than three months developed T2DM on average ten years later than women who did not breast feed their children [31]. Beyond that, recent findings suggest that everyone's individual intestinal microbiome is involved in the pathogenesis of T2DM [32].

1.2.2 Genetic risk factors

While the worldwide rising prevalence of T2DM can be explained by environmental factors, there is clearly an important genetic component, which is reflected in variations in T2DM prevalence by ethnicity [6, 33] and high rates of T2DM in families

[34]. Among identical twins, the co-occurrence of T2DM approaches 100%. Factors such as the Body Mass Index (BMI) or the glucose clearance rate and insulin levels as part of an OGTT appear to be highly inheritable [34]. Data from another study involving non-diabetic relatives of people with T2DM suggest that the function of the β-cells is passed down to the offspring [35].

The genetics of T2DM is polygenic, i.e. the result of combinations of multiple genetic mutations. Population based studies identified multiple common genetic variants in different genes, each having small individual effect on the risk for getting the disease. As of today, more than 65 such T2DM susceptibility loci have been revealed by Genome Wide Association Studies (GWAS), which all together explain approximately 6% of the disease's variance [36–39]. Given this small number of explained disease variance, it appears plausible that less common genetic variants with bigger individual effects on T2DM risk exist. However, data on such rare variants is still sparse as they cannot be easily screened for by population based approaches. And even if the risk loci are known, their functions have to be characterized and in many cases it remains to be resolved how they contribute to the pathogenesis of T2DM.

It is important to note that there exist rare monogenic varieties of diabetes with manifestations similar to those of T2DM. In contrast to the genetics of T2DM, these monogenetic forms of diabetes are characterized by relatively uncommon genetic mutations with high penetrance. Among all known monogenic forms of diabetes, Maturity-Onset Diabetes of the Young (MODY) is certainly the most common [40]. It is estimated that MODY accounts for 1-2% of all diabetes cases [41]. A population study in Saxony involving 865 children and adolescents (< 15 years) with newly detected diabetes showed that MODY accounted for 2.4% of these childhood diabetes cases (T1DM: 96%; T2DM: 0.6%) [42]. It is important to note that MODY is not a single entity but comprises at least 11 different subtypes (MODY 1-11). Here, each subtype is characterized by a specific mutation in a single autosomal dominant gene (40-90% penetrance), resulting in β-cell dysfunction [41]. First symptoms of MODY generally emerge between 10 and 45 years of age. Because the clinical features of MODY (e.g. mild to moderate hyperglycemia, sometimes insulin resistance, elevated blood sugar in combination with permanent thirst and urination) overlap with those of T1DM and T2DM, approximately 80% of MODY cases are misdiagnosed [41].

Unlike T2DM, for most of the monogenic forms of diabetes the pathogenic mechanisms where the mutation of a single gene only causes the onset of the disease is known.

1.3 Therapeutical concepts for the management of T2DM

Until today, there is no cure for T2DM. Current approaches for the management of T2DM distinguish between prevention with the aim to delay or stop the disease onset in early stages of the disease's progress and pharmacotherapeutical treatment in cases where the disease has already progressed or where it is manifest.

1.3.1 Strategies for the delay and prevention of T2DM onset

Most prevention strategies aim at reverting some of the modifiable risk factors before the onset of the disease, in particular overweight or obesity, sedentary lifestyle, and dietary factors. These changes are mainly achieved by lifestyle modifications such as regular physical activity or special regimens, which are sometimes supported by early pharmacotherapy with anti-diabetic drugs to keep blood glucose levels within the physiological range. Several studies which were conducted in people at high risk for T2DM (i.e. people with IFG or IGT), examined the potential benefits of different lifestyle modifications in disease delay and prevention [43–46].

For example, the Diabetes Prevention Programm (DPP) randomized controlled clinical trial [46] was conducted in 3,234 US adults with glucose intolerance. This study investigated the benefits of an intensive lifestyle modification (Low Fat Diet (LFD), regular sports) with the aim to reduce body weight by 7% versus the benefits of pharmaceutical treatment with Metformin on the disease's progress. After 3 years, the researchers showed that lifestyle intervention and Metformin treatement reduced T2DM incidence by 58% and by 31% respectively as compared to a placebo group

[46]. Based on their findings, the authors state that both lifestyle and drug intervention with Metformin reduces the risk for T2DM in the clinical cohort on the short-term. Moreover, Knowler et al. demonstrated the long-lasting benefits of both prevention strategies in a 10 year follow-up of the DPP [47]. Although the authors found similar incidence rates in the lifestyle, Metformin, and placebo groups during follow-up (4.9-5.9 per 100 person years), the cumulative incidence over 10 years was significantly smaller in the lifestyle group (34%) than in people treated with Metformin (18%) as compared to the placebo group [47]. The authors were also able to show that on average, the intensive lifestyle modification delayed the disease onset longer (4 years) than Metformin treatment (2 years) as compared to the placebo group [47].

1.3.2 Options for the pharmacotherapeutical treatment of T2DM

There is a broad panel of anti-diabetic drugs available today (Figure 1.3) [48]. These drugs act in different ways, achieving blood glucose lowering effects by targeting different processes and pathways. The most commonly prescribed anti-diabetic drugs on the market are Metformin and Thiazolidinediones (Glitazones), both mainly targeting the metabolic organs including liver, adipose tissue, and muscle tissue.

Glitazones, for example, are synthetic ligands for Peroxisome Proliferator-Activated receptors (PPARs), which is a group of nuclear receptors. In a mechanism which alters the transcription of several genes, activation of PPARs by binding of Glitazones promotes the storage of fatty acids in adipocytes. As more and more fatty acids are stored, less of them are available for oxidation and cells become more dependent on the oxidation of carbohydrates as an energy source. As a result, more circulating carbohydrates – notably glucose – are consumed, resulting in improved blood glucose levels [49].

Other anti-diabetic drugs such as Glucagon-like-peptide 1 (GLP-1) receptor agonists, Dipeptidylpeptidase 4 (DPP4) inhibitors, Glinides or Sulfonylurea act on the pancreas. Medical drugs that were established more recently target also the brain

(Bromocriptine), the kidneys (Sodium Dependent Glucose Transporter 2 (SGLT-2) inhibitors), or the intestines (Pramlintide, Colesevelam, α-glucosidase inhibitors) [48].

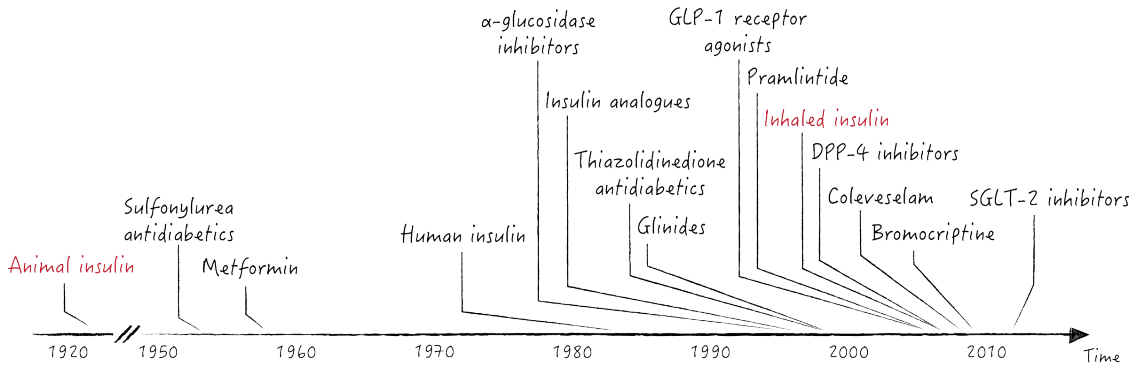

Figure 1.3 – Evolution of diabetes treatment. Market launch of established anti-diabetic drugs. Note that both animal insulin and inhaled insulin (red) are not longer administered in T2DM therapy. Data according to [48].

In most cases, these drugs allow to manage the disease over a relatively long period of time and the decline of insulin action and secretion can be compensated by increasing the doses. Sometimes, however, especially in advanced stages of T2DM, the administration of insulin to reduce circulating glucose represents the only treatment option that is left.

1.3.3 Limits of current therapeutical concepts in the management of T2DM

Although several studies provided evidence for short-term benefits of lifestyle or drug interventions in the management of T2DM, there is little known about their success over longer periods of time (> 10 years). In particular, it remains to be revealed whether glycemic control reduces clinical endpoints of the disease including micro- and macro-vascular complications, the latter being the main cause of deaths in diabetics. To date, there are several (ongoing) studies with the aim to assess the long- and longer-term benefits of the different therapy concepts in terms of managing hyperglycemia and their potential to minimize clinical complications [50–54].

For example, one of the older clinical trials investigating the effects of glycemic therapies including early pharmacotherapy on clinical complications and mortality

in people with T2DM was the United Kingdom Prospective Diabetes Study (UKPDS) randomized clinical trial [50]. The UKPDS took place between 1977 and 1998 and comprised 5,102 patients with newly diagnosed T2DM. In a 10 year follow-up study, Holman and Paul compared the long-term effects of these early anti-diabetic drug therapies (Sulfonylurea, insulin, or Metformin in overweight patients) to those of glycemic control by dietary restriction on T2DM related endpoints and microvascular disease [55]. Even though the differences in glycemic control in terms of Glycated Hemoglobin (A1c) levels were lost between the groups after a while, the authors found that patients who received early anti-diabetic drug treatment showed significant reductions in their relative risks for any T2DM related endpoints (9-21%), myocardial infarction (15-33%), and all-cause mortality (12-27%). Moreover, people on Sulfonylurea or insulin, but not Metformin, had a significantly smaller risk for microvascular disease (24%) than those managed by dietary restriction [55].

The Action to Control Cardiovascular Risk in Diabetes (ACCORD) randomized clinical trial conducted in 10,251 US american and canadian adults aged between 40 and 79 (mean age 62 years) investigated whether glycemic control reduces the occurence of major cardiovascular events (heart attack, stroke, cardiovascular death) in patients with T2DM which were at risk or had already a history of cardiovascular disease [51]. In addition, all participants showed more or less elevated levels of A1c (7.5-11.0%), which is a surrogate marker for blood glucose levels. After 3.4 years, Riddle et al. compared the intensive glycemic treatment strategy aiming at the reduction of A1c levels to less than 6% to standard glycemic treatment (A1c 7-9%). The authors found that intensive and standard treatment both produced a broad range of average A1c levels with a great overlap between the intervention groups. Although the all-cause mortality rates – approximately 50% of deaths were related to cardiovascular complications – were similar in the first 2 years, after 3 years it was twice as high in the intensive as in the standard treatment group [56]. In the intensive but not the standard treatment group, mortality linearly correlated with high average A1c levels greater than 7%, suggesting that for people who present high average A1c levels, intensive glycemic treatment has no positive or even adverse effects on cardiovascular outcomes [56].

Another clinical trial, the Look Action for Health and Diabetes (AHEAD) study [57], was conducted in 5,145 overweight or obese adults (mean age 58.7 years; mean BMI $\geq 36\,\mathrm{kg\,m^{-2}}$) with a history of T2DM (median 5 years). A primary goal of the AHEAD trial was to investigate the long-term effects of a lifestyle intervention designed to achieve and maintain weight loss on mortality rates related to certain cardiovascular complications including stroke, heart attack, and cardiovascular death. In the context of this study, 2,570 people underwent the intervention, including reduced caloric intake and increased physical activity (175 min per week) with the aim to reduce body weight by at least 7% from the baseline in these people. A second group of 2,575 participants attended counseling sessions in diabetes management and social support three times per year. After 10 years, Wing et al. found a similar number of deaths caused by cardiovascular events in both groups (mortality rates 1.92 vs. 1.83 per 100 person years; p-value = 0.51), despite the fact that the people which had undergone the lifestyle intervention displayed greater reductions both in body weight and A1c levels as compared to the counseling group. Based on their findings, the authors conclude that in terms of cardiovascular events, intensive lifestyle intervention does not have a greater effect than counseling in overweight and obese patients with T2DM [58]. In 2012, the AHEAD trial [57] was prematurely stopped on the basis that the intervention strategy had no positive effect on the primary outcome (cardiovascular disease). Post hoc analyses of the trial, however, suggest that the lifestyle intervention reduces the risk for other complications which are linked to cardiovascular disease, including chronic renal disease [59], cholesterol levels, and blood pressure [60]. Moreover, Espeland et al. argue that the reduced need for anti-diabetic drugs in the intervention group reduces the costs for medical treatment [61].

The Outcome Reduction With Initial Glargine Intervention (ORIGIN) trial examined the effects of insulin treatment versus standard care to maintain normal glucose levels (fasting glucose levels in blood or plasma below $5.3\,\mathrm{mmol\,l^{-1}}$) on total mortality, micro-, and macro-vascular outcomes. To this aim, 12,537 adults (mean age 63.5 years) with IFG, IGT, or early T2DM and cardiovascular risk factors were recruited. After about six years, researchers found no difference on cardiovascular outcomes between people receiving insulin treatment and those on standard care. Moreover, although it reduced the incidence of T2DM in people with IGT and IFG, insulin

treatment led to increased hypoglycemia and modest weight gain (median increase 1.6 kg).

In addition to the uncertain data basis on the long- and longer-term benefits of prevention strategies and medical treatment, management of T2DM is complicated by the effectiveness of medical treatment. All current anti-diabetic drugs loose their glucose lowering effect over time. Considering that worldwide more and more young people and children have the disease [62], ceasing drug effect will become a major problem in the treatment of T2DM. A lot of effort is therefore made to find alternative and more sustainable concepts to manage hyperglycemia in T2DM. Some recent studies investigated the effects of combined administrations of established anti-diabetic drugs [63, 64]. For instance, the Treatment Options for type 2 Diabetes in Adolescents and Youth (TODAY) trial [65] aimed at the investigation of the effects of Metformin, Metformin and Rosiglitazone combi-therapy, and Metformin therapy in combination with lifestyle intervention on insulin sensitivity and β-cell function in 699 overweight adolescents (10-17 years) with a history of T2DM [63]. The authors showed that the combi-therapy provides superior acute improvement on glycemic control within the first six months as compared to the other two treatments. Moreover, the failure rates of the combi-therapy (39%) are smaller than those of Metformin monotherapy (52%) or Metformin administration in combination with lifestyle intervention (47%) [63]. Between six months and four years, both insulin sensitivity and β-cell function declined in parallel in all three groups. Those participants who failed to maintain glycemic control displayed higher fasting glucose levels and lower β-cell function at baseline, with no differences in insulin sensitivity as compared to the others [63]. Based on their findings, the researchers claim that the combi-therapy improves short term glycemic control, which translates to smaller treatment failure rates. Thus, the initial reserves of pancreatic β-cells appear to be crucial for the long-term effect of the treatment, and preventing β-cell loss (for example by early treatment) should be of primary concern in adolescents with T2DM [63].

Promising data comes also from a recent study in mice on the potential benefits of a combi-therapie for T2DM treatment. Neschen et al. investigated the effect of the combined treatment of db/db mice with Metformin and an SGLT-2 inhibitor, which blocks the glucose reabsorption by the SGLT-2 transporter in the kidneys [64].

The authors showed that the combi-therapy of Metformin and the SGLT-2 inhibitor has a more sustainable effect on glycemic control than treatment with either one of the drugs alone [64]. Although the mechanism responsible for the improved effect of the combi-treatment remains to be revealed, based on their findings, the authors speculate that Metformin supports the glucose-lowering effect of the SGLT-2 inhibitor by restraining endogenous glucose production, leading to improved long-term glycemic control [64].

Another complication in T2DM management is that both prevention and treatment strategies, in particular lifestyle interventions and medical drugs, act rather unspecific. Just as disease progressions are unique to each person, the success of current treatment strategies varies from patient to patient. Drugs that work for one patient may have only a small effect in another patient. In some people, off-target effects of current anti-diabetics were shown to lead to other clinical complications [66]. Similarly, the success of lifestyle intervention has been shown to be quite different among individuals. For example, Schäfer et al. showed that moderate weight loss by increased physical activity and calorie restriction over roughly 9 months improved glucose tolerance significantly (2 h glucose during OGTT: -14%) in people with IGT and increased T2DM risk, however not in people with normal glucose tolerance and similar body-, and liver-fat, which are at risk for T2DM (2 h glucose during OGTT: $+2\%$) [67].

Finally, it is frequently questioned how much the broad population benefits from current therapy approaches, for example from the structured implementation of lifestyle programs. Livestyle modifications are neither simple nor straightforward and for many people (e.g. elderly people), such interventions are sometimes simply not practicable. In line with that, several community studies were not able to replicate the positive results from clinical trials. It appears that a key problem is that in the community setting, lifestyle modifications often do not result in similar reductions of weight as those achieved in clinical trials [68].

Taken together, it is obvious that new therapeutic concepts are needed for T2DM – pharmacological and non-pharmacological ones. These need to be more efficient, longer lasting, and rather personalized for each patient. Without doubt, to achieve

these goals, better knowledge about the etiology and pathogenesis of T2DM is required.

1.4 Approaches in T2DM research

Today, different research fields, including basic and clinical research, epidemiology, and translational studies, contribute equally to diabetes research. While clinical and epidemiological studies involve human beings, pre-clinical studies and basic research are usually limited to experiments in non-human (animal) models.

1.4.1 T2DM studies in human cohorts

The implementation of numerous epidemiological cohorts facilitated the search for heritable genetic variants contributing to T2DM risk. Before the advent of the different ›omics‹ fields (see Introduction 1.5), genetic variants were usually identified by so-called ›candidate gene studies‹. In such studies, the impact of genetic variation in an individual gene on a certain phenotypic trait such as T2DM is investigated. Suitable candidate genes for such studies are usually selected based on prior knowledge from previous studies. The selection is a costly and time-consuming process and the choice of the ›right‹ candidate is not straightforward. Yet, a few T2DM risk genes have been identified by candidate gene studies. For instance, Deeb et al. identified a Single Nucleotide Polymorphism (SNP) in a gene coding for one of the PPARs, PPAR-gamma. The authors claimed that this variant of the PPAR-gamma gene largely explains the variability in BMI and insulin sensitivity observed in a Finnish and a Japanese-American cohort [69].

The advent of genomics in the late 1990s and the introduction of DNA microarrays (see Introduction, 1.5.1) enabled large-scale screening for T2DM risk loci in GWAS. Rather than focussing on single pre-selected candidate genes, GWAS investigate hundreds of thousands of genes simultaneously. Comparing individuals with different phenotypic traits, genetic variants can be associated to these traits. The first GWAS

on T2DM were published in 2007 [36, 70–74]. Since then, according to the NHGRI-EBI GWAS Catalog, approximately 36 GWAS and meta-analyses identified around 114 T2DM risk loci (www.ebi.ac.uk/gwas; status as of 7/2015).

A surprising finding of these GWAS is that the variants for which functional roles could be assessed affected mainly β-cell function rather than obesity or insulin resistance [75]. Another interesting result is that several variants that associate with T2DM do not associate with insulin or glucose homeostasis in healthy populations [39, 76]. In general, the effect sizes of the currently known T2DM susceptibility loci are moderate or small, leaving a great gap between explained (5-10%) and estimated heritability (approximately 40%) [77, 78]. A potential explanation for this discrepancy between estimated and explained variance is that GWAS investigate only common SNPs, which are present in human populations very frequently. In the near future, new approaches and lower costs for DNA analyses will allow the study of rare variants ($< 1\%$ allele frequency), which may have greater effect sizes and explain more of T2DM's genetic variation. Moreover, most current studies are limited to SNPs as the only type of genetic variation, excluding other sources such as copy number variants, inversions, or structural variants, as well as factors such as gene-gene or gene-environment interactions, which may be equally crucial for the genetics of T2DM.

In addition to genetic markers, identification of non-genetic markers is equally important for the understanding of both etiology and pathogenesis of the disease. In particular the investigation of metabolic traits in Metabolome Wide Association Studies (MWAS) has been shown to provide crucial insights in disease-related perturbations of metabolic pathways in patients with T2DM [79–82] and prediabetes [83, 84], or related risk factors including obesity [80, 85–87] and NAFLD [88].

For instance, Newgard et al. applied targeted metabolomics to samples from lean (median BMI $23.2\,\mathrm{kg\,m^{-2}}$) and obese (median BMI $36.6\,\mathrm{kg\,m^{-2}}$) humans to study the metabolic traits of obesity [85]. In their study, the authors revealed a metabolic signature related to Branched Chain Amino Acid (BCAA) metabolism which differentiated obese from lean humans. Moreover, the alterations within this BCAA-related pattern correlated with increasing insulin resistance [85]. To test whether

this BCAA signature contributes to obesity-related comorbidities such as insulin resistance and glucose intolerance, they fed Wistar rats with a High Fat Diet (HFD) and a standard control diet with or without BCAA supplementation. Consistent with their hypothesis, the authors found that independently of the body weight, the intake of BCAA contributes to the development of insulin resistance in rats [85]. Based on these data, the authors conclude that BCAAs are likely to contribute to obesity-related insulin resistance in humans [85].

Another recently published metabolomics study analyzed 265 metabolites in plasma from 20 insulin-sensitive and 20 insulin-resistant subjects with NAFLD (matched for liver fat) before and after a 9-month lifestyle intervention [88]. During this intervention period, participants were advised to reduce calorie intake to reduce weight, mainly by eating less dietary fat and by increasing the intake of fibers. In addition to dietary counseling, they were asked to do at least three hours of moderate sports per week, for example walking or swimming [88]. In their work, Lehmann et al. found that characteristic changes in seven metabolites discriminate insulin-sensitive from insulin-resistant participants with NAFLD – to their surprise both before and after the lifestyle intervention [88]. Detailed analysis of these seven metabolites revealed that lyso-PC C16:0 correlates most strongly with insulin sensitivity in subjects with NAFLD. Based on their data, the researchers claim that a metabolic signature including lyso-PC C16:0 is likely to be an early marker for insulin sensitivity, and thereby T2DM risk, in people with NAFLD [88].

Although these different GWAS and Metabolome Wide Association Study approaches are very successful in identifying genetic and metabolic traits of the disease, they are very limited in studying the causal relation between the marker and the disease's physiology. There are several considerations to this limitation: First, many potential risk loci identified in GWAS lie in inter-genic regions for which the functional link is unknown. Second, variants are often located in genomic regions that contain more than one annotated gene and it is not clear which of the genes is functional in the disease context. Third, even if one is lucky and the locus lies in a gene region for which the product is known, considering the complex interactions between genetic and environmental factors it is hard to make statements about the causality of the elusive relations between the affected gene and the final phenotype.

1.4.2 Animal Models for T2DM research

Besides factors such as time and costs, functional and mechanistic studies in humans are complicated and limited to noninvasive procedures. Animal models, on the other hand, are usually cheap, less time consuming, and can be done under standardized conditions in the lab. Most importantly, in animal models physiological and invasive testing can be applied which is otherwise not allowed in humans for obvious ethical reasons. This is why today animal models and especially murine models are firmly established in (translational) T2DM research.

The first animal studies in diabetes research date back to the late 19th century. Oscar Minkowski described symptoms similar to those observed in diabetes mellitus in dogs whose pancreas was removed (pancreatectomy). Shortly after, Edouard Hedon and Minkowski both proved independently that the total removal of the pancreas was necessary for the development of the typical symptoms of the disease, suggesting that the pancreas is crucial for the pathogenesis. In 1893, Gustav-Edouard Laguesse hypothesized that the islets in the pancreas firstly described by Paul Langerhans produce an anti-diabetic substance. This unknown substance was referred to as ›insulin‹ for the first time by Jean de Mayer in 1909.

It took until 1922, when Frederick Banting and his graduate student Charles Best showed in the laboratories of John MacLeod that the administration of pancreatic extracts from atrophied pancreatic glands taken from dogs to other dogs whose pancreas were completely removed improved the diabetic-like conditions of the pancreatectomized animals. After these successful experiments, Banting and Best went one step further and tested their method on a human patient. Just like in their experiments with dogs, the injection of their pancreatic extract isolated from dogs into 14-year old diabetic Leonard Thompson resulted in a significant decrease of the boy's blood glucose concentrations to physiological levels. Banting named this anti-diabetic substance ›isletin‹, which was later changed to ›insulin‹, the name already given by de Mayer. For their discovery of insulin, which was at the same time the first treatment for diabetes, Banting and MacLeod were awarded with the the Nobel price in 1923. Their studies are also a perfect example of the successful translation of result from animals to humans.

Today, studies in animals are predominantly conducted in rodents, especially mice, which has several reasons. The genome sequences of mice and humans are 95% identical and many identified genes in human have orthologs in mice. This is why studies in mice are often favored for functional studies on potential risk genes identified in human trials, for instance by gene knock-outs. Other reasons which make mice so convenient for research are that they are relatively easy to breed and maintain, have short generation times, and an accelerated lifespan (1 mouse year corresponds to approximately 30 human years). Moreover, highly standardized phenotyping protocols from human diagnostics are also established in mice, including euglycemic-hyperinsulinemic clamp to measure insulin action, and OGTT to test insulin secretion and glucose tolerance [13].

Many genetic and non-genetic mouse models have been generated to recreate key symptoms and risk factors of human T2DM including obesity, insulin resistance, β-cell failure, or fatty liver disease [89]. These traits are generally the result of naturally occurring mutations, specific genetic manipulations, or special diets.

Classic genetic mouse models include the monogenic ob/ob and db/db strains originating from the Jackson Laboratory [90]. In both models naturally occurring autosomal recessive variants in singles gene coding for leptin (ob/ob) [91] or the leptin receptor (db/db) [92] induce obesity and hyperglycemia. Leptin and the leptin receptor build together the leptin-signaling axis which balances food intake. Disruption of this signaling pathway in ob/ob and db/db mice results in an inability to feel sated, leading to hyperphagia, obesity and other metabolic complications [93]. As a consequence of obesity, ob/ob and db/db mice become hyperinsulinemic and insulin resistant. In particular the db/db model is widely applied in T2DM research [94].

Beside these monogenetic models, a variety of polygenic mouse models of T2DM have recently been established including the New Zealand Obese (NZO) and TALLYHO/JngJ (TALLYHO) strains. NZO is a spontaneous model of polygenic obesity and insulin resistance. Mice of this strain become hyperinsulinemic and establish reduced insulin-stimulated glucose uptake in muscle and adipose tissues. In addition, they display elevated circulating triglyceride and suffer from high blood pressure. TALLYHO is another polygenic, naturally occurring model of T2DM [95].

TALLYHO mice become obese and diabetic and show symptoms of hyperlipidemia when exposed to a HFD. However, these polygenic models are more complicated than monogenic mouse models and some of them have not been completely characterized [96].

In addition to the mice having a specific genetic constitution, researchers often use special diets (e.g. HFD) to introduce human disease traits into them. For example, there are several more or less established mouse strains, including 129P2/OlaHsd (129), C57BL/6J (B6J), C57BL/6NTac (B6N), and C3Heb/FeJ (C3H), which establish the typical symptoms of NAFLD under HFD exposure. Because in dietary models, mice usually have the same genetic constitution, those models are supposed to be more straight forward to be interpreted than mono- or poly-genic models, where the different genetic constitutions have to be considered.

Most strains used in mouse models are ›inbred strains‹. Inbred strains are the result of repeated breeding of brother sister pairs over more than 20 generations. As a consequence, the genomes of these strains become fixed and individuals are genetically identical (›isogenic‹). Just like monozygous twins, individuals from inbred strains share identical phenotypes. Although inbred strains usually stay genetically stable for long periods of time, sometimes they change as a result of new mutations leading to new substrains. This substrain drift can be avoided by the maintaining banks of frozen embryos. The use of inbred strains for models has some advantages. For instance, the statistical power of such models is good even with small sample sizes. In addition, because of the (genetically) controlled biological variability, results obtained in inbred strains are also convenient to be interpreted and results from different studies carried out in the same inbred strain are assumed to be comparable. In contrast to inbred strains, ›outbred strains‹ are generated by random mating. Each individual of such an outbred strain possesses its own genetic constitution and models based on outbred strains are heterogenous genetically. Because of their genetic heterogeneity and the resultant phenotypic extremes, outbred strains are sometimes assumed to better reflect the situation of human populations, although they are obviously less variable genetically. However, because in outbred strains the genetic variation is not under the control of the researcher, results obtained in such models are far more complicated to be interpreted and less comparable among each other. It is therefore often suggested to do multi-strain experiments involving dif-

ferent inbred strains rather than using an outbred strain to cover genetic variability in animal models.

In the last years, large-scale screening (omics) methods (see 1.5, p. 27) have been of increasing interest for the application in animal experiments. As a result, researchers were enabled to do system-wide studies of complex diseases under rather controlled settings such as large-scale screenings for novel biomarkers [97–99].

For example, Simonson et al. applied transcriptomics to renal tissue samples in diabetic db/db versus nondiabetic wt mice to identify secreted proteins which may serve as new urinary biomarkers for kidney function in T2DM [99]. To this end, they searched for differentially expressed mRNA of genes that were predicted to encode secreted proteins and which have orthologs in human. As a result, the researchers found 36 of such candidate genes that were significantly affected in db/db mice [99]. In a cross-sectional study comprising 56 humans with T2DM, they tested whether the abundances of their corresponding ortholog proteins in urine correlate with the Glomerular Filtration Rate (GFR), which is a proxy for kidney function, for 17 out of the 36 candidates [99]. They found that 6 out of these 17 tested genes correlated with the GFR, irrespective of urine albumine concentrations, which is an established marker of renal dysfunction in diabetes [99]. Based on their findings, they state that these six genes represent promising candidates as early renal risk markers for kidney failure in T2DM [99].

In a large-scale comparative analysis, Ghazalpour et al. applied transcriptomics and proteomics to examine the concordance between levels of transcripts and proteins in liver tissue samples of 97 inbred and recombinant inbred mouse strains [98]. They compared the variation in 7,185 transcripts with that in 487 proteins. Overall, the concordance between variation in transcripts and the corresponding proteins was modest to small, most likely because of post-transcriptional processes including translational efficiency, alternative splicing, folding, assembly into complexes, transport and degradation [98]. Moreover, they found that the variation in transcript levels is more strongly associated with clinical traits than the variation in protein concentrations. Only 15% of significant associations between changes in transcript

levels and certain phenotypic traits have also been observed for the corresponding proteins [98].

1.4.3 Limitations in the translatability of results: Humans are not simply 70-kg mice*

*Citation taken from Leist and Hartung [100].

Undoubtably, many studies showed how valuable the mouse can be as a model to shed light on the functions of candidate genes which have been initially identified by human trials [101–104].

Beside these individual success stories, given the large number of published studies in mice, our knowledge about the pathogenic mechanisms of many complex diseases including T2DM is still very limited. In fact, quite often, findings obtained in mice cannot be reproduced in the human setting. Published estimates of irreproducible preclinical research range from 51-89% [105, 106]. Based on these numbers, Freedman et al. estimated that of the approximately 56.4 billion US dollars that were spent for preclinical research in the USA in 2012, 28.0 billion US dollars accounted for irreproducible preclinical research [107]. One major reason why many preclinical studies fail is that the results from the implemented mouse models in which the efficacy of the novel drugs are tested are irreproducible in humans [106, 108]. More importantly, this low predictivity of mouse experiments is not limited to comparisons of mice versus humans: the results obtained in one mouse model can often not be reproduced by others, even if they are using the very same model.

It is not surprising that mouse models cannot fully reproduce human disease phenotypes. There are obvious reasons for that, such as different anatomy, genetics and physiology. Mestas and Hughes highlighted significant differences in the immune system between mice and men [109]. In addition, as a result of the excessive inbreeding strategies applied in most mouse strains used for models, individuals from a particular model share the exact same genetic constitution and – as a matter of principle – cannot cover the genetic variation that is prevalent in human populations.

Although mouse models are generally well characterized on the phenotypic level, sometimes the same models display great variation in their physiological responses. This contributes to the translational gap among models or between species. For instance, Lai et al. recently examined the physiological responses of animal models of HFD induced obesity and T2DM systematically. On the basis of six studies implementing the murine B6J model, they found notable intra- and inter-laboratory variances among the dietary effects observed in these studies. This is most likely due to more or less variations in the lab protocols [110]. Moreover, the researchers argue that these phenotypic differences become greater for models which combine both genetic modifications and dietary interventions, which is not surprising because such genetically modified models display variable disease phenotypes irrespective of whether they are exposed to a dietary challenge or not. Based on these data, Lai et al. conclude that the benefits of studies in mice on our knowledge about the pathogenesis and treatment of obesity and T2DM in humans is negligible because the data from such models are confined to the strain, sex, protocol or simply the experimental conditions [110]. Instead, they suggest to redirect T2DM research back to humans, rather than spending further efforts on rodent models to study human conditions [110].

Another study from 2014 adressed the topic of translatability of results from animal models to humans based on rodent models applied in experimental stroke research [111]. The researchers claim that the physiology and pathophysiology of rodents is sufficiently similar to humans in order to make them a highly relevant model organism and at the same time sufficiently different to mandate an awareness of potential resulting pitfalls [111]. However, they argue that rather than turning their backs on mouse models and discarding relevant findings from the past, present, and future, researchers should focus on the improvement of the validity of the models [111].

In order to produce more reliable models to overcome the apparent translational failures, it is therefore essential to know the strengths and weaknesses of models in recreating the human disease's physiology. To this end, it will be essential to determine how well animal models reproduce the human disease's physiology on the phenotypic level and below (i.e. on the molecular level) in a more systematic fashion [112].

1.5 Omics: research in large-scale

Recent developments in biotechnology led to an increasingly common application of system-wide and data-driven methods in diverse research areas (Introduction 1.4). Rather than analyzing selected molecules, large-scale screening methods – collectively referred to as ›omics‹ – simultaneously measure thousands of molecules from individual biological samples and thereby provide systems-level readouts of cells, tissues, or even whole organisms. There are several omics fields that primarily differ in their objects of study. While genomics refers to the study of whole genomes, epigenomics, transcriptomics, proteomics, and metabolomics encompass the entirety of epigenetic modifications (epigenome), RNA (transcriptome), proteins (proteome), and metabolites (metabolome), respectively. The implementation of these different omics approaches constituted the start for system-wide analysis both in human and in non-human studies, most notably that of genome projects, GWAS, and MWAS.

1.5.1 Transcriptomics

The term ›transcriptome‹ refers to the total set of RNA molecules of an organism, tissues or a single cell at a specific time under a specific condition. Although there are other forms of RNA molecules including transfer RNA, ribosomal RNA and non-coding RNA, the term ›transcriptomics‹ generally refers to the study of mRNA molecules (i.e. the transcribed nucleotide sequences of expressed genes) only. While sinking costs make the application of Next Generation Sequencing (NGS) based approaches more and more attractive in transcriptomics, the predominant platform to measure the levels of individual mRNA molecules are still DNA microarrays.

Measuring techniques

There are basically two different methods for the production of DNA microarrays: spotted or cDNA microarrays and high-density oligonucleotide microarrays (›chips‹, Figure 1.4).

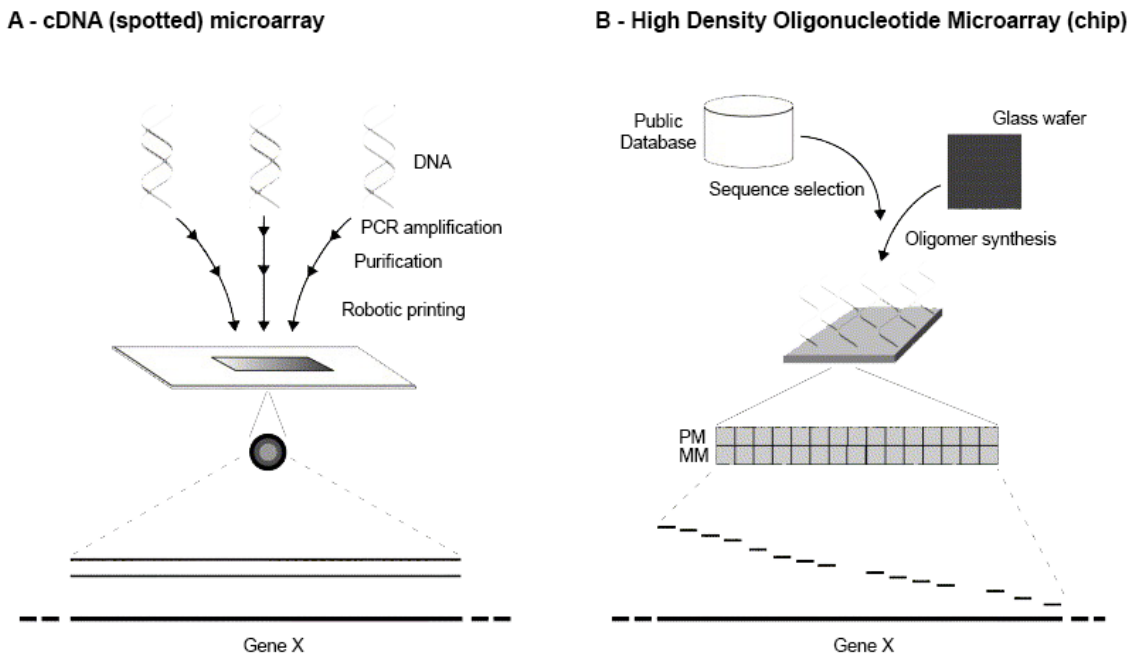

Figure 1.4 – Technical designs of coding DNA (cDNA) and high-density oligonucleotide microarrays. (A) DNA sequences of the genes whose expression should be measured is amplified and reversely-transcribed to cDNA. These cDNA strands, each corresponding to one gene, are printed on the microarray surface. (B) Short oligonucleotide sequences (25 bp), 16 to 20 per gene, are synthesized directly on the microarray surface using photolithography. Each oligonucleotide perfectly matches a different section of the gene's DNA sequence (PM). Some chip-based platforms include additional mismatch oligonucleotides (MM) containing intentional substitutions of single nucleotides which imperfectly match the genes' sequences. They are used to adjust for unspecifically hybridized mRNA. Figure adopted from [113].

In cDNA microarrays, cDNA strands of usually more than several hundred base pairs in length are synthesized beforehand and spotted onto specially manufactured glass slides in a process that is similar to inkjet printing.

In contrast, high-density oligonucleotide microarrays make use of short nucleotide sequences (25 bases) that are ›in situ‹ synthesized onto glass wafers using photolithography, a technique similar to that used in the production of computer chips. These short oligonucleotide sequences, also referred to as ›probes‹ or ›features‹, perfectly match parts of open reading frames known from nucleotide repositories such as GenBank® (http://www.ncbi.nlm.nih.gov). On some but not all oligonucleotide microarray platforms, a corresponding mismatch-probe is synthesized as a specificity negative control for each probe. Such mismatch-probes have the same

nucleotide sequence except for a single substitution of a nucleotide in a central position. These negative controls can be used to correct for false-positive signals from local background or cross-hybridization. Pairs of 16 to 20 matching – and possibly mismatching – probes are summarized in so called ›probesets‹.

These probesets can then be collected into greater assemblies of ›transcriptclusters‹. Other than probesets representing exons, transcriptclusters represent entire strands of transcribed RNA (e.g. the mRNA of a gene). Consequently, the analysis of differentially expressed probesets aims at the study of alternative splicing, whereas the collection of probesets into transcriptclusters allows the investigation of differentially expressed genes.

The final expression values of probesets or transcriptclusters are calculated from the measured intensities of the individual probes (e.g. by taking the mean over the corresponding probe intensities).

A typical workflow in gene expression profiling

A typical microarray experiment compares the abundance of RNA in samples from contrasting conditions (e.g. diseased vs. healthy). Although the detailed procedure may be different depending on the microarray platform and the sample types, the major steps are similar (Figure 1.5).

Using cDNA microarrays, mRNA is extracted from samples and color-labeled with fluorescent dyes (one color for each condition). The labeled RNA is then hybridized altogether to strands of coding DNA on a single array. After a washing step, a laser scans the microarray to determine the intensities of the different fluorescent dyes. Here, the ratio of the dye intensities measured for each spot on the array corresponds thereby to the relative abundance of hybridized RNA from the different samples.

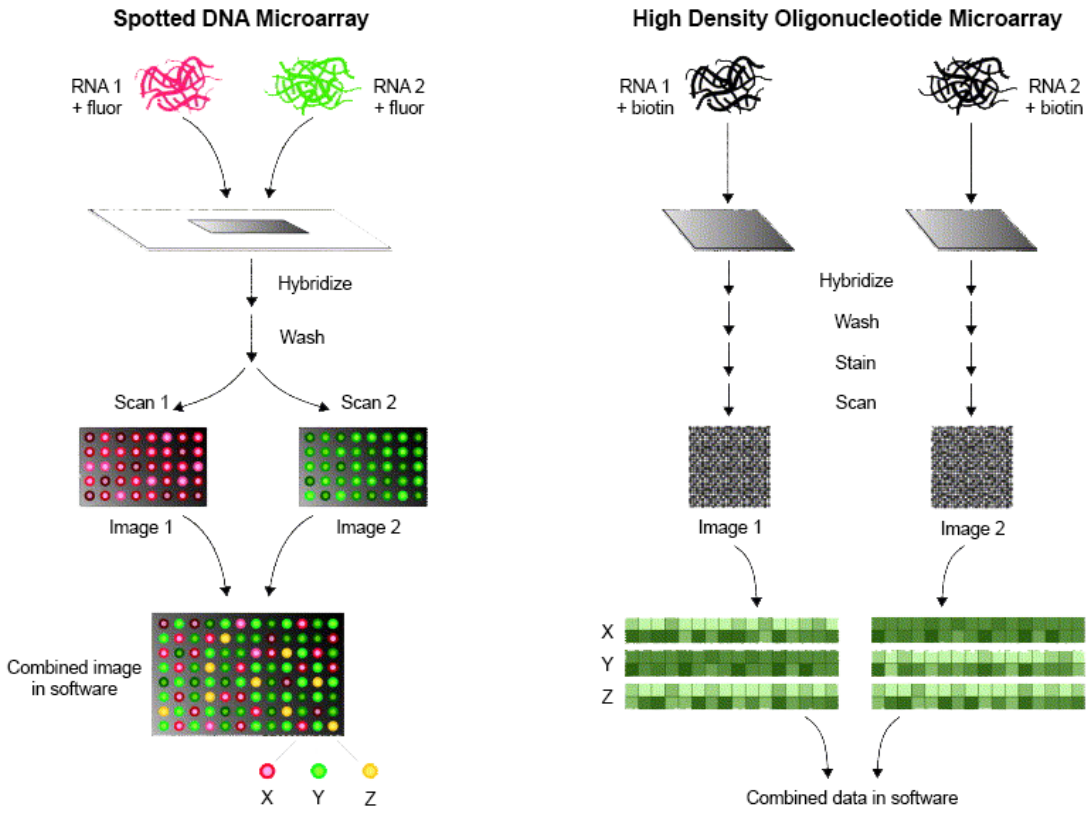

Figure 1.5 – Typical workflows in cDNA and oligonucleotide microarray transcriptomics experiments. (A) Two mRNA samples from two different conditions (e.g. case and control) are labelled with fluorescent dyes (one dye for each condition, e.g. case = green; control = red). The labelled mRNA is hybridized to a single microarray. After processing, the microarrays are scanned twice to determine the intensity of each dye (i.e. amount of mRNA in case and control) on the microarray. Combining the results of both scans, the color overlay at each spot indicates the corresponding gene's relative expression change between the two conditions (i.e. green = gene is more expressed in case than control). (B) All mRNA samples are similarly labelled with biotinylated uridine- and cytidine-triphosphate, irrespective of the samples' conditions (e.g. case and control). mRNA from each sample is hybridized to its own microarray. After processing, the microarrays are separately scanned to determine the amount of labelled mRNA bound to each microarray. The data are then normalized to get the genes' absolute expression values within each sample. Comparing the expression values between samples or the mean expression values between groups of samples, the relative expression changes of genes are determined. Figure adapted from [113].

For chip based experiments, biotinylated uridine- and cytidine-triphosphate are used to label the RNA. The biotinylated RNA is then hybridized to different chips (one chip per sample). After washing, the biotinylated RNA on each chip is stained with

a fluorophore. A laser subsequently determines the intensity of this fluorophore (i.e. bound RNA) for each chip separately. From these intensities, the expression values for each RNA probe on the chips are calculated. Finally, to determine the relative RNA abundances between samples, the expression values of the respective chips are compared.

Because photolithography enables the parallel synthesis of hundreds of thousands of oligonucleotide probes on a single chip, oligonucleotide microarrays are often preferred over cDNA microarrays for whole genome gene-expression profiling or genotyping experiments [113, 114].

1.5.2 Metabolomics

Just like the transcriptome comprises the totality of DNA and RNA molecules, the term ›metabolome‹ refers to all metabolites present in a biological sample. Equally, the term ›metabolomics‹ denotes the study of metabolomes. Metabolomics profiles the endpoints of epigenetic and transcriptional changes, enzymatic reactions, as well as environmental impact. Therefore, metabolomics is generally believed to track the phenotype more closely than any other omics technology. As a result, changes in the metabolome are often referred to as ›intermediate traits‹.

Measuring techniques

Numerous techniques have been employed for metabolomics, notably Nuclear Magnetic Resonance spetroscopy (NMR) [115, 116] and Mass Spectrometry (MS)-based methods [117, 118]. Each of these techniques has its own individual strengths and weaknesses. Most importantly, none of the currently available techniques is exhaustive and able to measure all metabolites. Thus, in contrast to the other omics fields such as transcriptomics (see above), which can be typically handled by a single technique, the study of the metabolome requires the combined application of multiple, complementary techniques rather than individual methods. Moreover, other than genomic data, the chemical annotations of metabolomes remain largely incomplete.

NMR is fast and cheap and usually nondestructive because it can be performed directly on the samples with little or no need for sample preprocessing. It is not selective for certain classes of metabolites, can theoretically detect any molecule containing carbon or hydrogen, and is robust, i.e. metabolite profiles are reproducible (although factors such as sample aging might change the metabolite profiles). The main weakness of NMR is its relatively low sensitivity (i.e. only medium and highly abundant metabolites can be detected) and the overlap of signals from different metabolites, which limits the number of quantifyable distinct metabolites to about 100 in practice. In addition, the post-processing and identification of metabolites from the spectra generated by NMR is often not straight-forward and in practice, NMR-based metabolomics is limited to the study of about 100 distinct metabolites.

MS-based approaches are highly sensible and provide unmatched mass resolutions down to 10^{-15} mol [118]. In metabolomics, MS is often combined with separation techniques such as Gas Chromatography (GC) or Liquid Chromatography (LC). Using separations, MS-based metabolomics is able to distinguish isobaric metabolites and provides further information about the physico-chemical properties of metabolites. However, MS-based approaches require a fairly extensive and destructive sample preprocessing (i.e. the sample cannot be reused for further analyses), which is costly, time-consuming, and a potential source for variation or loss. In addition, MS-based methods are usually not equally sensitive to all classes of metabolites. Thus, when using MS-based approaches, the parallel application of different techniques (e.g. GC-MS and LC-MS) is recommended.

Because the metabolomics data used in this thesis was exclusively measured using GC-MS and LC-MS, I will give a brief introduction on the principles of MS-based approaches only. Please refer to Blümich [119] for detailed information on NMR theory.

MS in combination with chromatographic separation has become a widely applied tool in metabolomics. Although the detailed procedure might differ depending on the samples and the nature of the study, MS approaches generally comprise the following steps: (1) sample preprocessing, (2) separation of the metabolites using chromatography, (3) ionization of the separated metabolites in an ion source, (4)

fragmentation, and (5) sorting and detection of the charged metabolites and fragments.

(1) In the preprocessing step, the metabolites are extracted from the biological matrix (e.g. blood serum or plasma, tissue homogenates) using appropriate solvents (e.g. methanol). In targeted metabolomics, where the analytes are known beforehand, this preprocessing step is usually optimized to maximize the extraction for the metabolites of interest. (2) After sample preprocessing, the extracted metabolites are separated by chromatographic methods such as GC or LC. (3) During separation, the stream of separated metabolites enters an ion source, where the metabolites are charged either physically or chemically. Typical ionization techniques are Electron Spray Ionization (ESI) or Chemical Ionization (CI). Depending on the specific procedures, metabolites sometimes already break into smaller fragments or build adducts with other ions in the ion source, which is generally an undesirable effect. (4) In the collision zone, the ions collide in the gas phase with a neutral gas (e.g. helium) and break into smaller ion fragments. (5) The ionized molecules and fragments are then sorted for their masses based on the mass-to-charge ratio (m/z) using electric and magnetic fields. Finally, the relative abundance of each ion is determined by recording how many of them hit the detector. As a result, the mass spectrum, which shows the abundance of ions as a function of their m/z ratio, is produced.

Analysis strategies: targeted and non-targeted metabolomics

Approaches in the field of metabolomics fall in general into two main classes: targeted (bottom-up) and non-targeted (top-down) metabolomics (Figure 1.6).

Targeted metabolomics is usually applied in hypothesis-driven studies. Based on the research question, the metabolites of interest are selected prior to the measurements. Knowing beforehand which metabolites are to be measured has the advantage that the analysis can be optimized for the selected metabolites. Notably, in targeted metabolomics, internal isotope-labeled standards (spikes) are added to the samples prior to the actual analysis. Using these internal standards, metabolite abundances

can be quantified absolutely and reported in concentrations, usually µmoll^{-1}. Naturally, targeted metabolomics approaches are restricted to metabolites for which internal standards are available.

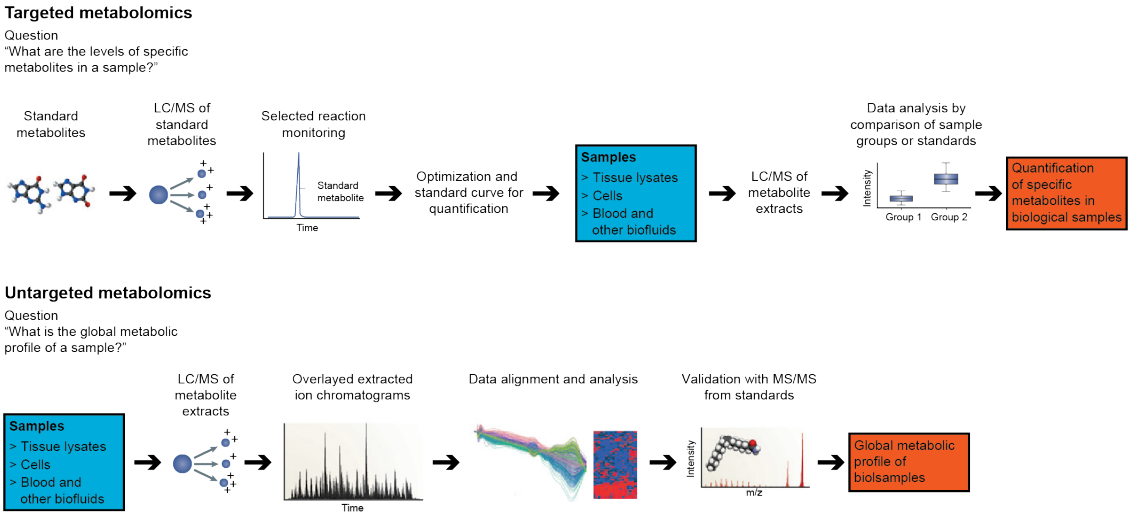

Figure 1.6 – Targeted and Non-Targeted Metabolomics. Targeted metabolomics use a predefined set of standard metabolites, allowing for the absolute quantification of their concentrations. In contrast, non-targeted metabolomics reports every measurable metabolite in a sample, however, is limited to qualitative comparisons of metabolite levels between samples. In non-targeted analyses the measured metabolites' identities are initially unknown and need to be clarified by comparing features of the recored spectra to those of known metabolites. Moreover, measurements from non-targeted analyses always have to be confirmed by targeted analyses. Figure adapted from [120].

Current targeted metabolomics approaches are able to detect less than 300 discrete metabolites. Considering estimates of 6,500 total metabolites in the metabolome, targeted metabolomics covers obviously only small parts of the metabolome [120, 121].

In contrast to targeted metabolomics, non-targeted metabolomics is considered an explorative, hypothesis-generating approach. Non-targeted approaches do not work with predefined standards and report every measurable metabolite in a biological sample, regardless of its chemical class. Using state-of-the-art technologies (see below), non-targeted approaches are in principal able to measure thousands of metabolites. However, the lack of internal standards in non-targeted metabolomics means at the same time that the measurements of such approaches are at best semi-

quantitative. Non-targeted metabolomics is therefore generally limited to the study of qualitative differences of metabolite levels (e.g. between contrasting conditions). In addition, also as a result of the missing internal standards, non-targeted metabolomics approaches are semi-informed, i.e. the identities of the detected metabolites are initially unknown. Although many identities can be clarified by comparing features of the recorded spectra to those of known metabolites, in non-targeted metabolomics researchers are usually left with a considerable number of analytes that cannot be identified. Regardless of whether the identity is known or not, results from non-targeted analyses need to be ultimately confirmed by additional targeted analyses, comparing the candidate metabolites to their corresponding standard compounds [120].

1.5.3 Comparative omics: quantifying within- and between-species similarities and differences

With the increasing use of omics, physiological changes can be comprehensively described on a whole new level of detail on the basis of molecular traits such as altered gene expression or changing metabolite concentrations. As a result, using omics data within- or cross-species comparisons, for example to determine the validity of mouse models in reproducing human disease traits, are not limited to a handful of phenotypic traits anymore, but can rather be done on the basis of thousands of molecular traits.

There are several examples for comparative gene expression studies in the scientific literature, facilitated by more and more gene expression profiles that are publicly available in repositories such as the Gene Expression Omnibus [122]. For instance, Zheng-Bradley et al. studied the conservation of tissue-specific gene expression of orthologous genes in mice and humans using a large collection of publicly available human and mouse microarrays. The authors showed that both the most variable genes and the most ubiquitously expressed genes co-vary across both species and found the greatest overlap for genes expressed in brain and neural tissue. Based on their observations, they conclude that gene expression patterns are more similar

among identical tissues within different species than those among different tissues within a single species [123].

Another study compared significantly affected genes in response to dietary restriction obtained from 22 studies in 6 different organisms including mouse and rat [124]. They found that there was no single gene commonly affected across all species examined in their study. However, when they focussed on the functions of the altered genes rather than the individual gene expression traits, they indeed found some overlap among species in response to dietary restriction [124]. This finding was in line with Kumar et al., which stated that abstracting genes to gene ontology terms allowed comparison across multiple species [125].

Some studies, however, come to contrary conclusions. For instance, only few changes in the whole genome mRNA expression in leukocytes after ischemic stroke are common to rodents and humans [126, 127]. Two other studies recently revealed key differences in the molecular constitutions of distinct mouse models of amyotrophic lateral sclerosis [128] and human inflammatory diseases [112]. Even though the models examined in these studies perfectly mimic the key characteristics of the corresponding human disease physiologies on the phenotypic level, the gene expression changes in the models and humans did not correlate significantly. However, using a slightly different analysis approach, Takao and Miyakawa conclude the exact opposite of [112] and claim that genomic responses in mouse models greatly mimic human inflammatory diseases [129].

The field of comparative omics is not limited to the analysis of gene expression and there are some metabolomics studies addressing the similarities and differences of metabolic traits between studies. For instance, in a systematic cross-species metabolomics study, Salek et al. compared the urinary metabolic profiles of diabetic db/db mice, obese Zucker Diabetic Fatty (ZDF) rats, and that of untreated diabetic patients [130]. They used 1H-NMR spectroscopy and identified 27, 31 and 44 metabolites in mice, rats, and humans, respectively. Comparing these urinary profiles, the researchers found different metabolic processes that are perturbed in all three species, although the individual changes of metabolites were sometimes different between rodents and humans [130].

Another recently published study combined gene expression and metabolomic profiling in liver from humans, chimpanzees, and rhesus macaques to investigate the differences in their metabolomes as a result of gene regulatory differences within these species [131]. In line with previous studies which showed that – probably because of different eating habits – genes with metabolic functions are enriched among differentially regulated genes in humans and non-human primates, the researchers revealed similar inter-species differences among metabolic concentrations [131]. Furthermore, they showed that the metabolic differences between the three species correlate with the altered expression of those enzymes which control the corresponding metabolic reactions. Finally, they present several metabolites that change species-specifically, which is probably due to dietary differences between humans and non-human primates [131].

1.6 Aims and structure of the thesis

Experiments in model animals represent an important tool in T2DM research. Searching for the term ›type 2 diabetes‹ with the filter ›other animals‹ on Pubmed to get a rough estimate of animal experiments done in diabetes research results in more than 18,221 documents (status as of June 2015). Dispite this large number, our understanding about the pathogenic mechanisms of human T2DM is still limited. Clearly, the translation of animal research into humans is complicated for various reasons, most obviously because of the species' different anatomy, genetics, and physiology. But even across models from the same species the findings often fail to replicate (see Introduction 1.4.3). Although most animal models are usually well characterized on the phenotypic level at which they are supposed to mimic the human phenotype, indeed, for many models only little is known about their underlying molecular constitutions. As of today, there are no comprehensive characterizations and comparisons of the molecular constitutions of diabetes in mouse models and human diabetic patients available.

In this thesis, I present a generic meta-analysis workflow which allows to systematically study universal and species-specific molecular characteristics based on high-throughput omics data. Applying this workflow on transcriptomics and metabolomics data from two different mouse experiments, I address two points outlined above: first, the reproducibility of findings across different mouse models for the same disease, and second the translatability of findings across mouse models and the corresponding human disease.

After summarizing the data and methods used in this thesis in **Chapter 2**, I exemplify the use of my meta-analysis workflow for the study of mouse models in the following two chapters. In **Chapter 3**, I apply my workflow to whole genome liver transcriptomics data from four genetically heterogeneous mouse models of NAFLD to investigate universal and species-specific disease related genomic responses (i.e. differentially expressed genes). I discuss how the similarities and differences between the models as revealed by my analysis might influence study outcomes. In **Chapter**

4, I use my workflow for the comparative study of metabolomics data across species. Comparing the metabolic signatures of the db/db model of obesity and T2DM to those observed in obese diabetic humans, I explore how well the model mimicks the metabolic constitution of human diabetes. I discuss which aspectes of the disease are well reflected and which are not, and provide possible explanations for specificities in the model's metabolic make-up.

Finally, I summarize my results in **Chapter 5** and provide further thoughts on the limitations and potential of my workflow and future perspectives.

Chapter 2

Data and Methods

2.1 Mouse models of NAFLD: 129, B6J, B6N and C3H

In collaboration with the German Mouse Clinic II, 72 male mice from four different inbred mouse strains C3Heb/FeJ (C3H), C57BL/6NTac (B6N), C57BL/6J (B6J), and 129P2/OlaHsd (129) were bred and housed under standard vivarium conditions. At an age of 14 weeks, animals of each strain were single-housed and allocated to two groups in a litter-matched manner. One group of each strain was subsequently fed a High Fat Diet (Ssniff Spezialdiäten, Soest, Germany) to induce the NAFLD phenotype, while the remaining mice stayed on a Low Fat Diet (Diet#1310, Altromin, Lage, Germany). After 21 days, all 72 mice were sacrificed. Liver samples were taken and quickly freeze-clamped in liquid nitrogen or immersed in paraformaldehyde. Blood and liver samples were deep frozen to $-80\,^{\circ}\mathrm{C}$ and stored until analysis.

Animal experiments were approved by the Upper-Bavarian district government (Regierung von Oberbayern, Gz.55.2-1-54-2532-4-11). For a detailed description of the experimental conditions and sampling refer please to Kahle et al. [132].

2.2 Mouse model of T2DM: db/db

20 male BKS.Cg-Dock7m+/+ Leprdb/J (db/db) mice were used as a model for T2DM and obesity and 20 male Dock7m+/+ (wt) littermates were used as non-diabetic, lean, ›wild-type‹ controls (Figure 2.1, B). From an age of three weeks, all 40 mice were fed a HFD (Ssniff Spezialdiäten, Soest, Germany). All 40 db/db and wt mice received vehicle treatment by gavage, as they served as control animals in a pharmacological treatment experiment [64]. After 8 and 10 weeks, plasma samples of 10 db/db and 10 wt mice were taken after 2 h fasting and deep frozen to −80 °C until further analysis. Thus, a total of 40 plasma samples were collected.

Animal experiments were approved by the Upper-Bavarian district government (Regierung von Oberbayern, Gz.55.2-1-54-2532-4-11).

2.3 Human cohort of the general population: KORA F4

All human samples were taken from the Cooperative Health Research in the Region of Augsburg (KORA) F4 cohort study conducted in 2006 to 2008. KORA F4 is an extensively phenotyped sample (n = 3,080) from the general population for which several high-throughput data sets are available in addition to anthropometric phenotypes and clinical outcomes.

Here, we took a subsample (n = 1,768) of the KORA F4 survey for which targeted as well as non-targeted metabolomics data were available. The results of an OGTT after overnight fasting were used to divide individuals into ›diabetic‹ (n = 72) and ›healthy‹ (n = 1,138) groups according to [12]. Diabetic and healthy individuals were further stratified for weight differences into three groups: (1) 45 obese diabetic (od) individuals (BMI $\geq 30\,\mathrm{kg\,m^{-2}}$), (2) 231 obese healthy (oh) individuals (BMI $\geq 30\,\mathrm{kg\,m^{-2}}$), and (3) 390 lean healthy (lh) individuals (BMI $18.5 - 25\,\mathrm{kg\,m^{-2}}$). See Figure 2.1 (A) for additional sample parameters.

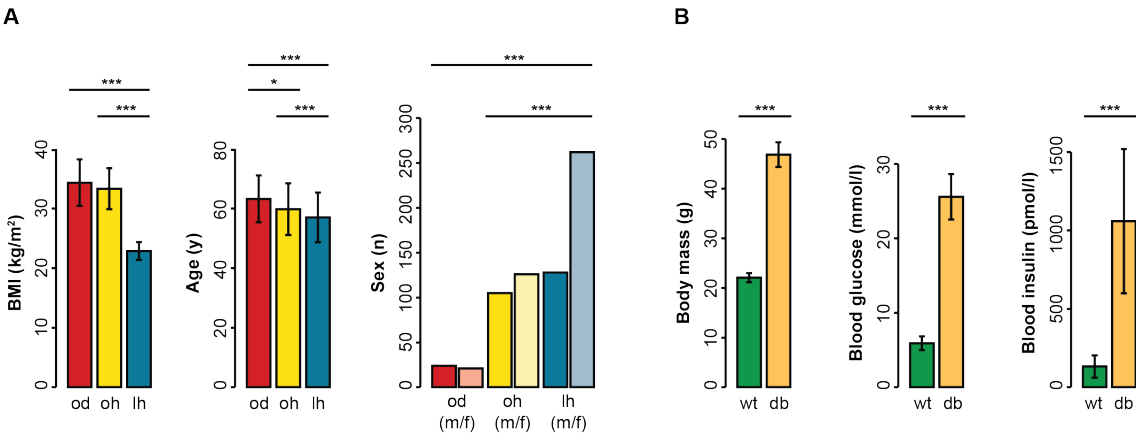

Figure 2.1 – Descriptive characteristics of human and murine samples. Parameters were tested for significant differences between groups using Wilcoxon test for continous (BMI, age) or Fisher Exact Test for categorical variables (sex). Abbreviations: od = obese diabetic (n = 45); oh = obese healthy (n = 231); lh = lean healthy (n = 390); db = db/db (n = 20); wt = wild-type (n = 20); $^{*}P < 0.05$; $^{**}P < 0.01$; $^{***}P < 0.001$.

Diabetic participants were not under any anti-diabetic drug treatment because they were firstly diagnosed with the disease at the time of the sampling. Serum samples were taken after overnight fasting and were processed and deep frozen at $-80\,^{\circ}C$ until further analysis [133].

Written informed consent has been given by all participants. The KORA study has been approved by the ethics committee of the Bavarian Medical Association (Bayerische Landesärztekammer).

2.4 Transcriptomics measurements

To examine NAFLD related changes in the liver transcriptomes of the four mouse models, we applied high-throughput expression profiling on Affymetrix® GeneChip® Mouse Gene 1.0 ST arrays, which cover a broad spectrum of known murine protein coding genes.

2.4.1 Sample preparation and RNA isolation

Total RNA was isolated from frozen liver homogenates using the miRNeasy Minikit (Qiagen) including DNAse treatment. RNA quality was assessed with an Agilent bioanalyzer kit and total RNA (200 ng, RNA integrity number > 5) was amplified using the Affymetrix® GeneChip® Whole Transcript Sense Target Labeling Assay. The amplified cDNA was subsequently hybridized on Affymetrix® GeneChip® Mouse Gene 1.0 ST oligonucleotide arrays. The preparation of tissue samples for mRNA profiling has been described in detail in [132].

2.4.2 Quality control and data preprocessing

The latest gene-level annotation data was collected for Affymetrix® GeneChip® Mouse Gene 1.0 ST arrays from Affymetrix®, Inc. (http://www.affymetrix.com, state as of 04/2015). All arrays were processed separately for each strain using the Robust Multichip Average (RMA) algorithm for background-adjustment and normalization. Briefly, in RMA, intensities are adjusted for non-specific binding and optical noise using a background plus signal model, assuming that the intensity of each measured probe set is the convolution of exponentially distributed signals and normally distributed noise. The background-adjusted intensities are then normalized by quantile normalization, making the distributions of the probe set intensities equal for all arrays. Finally, the expression values of each probe set are represented as an additive linear model of the background-adjusted and normalized probeset intensities. For a detailed description and evaluation of the RMA method, please refer to the original text in Irizarry et al. [134].

Before and after normalization, and for each strain separately, we checked the arrays for possible outliers. To this end, we used three different summary metrics and inspected the corresponding quality plots.

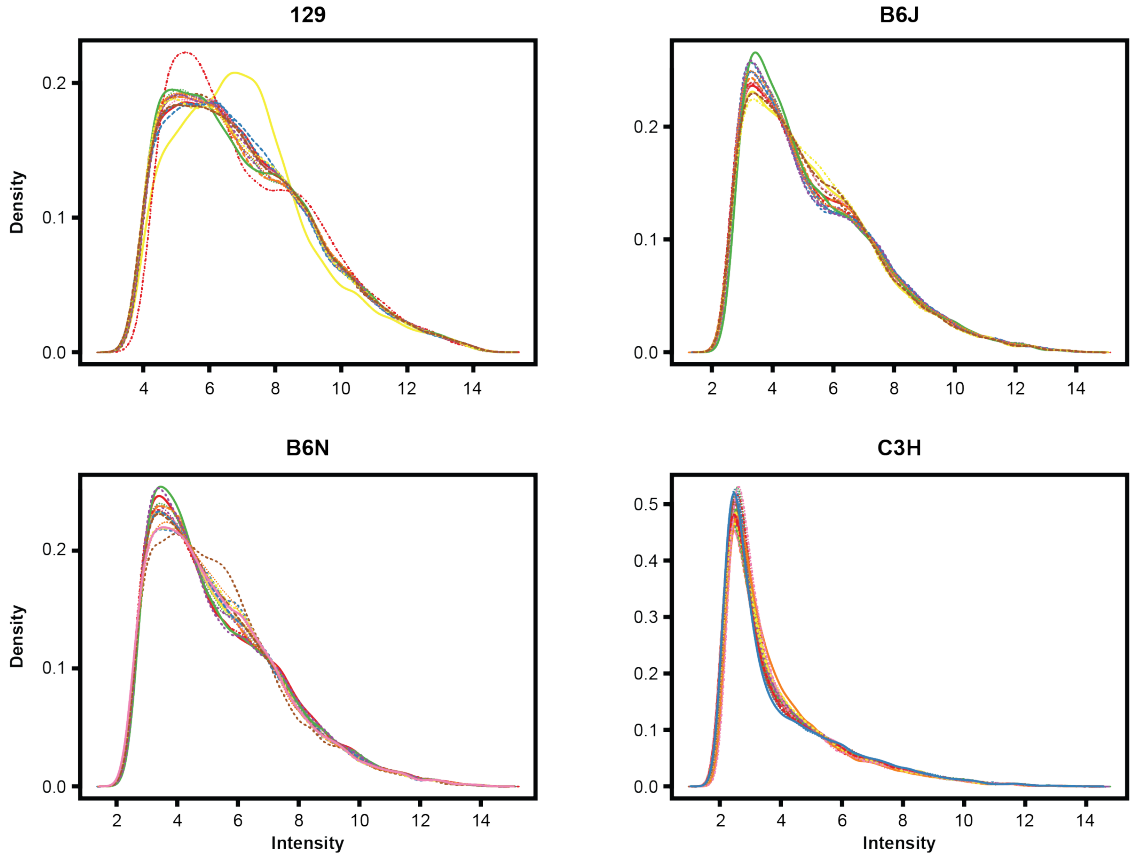

Figure 2.2 – Distributions of normalized expression values. In 129 and B6J, the intensity distributions of some samples diverge significantly from each other as determined by the Kolmogorov-Smirnov test.

In short, all these metrics are calculated from the M (minus) values (that is the log-ratios of the expression values of each probe) and the A (average) values (i.e. the arithmetic mean of the logarithmized expression values of each probe), which are defined as follows:

$$M = log_2(l_1) - log_2(l_2) \tag{2.1}$$

$$A = \frac{log_2(l_1) + log_2(l_2)}{2} \tag{2.2}$$

where l_1 denotes the measured intensity of a certain probe on the array of interest, and l_2 the intensity of a ›pseudo‹-array, representing the median of the same probe's intensity across different arrays. For a detailed description of the applied metrics and on how they help to decide whether an array is a possible outlier or not, please refer to Kauffmann and Huber [135].

The evaluation of the different Quality Control (QC) metrics led us to exclude 2 of 15 samples from the 129 strain, because samples 6 and 9 exceeded a critical Manhattan distance to the other arrays (Figure 2.3) and their intensity distributions diverged significantly from those of other samples' measurements (Figure 2.2). For the same reasons, we removed one sample (sample 11) from the B6J study (Figure 2.3; Figure 2.2). No samples of strains B6N or C3H were considered as potential outliers in terms of the three QC criteria outlined above.

The measurements of strains B6J, B6N and C3H showed (even after normalization) batch effects (Figure 2.3), corresponding to the three (C3H) and two (B6J, B6N) different measurement dates in these studies. However, because in all studies HFD and LFD samples were randomly and evenly split over the different measurement dates, it is safe to assume that the batch effects do not interfere with the comparison of interest (i.e. HFD vs. LFD).

After QC, 69 out of 72 arrays from the 4 mouse strains were left in the analysis (Table 2.1).

Table 2.1 – Microarrays left after QC.

Strain	High-fat diet (Case)	Chow (Control)
129 (13)	6	7
B6J (14)	6	8
B6N (16)	8	8
C3H (26)	8	18
Total	**30**	**42**

After removing low-quality arrays, 69 out of the 72 Affymetrix GeneChip® Mouse Gene 1.0 ST arrays were left for the comparison of transcriptomic responses in the four different mouse strains of NAFLD. Because of the experimental design, for C3H the LFD samples (controls) were pooled from mice of different age (age differences between 5 to 33 days).

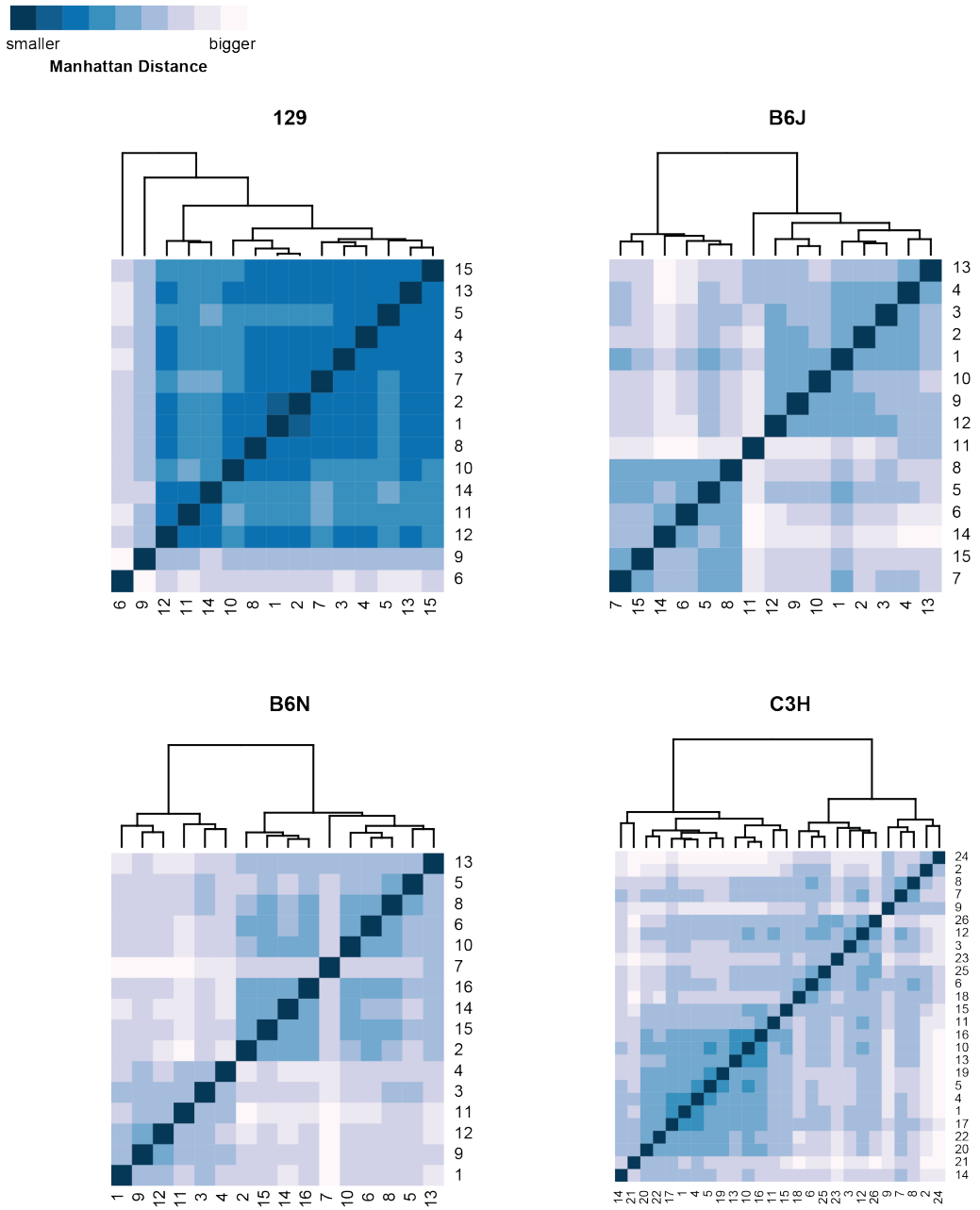

Figure 2.3 – Similarity of samples based on their expression profiles. Pairwise Manhattan distances (L_1 distances) between samples of each mouse strain, calculated from the normalized expression values. Dendrograms show the hierarchical clustering (Ward's method [136]) of samples based on their distances. Samples with large distances to the remaining ones are considered as outliers. We find potential outliers for strains 129 (samples 6 and 9) and B6J (sample 11). Note that in strains B6J, B6N, and C3H, clear batch effects are visible, because the measurements in these studies had to be split over several dates.

2.4.3 Filtering

After QC, the RMA processed data was filtered for unspecific criteria (i.e. features irrespective of the samples' phenotypes) to exclude non-informative probesets.

(1) We excluded probesets belonging to non-protein coding sequences that are present on chips of the GeneChip® Mouse Gene 1.0 ST oligonucleotide platform such as non-murine sequences (negative controls) or microRNA. In total, 6,615 of such probesets were excluded from each of the 69 datasets. (2) In addition, we removed 4,106 probesets without gene annotations. (3) Finally, we collapsed probesets representing the same gene to a single value by selecting the probeset which shows the greatest relative expression change, i.e. the greatest absolute $\log_2$ fold-change between HFD and LFD groups. As a result, another 2,805 probesets were excluded from each dataset. After these filtering steps, the final datasets of each study contained the expression values of 22,030 unique genes (Table 2.2).

Table 2.2 – Filtered transcriptclusters

Strain	Total	Protein coding	With annotation	Unique genes	Fold change > 1.3
129	35,556	28,941	24,835	22,030	561
B6J	35,556	28,941	24,835	22,030	329
B6N	35,556	28,941	24,835	22,030	436
C3H	35,556	28,941	24,835	22,030	341

Transcriptclusters fulfilling certain criteria, starting from 35,556 total transcriptclusters measured on each GeneChip® Mouse Gene 1.0 ST array. Annotated transcriptclusters are those with gene annotations.

For certain statistical analyses, we constrained the data to genes with absolute linear fold changes greater than 1.3 between HFD and LFD groups for each strain separately to exclude genes which are not differentially expressed (Table 2.2).

2.5 Metabolomics measurements

To obtain a comprehensive picture of the murine and human blood metabolomes, we applied both a targeted metabolomics approach with a specific focus on lipids and a non-targeted metabolomics approach which broadly covers the spectrum of known metabolic pathways.

2.5.1 Targeted metabolomics

For targeted metabolite quantifications in human and murine blood samples, we used the mass spectrometry (MS) based AbsoluteIDQ™ kits p150 and p180 (Biocrates Life Sciences AG, Austria). Sample preprocessing and analyses were performed according to the manufacturer's instructions, which was described in detail in [133, 137] for the kit p150. Briefly, after methanolic metabolite extraction from 10 µL of human serum samples, a flow injection analysis method combined with appropriate internal standards enables the absolute quantification of 14 amino acids, hexose (about 90-95% glucose), free carnitine, 40 acylcarnitines, as well as the semi-quantitative assessment of 92 glycerphospho- and 15 sphingo-lipid abundances. Kit p180, which was applied to murine plasma samples, works similar. An additional liquid chromatography step in the p180 assay allows for quantification of further 7 amino acids and 21 biogenic amines. 161 of 163 metabolites measured by kit p150 are also measured by the p180 kit.

Liquid handling was performed on a Hamilton Microlab STAR™ robot (Hamilton AG, Switzerland) and a Ultravap nitrogen evaporator (Porvair Sciences, Leatherhead, U.K.). MS were performed on an API 4000 LC/MS/MS System (AB Sciex Deutschland GmbH, Darmstadt, Germany) equipped with a 1200 Series HPLC (Agilent Technologies Deutschland GmbH, Böblingen, Germany) and a HTC PAL auto sampler (CTC Analytics, Zwingen, Switzerland) controlled by the software Analyst (version 1.6.1). Quantification of metabolite concentrations and quality assessment was performed with the MetIDQ™ software package, which is part of the AbsoluteIDQ™ kit.

2.5.2 Non-targeted metabolomics

For non-targeted metabolite profiling, human and murine blood samples were sent to Metabolon Inc. (Durham, USA), a commercial supplier of metabolomics analyses. Profiling was performed on gas and liquid chromatography coupled to mass spectrometry (GC/MS and LC/MS, respectively). Sample preparation was performed on a Hamilton Microlab STAR™ robot (Hamilton AG, Switzerland). LC/MS was done on an LTQ mass spectrometer (Thermo Fisher Scientific, Waltham, MA) equipped with a Waters Acquity UPLC system (Waters Corporation, Milford, MA). GC/MS analysis was done on a Thermo-Finnigan Trace DSQ fast-scanning single-quadrupole mass spectrometer. Metabolites were identified from the MS data by semiautomated multiparametric comparison with a proprietary library, containing retention times, m/z ratios, and related adduct/fragment spectra. Non-targeted profiling for human and murine samples resulted in 377 and 440 metabolites, respectively, covering a broad spectrum of metabolic pathways.

2.5.3 Quality control and pre-processing

For the targeted data, we applied the QC procedure described in Jourdan et al. [86]. Briefly, in the human data, 11 of 163 metabolites were excluded because of high variance of measured values in reference serum samples (coefficient of variation $> 25\%$). Another metabolite was excluded because its number of missing values exceeded 5%. Similarly, 14 of 188 metabolites from the targeted data obtained in mouse were excluded because of high variation, and 3 measurements because of more than 5% missing values. Outliers were defined as data points with values greater or less than the mean ± 5 standard deviations for each metabolite over all human or murine samples. In human, samples with more than three independent outlier data points (i.e. their correlation with all other outliers in this sample is less than 0.7) were excluded from further analysis. In mouse, there was no metabolite with more than three outlying data points. Remaining outlier data points were set missing. All missing values were imputed using predictive mean matching as implemented in the R package ›MICE‹.

QC of the non-targeted data was implemented as described in more detail in Shin et al. [138]. Accordingly, all 377 and 440 measured raw ion counts in the human and murine samples were divided by the metabolites' median of the respective run day to adjust for instruments' inter-day variations. The normalized values were log-transformed ($\log_{10}$), because values show log-normal distributions for the majority of metabolites. We removed individual outlier data points that lay more than four standard deviations from the mean of the particular metabolite over all human or murine samples. Metabolites with more than 30% missing values in one of the human study groups (od, oh, lh), db/db or wt mice were excluded from analysis.

After QC, the human dataset contained 524 and the murine dataset 516 metabolites. Thereof, data on 319 metabolites were available in both human and murine blood samples. 26 out of 319 metabolites were measured on each of the two platforms (Table 2.3). In addition, 13 metabolites detected on the non-targeted platform represent isobaric molecules that are measured together in 6 sum measures on the targeted platform (Table 2.4). Thus, the 319 metabolites measured both in humans and mice correspond to 287 distinct molecules.

Table 2.3 – Metabolites measured on both platforms

#	Targeted (Names as in Biocrates)	Non-targeted (Names as in Metabolon)
1	Gly	glycine
2	Ser	serine
3	His	histidine
4	Tyr	tyrosine
5	Phe	phenylalanine
6	Trp	tryptophan
7	Val	valine
8	lysoPC.a.C17.0	1-heptadecanoylglycerophosphocholine
9	C2	acetylcarnitine
10	C0	carnitine
11	C6 (C4:1-DC)	hexanoylcarnitine
12	C3	propionylcarnitine
13	lysoPC a C20:4	1-arachidonoylglycerophosphocholine*
14	SM C16:0	palmitoyl sphingomyelin
15	C5	isovalerylcarnitine
16	Gln	glutamine
17	Arg	arginine
18	C16	palmitoylcarnitine
19	Met	methionine
20	lysoPC a C20:3	1-eicosatrienoylglycerophosphocholine*
21	Thr	threonine
22	Pro	proline
23	C18	stearoylcarnitine
24	C18:1	oleoylcarnitine
25	lysoPC a C14:0	1-myristoylglycerophosphocholine
26	lysoPC a C16:1	1-palmitoleoylglycerophosphocholine*

*Pure substance was not available for spectra comparisons within the same platform.

Table 2.4 – Isobaric molecules

#	Targeted (Names as in Biocrates)	Non-targeted (Names as in Metabolon)
1	H1	glucose, fructose, mannose
2	lysoPC a C16:0	1-palmitoylglycerophosphocholine, 2-palmitoylglycerophosphocholine*
3	lysoPC a C18:0	1-stearoylglycerophosphocholine, 2-stearoylglycerophosphocholine*
4	lysoPC a C18:1	1-oleoylglycerophosphocholine, 2-oleoylglycerophosphocholine*
5	lysoPC a C18:2	1-linoleoylglycerophosphocholine, 2-linoleoylglycerophosphocholine*
6	C4	butyrylcarnitine, isobutyrylcarnitine

Isobaric molecules measured on the non-targeted platform that are jointly detected as sum measures on the targeted platform.

2.6 Statistical analysis

All statistical analyses were done in R (http://www.r-project.org).

2.6.1 Determining the significance of gene expression traits of NAFLD

For each of the 22,030 measured gene transcripts, the $\log_2$ fold change was calculated as the difference of the mean $\log_2$-transformed expression values in the HFD and LFD groups for each mouse strain separately. The statistical significance of the $\log_2$ fold changes (i.e. whether a gene is significantly differentially expressed or not) was tested using a moderated T-statistic [139].

For the selection of significantly altered gene expression traits (see below), only genes which showed fold changes greater than 1.3 between groups were considered

(Table 2.2). The p-values of these genes were adjusted for multiple testing using conservative Bonferroni correction, which controls the Family Wise Error Rate (FWER).

2.6.2 Determining the significance of metabolic traits of T2DM or obesity

For each metabolite measured in human and mouse, we applied linear regression models to identify the change in the metabolite's normalized $\log_{10}$-transformed blood levels (regression coefficient β) between case and control samples. We used the metabolite levels as continuous dependent variables and adjusted all regression models for potential confounding by age and sex (human) or the time of sacrifice (mouse; 8 weeks/10 weeks).

For each metabolite, the statistical significance of its estimated regression coefficient β is derived from a T-statistic:

$$t_\beta = \frac{\beta}{\sigma_n(\beta)} \tag{2.3}$$

where t_β corresponds to β, standardized by the model's standard error $\sigma_n(\beta)$.

All p-values were adjusted for multiple testing using conservative Bonferroni correction (FWER) and less stringent False Discovery Rate (FDR) [140].

2.6.3 Ranking differential gene expression and alterations in metabolite levels

For each case-control comparison in the murine models and human, we ranked the corresponding lists of gene expression and metabolic traits according to their $-\log_{10}$-transformed p-values multiplied by the sign of the $\log_2$ fold change (gene expression) or the regression coefficient β (metabolites):

$$r_i = -log_{10}(p_i) \cdot sign(\beta_i) \tag{2.4}$$

where r_i denotes the rank, p_i the p-value, and $sign(\beta_i)$ the effect direction of the i_{th} gene or metabolite.

Accordingly, genes or metabolites with the most significant increases are placed at the top of the ranked list, and those with the most significant decreases are placed at the bottom of the ranking. In the middle of the ranked lists are gene expression or metabolic traits with small or zero effects.

2.6.4 Determining the global similarities of differential gene expression or metabolic traits between strains or species using correlation

We calculated the six pairwise correlations between the four strains of NAFLD (129, B6J, B6N, C3H) based on their gene expression traits, as well as the three pairwise correlations between the human study groups (od, oh, lh) and the db/db model based on their metabolic traits. To avoid an overestimation by the false assumption that gene expression changes and differences in metabolite levels are normally distributed, we calculated non-parametric Spearman's rank correlation on the estimated effects.

As measures of effect size, we used the $\log_2$ fold changes of the means for mRNA expression data and the standardized regression coefficients (Equation 2.3) for the metabolomics measurements. To visualize the general agreement of the estimated effects on gene transcription across strains or metabolite levels between species, we generated scatter plots contrasting the estimated effects of one against the other study.

2.6.5 Determining the global similarities of differential gene expression or metabolic traits between strains or species using a weighted sum on ranked lists

Yang et al. introduced a measure to determine the similarity of ranked lists of gene expression traits [141]. The authors claim that their measure regards the nature of the studies of interest, considering only ›biologically relevant‹ traits for their comparison. To this end, the authors calculated a weighted sum of overlapping up- and down-regulated genes at each rank, putting more weight on the most up- and down-regulated genes. Although designed for microarray studies, this method for comparing ranked lists can be applied to results from other differential analyses [141].

The method compares two studies A and B based on the results of the differential analyses, which are summarized in two lists $L_A = \{a_1, \ldots, a_n\}$ and $L_B = \{b_1, \ldots, b_n\}$. Here, each of the two lists contains the names of the n molecules (e.g. gene names, metabolite names) measured in both studies and is ranked by the estimated effects (Methods 2.6.3, Equation 2.7) on the individual molecules. Given the ranked lists L_A and L_B, the partial overlap $O(i)$ between their i top and i bottom ranked molecules is defined by:

$$O(i) = |\{a_1, \ldots, a_i\} \cup \{b_1, \ldots, b_i\}| + |\{a_{n-i}, \ldots, a_n\} \cup \{b_{n-i}, \ldots, b_n\}|. \tag{2.5}$$

The final similarity score between studies A and B based on their ranked lists of results is the weighted sum of all partial overlaps, which is calculated as follows:

$$S = \sum_{j=1}^{n} w_j \cdot O(j),\ j \in \{1, \ldots, n\}. \tag{2.6}$$

Here, w_j denotes the rank-dependent weight at rank j. The weighting function w_j is defined as:

$$w_j = e^{-\alpha \cdot j},\ j \in \{1,\ldots,n\} \tag{2.7}$$

where α is a tuning parameter which has to be individually tuned for each comparison.

The tuning parameter α determines not only how much weight is put on the top and bottom ranks in the calculation of the overall score, but also how many genes or metabolites are used to determine the similarity between two ranked lists because the weights decay exponentially and approach zero with increasing ranks (Equation 2.7). For choices of large α, only the top ranking up- and down-regulated molecules are considered for the comparison of the ranked lists, whereas for choices of small α, more and more molecules up to the middle of the ranked lists are considered to be ›biologically relevant‹.

Instead of arbitrarily choosing an α, we searched for an optimal choice of α by resampling as described in [141]. To this end, we used the orignial datasets (gene expression intensities, metabolite levels) of studies A and B. From these datasets, k random subsamples were drawn so that each subsample contained 80% cases and controls from each study. For each of the k subsamples, the differential analyses were done and the ranked lists generated. As a result, we obtained two sets, each containing k ranked lists, one set for the results based on the subsamples from study A, and one for those based on the subsamples of study B. Then, the similarity scores for all pairs of ranked lists from both sets were calculated, which gave us a list of k similarity scores $S_s = \{s_{s_1},\ldots,s_{s_k}\}$ (signal). To get an estimate for random similarity scores for studies A and B, the complete resampling procedure was done on another k subsamples. In this run, however, the class labels within the datasets of study A and study B were shuffled beforehand. As a result, we obtained a second list $S_n = \{s_{n_1},\ldots,s_{n_k}\}$ of k random similarity scores calculated on noise.

The resampling was done for l different choices of α. To determine an optimal choice of α for the comparison of studies A and B, we calculated the Partial Area Under the Curve (pAUC) score, which measures the ›separability‹ of signal and noise scores. The pAUC for one particular $\alpha \in \{\alpha_1, \ldots, \alpha_l\}$ is the integral of the corresponding Receiver Operating Characteristic (ROC) function for this α over a given range:

$$pAUC_\alpha(t_0,t_1) = \int_{t_0}^{t_1} ROC(t)\,\mathrm{d}t,\ t_0,t_1 \in [0,1] \tag{2.8}$$

where the ROC function is defined by the True Positive Rate (TPR) and the False Positive Rate (FPR):

$$TPR(t) = \frac{|\{s_s \in S_s | s_s \geq t\}|}{k} \tag{2.9}$$

$$FPR(t) = \frac{|\{s_n \in S_n | s_n \geq t\}|}{k},\ t \in S_t, S_t = \{s_s \in S_s \vee s_n \in S_n\}. \tag{2.10}$$

Here, k = 1,000 resamples were drawn for each choice of α, i.e. 1,000 subsamples from the original data and 1,000 subsamples from the data with shuffled class labels. For the pairwise comparisons of the four mouse models of NAFLD (129, B6J, B6N, C3H), we specified a set of 20 α so that in each case, the 25 to 500 top and bottom ranked genes (i.e. 50 to 1,000 ranks in total) were considered. For the comparison of the changes in metabolite levels in humans and in the db/db mouse model, we specified a set of 30 α, considering the 5 to 150 top and bottom ranked metabolites (that is 10 to 300 ranks in total). According to Yang et al. [141], the α whose ROC function achieves the greatest pAUC score for FPR values from 0 to 0.1 was chosen as the optimal tuning parameter for the respective comparison.

The statistical significance for the final similarity score for two lists was empirically determined using 1,000 random rankings of these lists.

2.6.6 Examining local overlaps of differential gene expression or metabolic traits between strains or species using the rank-rank hypergeometric overlap

To examine local overlaps of ranked gene expression changes among the four NAFLD mouse strains or of ranked changes in metabolite levels between humans and the db/db mouse model, which in contrast to the weighted sum approach are not limited to the top- and bottom-ranks, we applied the Rank-Rank Hypergeometric Overlap (RRHO) method. Here, the optimized implementation of the RRHO method [142] was used.

In brief, given two studies A and B with the results of the differential analyses summarized in lists $L_A = \{a_1, \ldots, a_n\}$ and $L_B = \{b_1, \ldots, b_n\}$, respectively. Here, L_A and L_B contain the names of the n molecules (e.g. gene names or metabolites) measured in both studies, ranked by the individual effects (Methods 2.6.3, Equation 2.7). For each combination of $i,j \in \{1, \ldots, n\}$, the RRHO determines the over- or under-representation of overlapping molecules within subset L_{A_i} up to rank i in L_A and L_{B_j} up to rank j in L_B. The statistical significance for observing an overlap of size k between L_{A_i} and L_{B_j} is given by the hypergeometric probability distribution:

$$h(k; i, j, n) = \frac{\binom{j}{k}\binom{n-j}{i-k}}{\binom{n}{i}},\ i,j \in \{1, \ldots, n\} \tag{2.11}$$

where k denotes the number of overlapping molecules between the subsections of L_A and L_B given the current rank combination (success in sample). Because the hypergeometric probability distribution is symmetric, an over-representation between L_A up to rank i and L_B up to rank j is equivalent to an under-representation between L_A up to rank i and L_B from rank j downwards.

Plotting the $-\log_{10}$-transformed hypergeometric p-values for all combinations of i,j in a heatmap for example, different types of overlap between studies such as full correlation or partial overlaps can be revealed, where the overlaps with the smallest hypergeometric p-values can be used as an estimate for the total accordance between results from study A and study B [142].

Note that the actual computation of the hypergeometric p-values was done on binned data, meaning that not every combination of i,j was tested. Instead, bins of size $n \cdot 10^{-2}$ were used for the computation of the RRHO, with n denoting the total number of genes (22,030) or measured metabolites (319).

2.6.7 Selection of joint and disjoint metabolic changes in humans and db/db mice

To dissect the changes in the blood metabolomes of humans and db/db mice with T2DM and obesity in more detail, we defined sets of joint and disjoint metabolic changes based on their effect directions and statistical significance.

Generally, we distinguished between joint and disjoint metabolic effects. Metabolites that reached statistical significance after Bonferroni correction ($\alpha = 5\%$) in humans and the db/db model were, irrespective of their effect direction, regarded as jointly affected in both species. Moreover, to include also borderline cases, we considered metabolites that meet the Bonferroni criterion ($\alpha = 5\%$) in one, and the less stringent FDR $< 1\%$ in the other study also to be jointly affected. Correspondingly, metabolites with p-values below 0.05 after Bonferroni correction in human and FDR greater than 1% in the db/db mouse model and vice versa were regarded to be distinctly affected in humans or mice.

We further distinguished the sets of joint effects into metabolites which changed in the same direction (e.g. metabolites whose levels are increased in od humans and db/db mice) and those changing into different directions (i.e. metabolites whose levels are increased in od humans but decreased in db/db mice and vice versa).

Note that metabolites which were measured more than once (Table 2.3) were considered as jointly affected in human and mouse if one of the individual metabolic measures met the selection criterion.

Chapter 3

Comparative transcriptomics in four mouse models of diet-induced non-alcoholic fatty-liver disease: universal and unique Adaptions in their genetic responses

This chapter bases on a collaboration with the Institute of Experimental Genetics of the Helmholtz Center Munich. The goal of this cooperation was the deep phenotypic comparison of four genetically heterogenous mouse models commonly used for the study of NAFLD to determine similarities and strain specific phenotypic features under highly standardized conditions. In this context, I contributed to the interpretation of the liver transcript signatures including the preprocessing of the measured messenger RNA (mRNA) microarrays, their differential anaylsis and the set-based meta-analysis of differentially expressed genes across strains. The results of this study were published in Kahle et al. [132].

In addition, I performed a comprehensive meta-analysis of the transcript signatures measured in this collaborative study that goes beyond the simple set-based comparison of significant results as presented in the publication. Here, I developed a generic workflow for the comparative analysis of the genomic repsonses in the different mouse strains. In contrast to established meta-analysis workflows, this workflow

combines correlation analysis with rank-based statistics and set-based meta-analysis methods to characterize similarities and differences between studies in an unbiased fashion, covering several levels of detail, starting at the global level (correlation, rank-based statistics) and ending up with the comparison of single transcripts (rank-based, set-based). Most imporantly, I aimed to avoid assumptions that hamper the transfer of the workflow to other scenarios, i.e. other studies, data types or even species. As a result, I was able to use this workflow for the cross-species comparison of metabolic signatures between human and mouse as presented in Chapter 4.

In the following, I introduce the generic meta-analysis workflow and examplify its application to mRNA microarray profiles measured in the liver from the four different mouse models of NAFLD, and discuss its potential for the comprehensive comparison of these mouse models on the molecular level based on their genomic repsonses.

3.1 Research Design

To estimate the reproducibility of genetic responses across different mouse strains, I investigated the transcriptomic profiles from four genetically heterogenous mouse strains for the study of NAFLD. The study was based on a total number of 72 liver samples from 129, B6J, B6N, and C3H mice: 30 animals exposed for 21 days to a HFD to induce the NAFLD phenotype and 42 control animals fed a LFD. All samples were phenotypically characterized using key parameters of clinical chemistry and histological stains. In addition, in each liver sample, the expression levels of 22,030 genes were measured using mRNA micro arrays. The relative expression changes (›gene expression traits‹) of these genes were determined between HFD and LFD groups by differential analysis for each of the four mouse strains separately.

Based on the results of the differential analyses between HFD and LFD groups within each model, for each pairwise comparison between the four models, I examined the overall agreement of changes in the genes' expression in response to the HFD induced NAFLD phenotype. To estimate the global agreement between the models' responses,

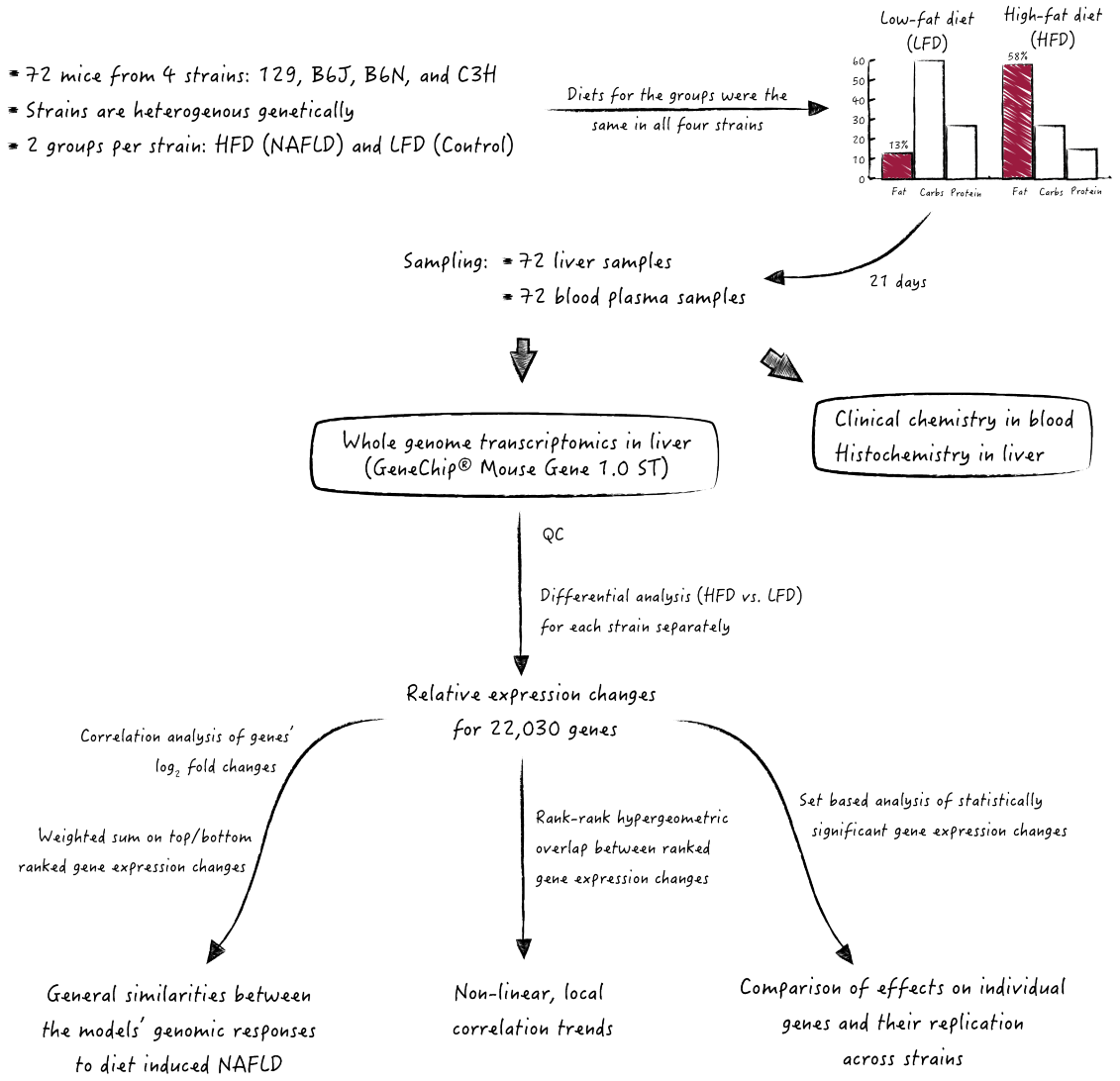

Figure 3.1 – Schematic workflow of the comparison of the transcriptomic responses in response to diet induced NAFLD in livers of 129, B6J, B6N, and C3H mice.

I used correlation analysis and calculated the weighted sum on the ranked results. To detect non-linear and local correlation trends, I used the RRHO hypergeometric overlap statistic. Finally, to characterize the effects of NAFLD on the expression of individual genes and to determine how well these effects replicate across the four strains, I used a set-based approach.

3.2 Results

3.2.1 Phenotypic effects of HFD exposure

We measured anthropometric and clinical features to examine the phenotypic effects of the HFD and LFD on animals of each strain. Except for the strain 129, all control animals that were fed the LFD did not show significant differences in whole body mass and whole body fat mass between the start of the study and the time of sacrifice (Figure 3.2, A-B). LFD fed 129 mice gained both whole body mass and whole body fat mass over the survey. We observed a small increase of hepatic triacylglycerol concentrations (averaged over three timepoints in each study) in response to the LFD in control mice from all four strains, ranging from 1.5% to 2.5% in B6J and 129, respectively (Figure 3.2, C).

Without exception, the HFD fed mice displayed an increased body mass and whole body fat mass at the time of sampling as compared to the start of the study (Figure

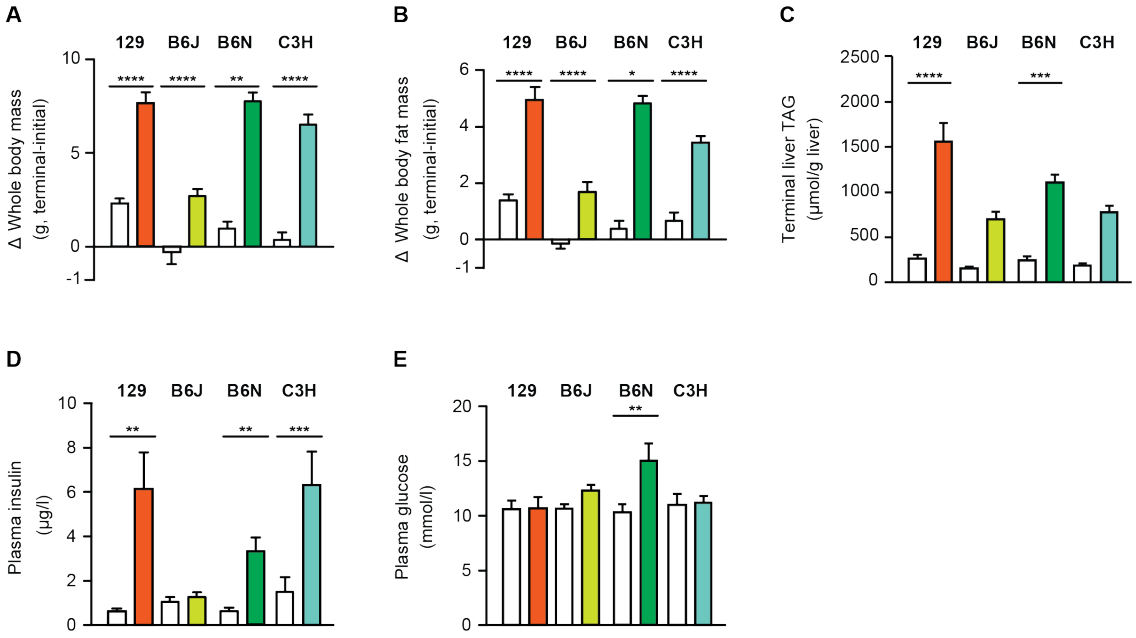

Figure 3.2 – Clinical chemistry of key parameters measured for all four models. Closed bars = HFD; Open bars = LFD; $^{*}P < 0.05$; $^{**}P < 0.01$; $^{***}P < 0.001$; $^{****}P < 0.0001$; Figure adopted from Kahle et al. [132].

3.2, A-B). Histological stains of liver tissue revealed that these increases in body mass and fat mass were paralleled by an extension of hepatic lipid-storage (Figure 3.2, C; Figure 3.3). In all four strains, body mass, whole body fat, and hepatic triacylglycerol concentrations were significantly higher in the HFD groups than in the LFD group (Figure 3.2, A-C).

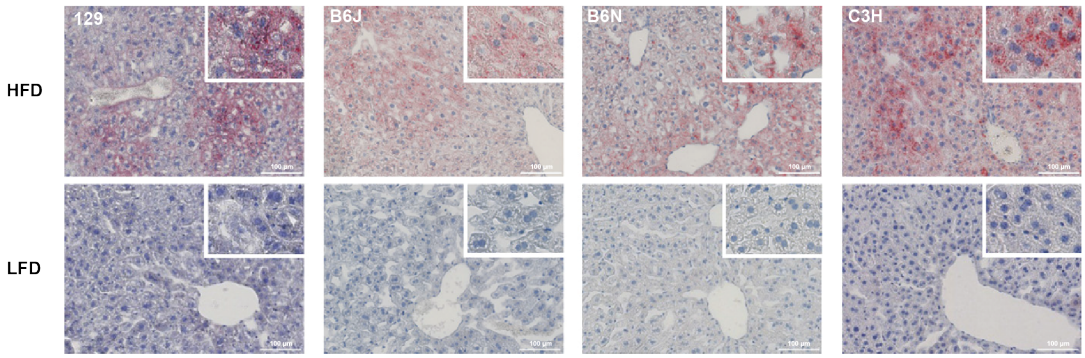

Figure 3.3 – Histological stains of liver tissue. Neutral lipid (red) in liver tissue of animals exposed to HFD (upper panel) or LFD (lower panel). Nuclei (blue) are visualized with hematoxilin. Shown are 20× and 100× magnifications. Figure adapted from Kahle et al. [132].

In strains 129, C3H, and to a lesser extend in B6N, we observed significant increases in plasma insulin concentrations between HFD and LFD samples (Figure 3.2, D). In contrast, in strain B6J the HFD did not significantly change the plasma insulin concentrations as compared to the LFD. In B6N, but not the other three models, the concentration of plasma glucose was significantly higher in HFD than in LFD samples (Figure 3.2, E).

3.2.2 Global accordance of differential gene expression across models

Pairwise correlations of the transcript signatures based on all 22,030 measured gene expression changes

To examine the agreement of the gene expression changes in the liver transcriptomes of the four mouse strains of NAFLD on the global level, I determined the pairwise cor-

relations over the relative expression changes ($\log_2$ fold changes) in the four strains. For each of the six pairwise comparisons between the strains 129, B6J, B6N, and C3H, the correlation over the changes in all 22,030 measured genes is significant (Methods 2.6.4). The comparisons B6J×B6N, 129×B6J, and B6N×C3H reveal significant pairwise correlations greater than 0.2. In contrast, for 129×B6N and 129×C3H the correlations are below 0.1 (Figure 3.4), indicating slightly smaller overall similarities between these strains.

Pairwise correlations of transcript signatures based on ›responding‹ genes

To verify whether the similarity across the four mouse strains is greater for ›responding‹ genes that change in response to NAFLD than for all 22,030 genes, I constrained the individual datasets to genes with absolute linear fold changes greater than 1.3 between the HFD and the LFD group and repeated the correlation analysis. Considering only responding genes, the correlations of the gene expression changes improved for all six pairwise comparisons between models (Figure 3.5). I found strong and significant correlations for the pairwise comparisons of strains 129, B6J, and B6N ($r = 0.84$-0.87; p-values < 0.001), whereof the two closely related strains B6J and B6N featured the highest correlation ($r = 0.87$; p-value < 0.001). In contrast, the correlations of C3H versus the other three strains were smaller, with 129×C3H correlating the least ($r = 0.21$). In C3H, the expression of many genes changed to the opposite direction in response to the HFD exposure as compared to the other three strains (Figure 3.5, quadrants II and IV).

Hierarchical clustering (Manhattan distance, Ward's method) of the four strains based on their gene expression changes in response to the HFD (absolute linear fold change greater than 1.3) illustrates the high similarity between the strains B6J, B6N, and 129, while the $\log_2$ fold changes of the genes' expression in strain C3H appear to be different (Figure 3.6).

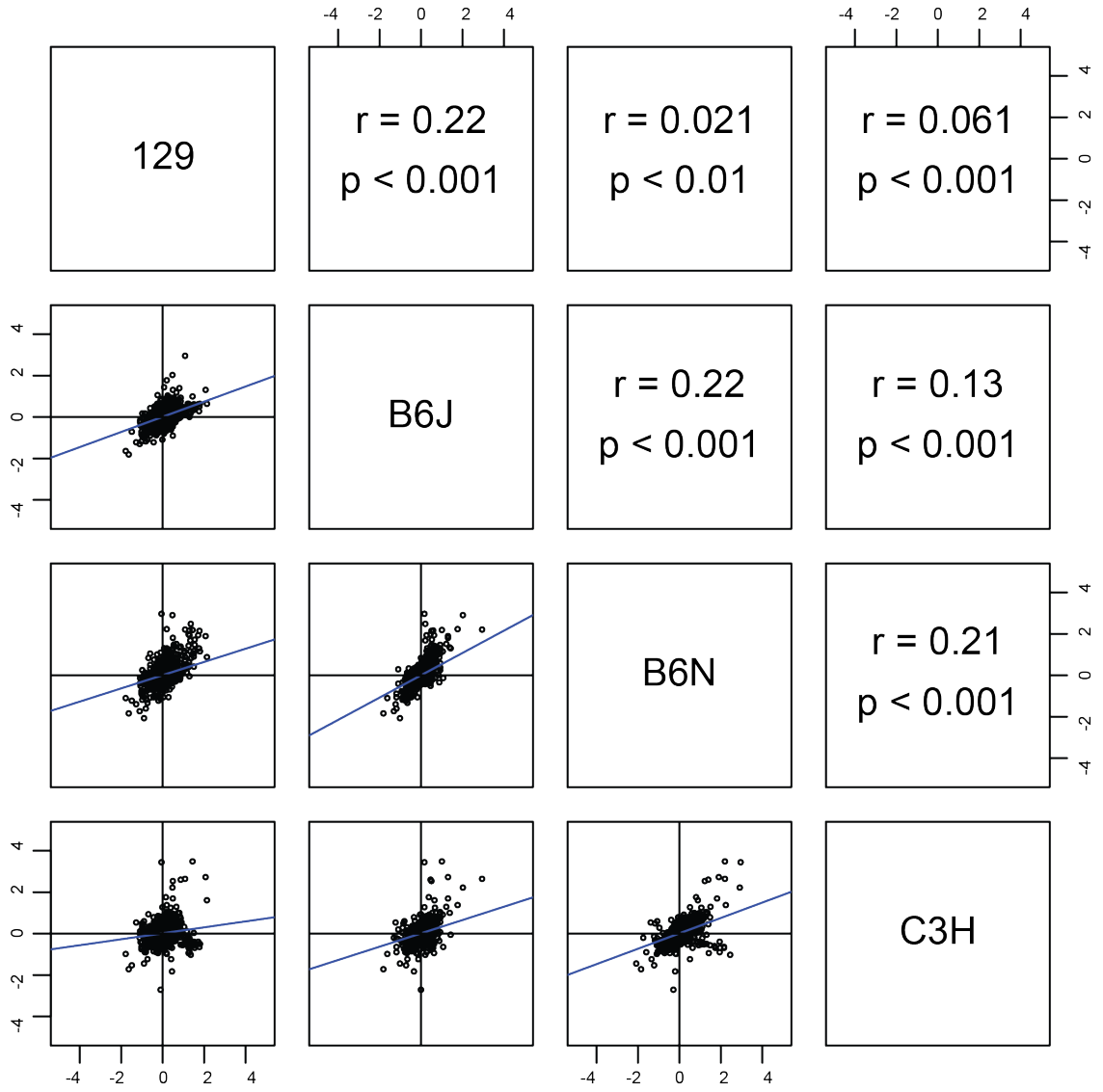

Figure 3.4 – General similarity of gene expression changes between HFD and LFD groups in the four models of NAFLD. Scatterplots and correlation coefficients r (Spearman correlation) of the gene's $\log_2$ fold changes) are plotted for each pairwise comparison between the four mouse strains 129, B6J, B6N, and C3H. Regression lines are depicted in blue.

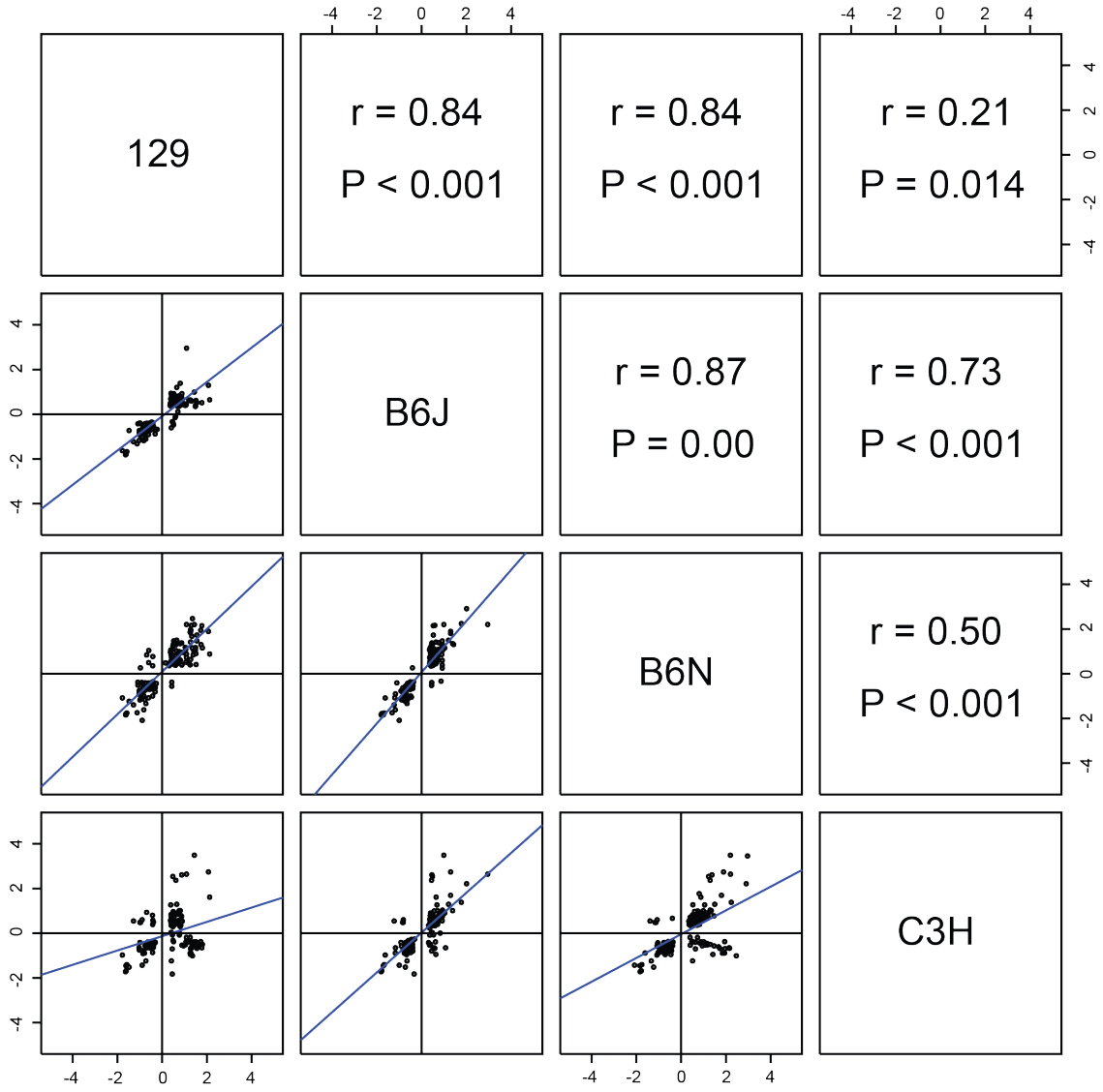

Figure 3.5 – General similarity of expression changes in responsive genes between HFD and LFD groups in the four models of NAFLD. Considering only responsive genes with absolute linear fold changes greater than 1.3, scatterplots and correlation coefficients r (Spearman) of the gene's $\log_2$ fold changes) are plotted for each pairwise comparison between the four mouse strains 129, B6J, B6N, and C3H. Regression lines are depicted in blue.

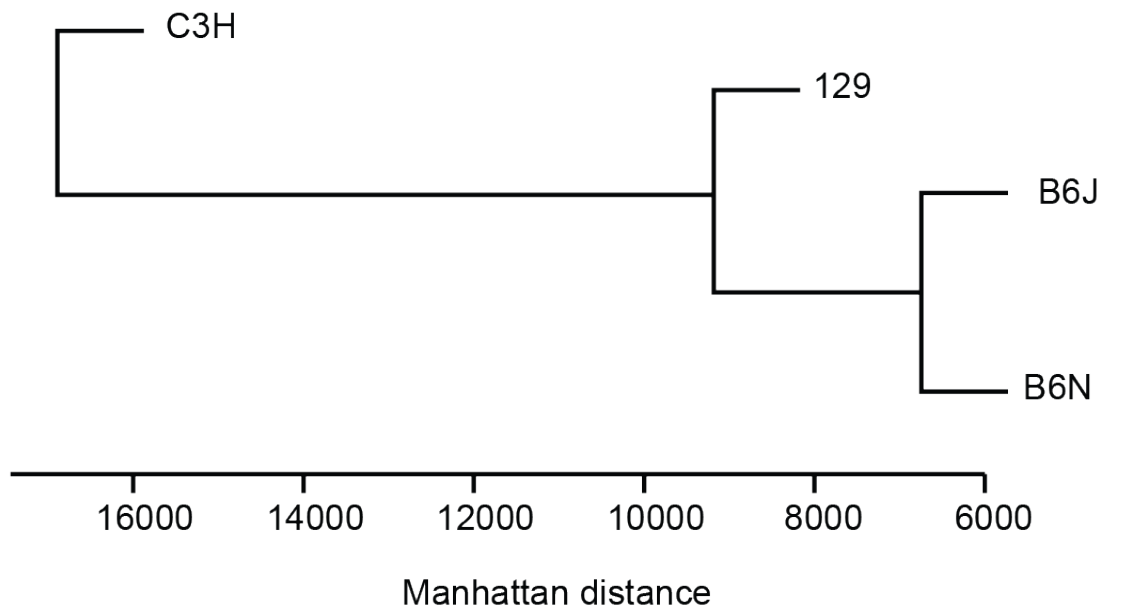

Figure 3.6 – Hierarchical clustering of models of Non-Alcoholic Steatohepatitis (NASH). For each study pair, the Manhattan distances between the $\log_2$ fold changes of the genes' expression with absolute linear fold changes greater than 1.3 were calculated and subsequently clustered using Ward's method.

Global similarity of transcript signatures in terms of the weighted-sum rank-based statistic

Correlating the effect sizes ($\log_2$ fold changes, cf. Methods 2.6.4) across independent studies is either sensitive to non-responding genes with small changes in their expression or subject to selection bias when defining an arbitrary cut-off to exclude these non-responding genes. In my workflow for comparative omics analysis, I address this issue by applying additional ranked-based statistics to determine the similarity of gene expression changes in response to the HFD induced NAFLD phenotypes in the four mouse models.

For each strain, I ranked the 22,030 genes according to their $-\log_{10}$-transformed p-value from the differential analysis multiplied by the sign of the $\log_2$ fold change (Methods 2.6.3). Based on these ranked lists of gene expression changes, I calculated for the six pairwise comparisons between the strains 129, B6J, B6N, and C3H the weighted sum measure (Methods 2.6.5). Here, the tuning parameter α determines the

number of ›biologically relevant‹ genes that are considered for the calculation of the similarity of the individual study pairs. For each comparison, the weighted sums for the same 20 choices of α were calculated, so that between 25 and 500 top and bottom ranked gene expression changes were considered to determine the similarity between strains. For all choices of α, the weighted sums for the six pairwise comparisons were significant (p-values < 0.01). Although all models showed significant pairwise overlaps among the ranked gene expression changes, I found substantial differences in the mean similarity scores of the individual comparisons. On average, the ranked gene expression traits displayed the smallest similarity scores for the comparisons of 129×C3H and 129×B6N, while the comparison of B6J×B6N achieved the greatest weighted sum (Table 3.1).

Table 3.1 – Weighted sum over top ranked gene expression traits

# Genes	129×B6J	129×B6N	129×C3H	B6J×B6N	B6J×C3H	B6N×C3H
⋮	⋮	⋮	⋮	⋮	⋮	⋮
425	660.31	592.15	516.21	1267.51	808.51	1166.22
450	740.28	661.95	578.31	1416.03	914.26	1313.46
475	824.43	734.94	643.29	1571.50	1025.69	1468.60
500	912.72	811.05	711.10	1733.75	1142.67	1631.49
Mean score	323.55	289.08	249.84	626.44	382.66	564.09

Empirical P-Value = 0 for all scores.

To select an optimal tuning parameter α for each comparison, I resampled the underlying gene expression data and the same data with randomized group labels (HFD, LFD) 1,000 times. From the 20 choices of α, I chose the one which achieved the best separation between similarity scores calculated from the 1,000 subsamples drawn from the original datasets (signal) and those calculated from the 1,000 subsamples drawn from the datasets with randomized class labels (noise). The pAUC score (Methods 2.6.5) was used as a measure of separability. For all comparisons, $\alpha = 0.023$ achieved the largest pAUC score, i.e. results in the best possible separation between signal and noise scores, considering the top and bottom 500 gene expression traits. Based on this choice of α, strain 129 shows the smallest similarity to the three other models (weighted sums 711-913), while with 1,631 and 1,734, the weighted

sums were almost twice as large for the comparisons of B6N×C3H and B6J×B6N, respectively (Table 3.1).

Local correlation patterns between transcript signatures

Both correlation analysis and the weighted sum approach determine similarity based on all effects or those with the highest ranks but do not consider local correlation trends. To identify and visualize such local patterns of similarity between two strains, I calculated the RRHO for all pairwise comparisons of the strains (Figure 3.7). Given two lists of ranked gene expression changes (Methods 2.6.3), the RRHO determines the over- or under-representation of common genes between both lists, where the combination of two rank thresholds i and j (one for each list) limits the comparison up to rank i in the first list and up to j in the second list. The RRHO is calculated for all possible rank combinations. Because the lengths of the individual ranked lists are identical for all strains, the results from the RRHO can be directly related to each other.

I found significant overlaps of gene expression changes for all pairwise comparisons. In the case of the comparisons of 129×B6J, B6J×B6N, and B6N×C3H, the ranked lists of gene expression changes overlapped in large parts. For the comparisons of 129×B6N, 129×C3H, and B6J×C3H, the overlaps between the ranked lists were smaller. In particular, for the comparisons of 129×B6N and 129×C3H the overlap was rather limited to the top and bottom ranked gene expression changes (Figure 3.7).

Considering ›up-regulated‹ genes whose expression is higher in HFD than LFD mice and which are ranked at the tops of the ranked lists, B6N and C3H displayed the greatest similarity, i.e. the most significant enrichment for common gene expression changes (p-value = 2.19×10^{-186}). Of 273 top up-regulated genes in each of the two studies, the strains B6N and C3H had 175 in common (Figure 3.8). For the comparison of B6J×B6N the most significant enrichment was found for 319 common genes (p-value = 3.84×10^{-154}) which are shared between the 1,789 and 746 top ranked up-regulated genes in B6J and B6N, respectively. In terms of the number of

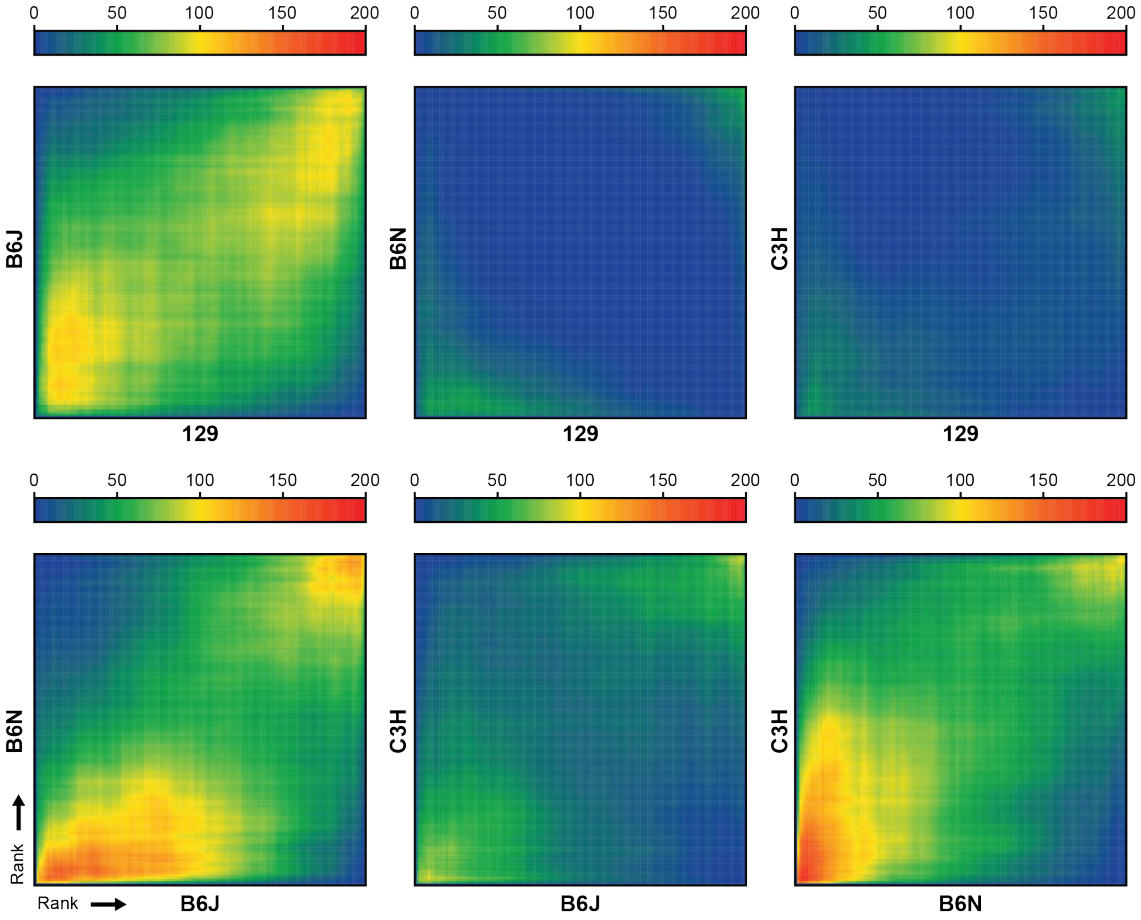

Figure 3.7 – Pairwise local overlaps of gene-expression changes. Heatmaps of hypergeometric p-values (-$\log_{10}$) for each rank combination between study pairs (x- and y-axes).

shared genes, I found the greatest similarity between the strains 129 and B6J, which share 475 up-regulated genes (p-value = 2.54×10^{-111}). The remaining comparisons (129×B6N, 129×C3H, and B6J×C3H) display less significant enrichments of common up-regulated genes (p-value = 7.6×10^{-46}-1.61×10^{-52}).

Among ›down-regulated‹ genes (i.e. genes whose expression is higher in the LFD than HFD groups) which are ranked at the bottoms of the ranked lists, strains B6J and B6N show the greatest similarity (overlap 209; p-value = 3.04×10^{-134}). In terms of the number of common down-regulated genes, strains 129 and B6J show the largest agreement (overlap 306; p-value = 5.73×10^{-106}) again. For the comparisons of 129×B6N and 129×C3H, the sizes of enriched sets of shared genes are smaller (overlap

45-81) and less significant (p-value = 2.42×10^{-47}-2.56×10^{-55}) as compared to the RRHO between the remaining strains.

3.2.3 Shared and species-specific gene expression traits

This part of my workflow was the basis of the comparative transcriptomic analysis published in Kahle et al. [132].

Differential analysis to define sets of statistically significant gene expression changes within each strain

In addition to general similarities across the genomic responses of the four mouse models in response to the HFD induced NAFLD phenotype, I studied the individual gene expression changes in more detail. In particular, I looked into the individual genetic responses of each strain and searched for patterns which are common to all four strains, some but not all strains, or wich are strain-specific. To this end, I defined sets of statistically significantly changed genes between the HFD and LFD groups in each strain by filtering the 22,030 measured genes for responding genes, i.e. genes with absolute linear fold changes greater than 1.3) for each strain separately. As a result, I obtained four sets of responding genes, one for each strain. For each of these sets separately, the moderated t-statistic was calculated on the $\log_2$ fold changes of the individual genes to determine the statistical significance of their changes of expression.

Among the four strains, with 87 significantly affected genes (Bonferroni adjusted p-value, $\alpha = 5\%$) B6N displays the most changes between the HFD and LFD group (Figure 3.9). In strains C3H and B6J, 76 and 49 genes are differentially expressed, respectively. Strain 129 showed the fewest changes. Here, the expression of 15 genes is significantly altered in the livers of mice after 21 days of HFD exposure. In strain 129, 87% of the significantly altered genes are up-regulated (i.e. their expression is higher in HFD than LFD fed mice). By contrast, with 47% and 53%, respectively, the proportions of up- and down-regulated genes are almost the same. In turn, in strains

Figure 3.8 – Overlapping sets of top- and bottom-ranked gene expression traits which display the smallest hypergeometric p-values. For each pairwise comparison, the rank-rank combination achieving the smallest hypergeometric p-value is shown. Divided by top- and bottom-ranked gene expression traits.

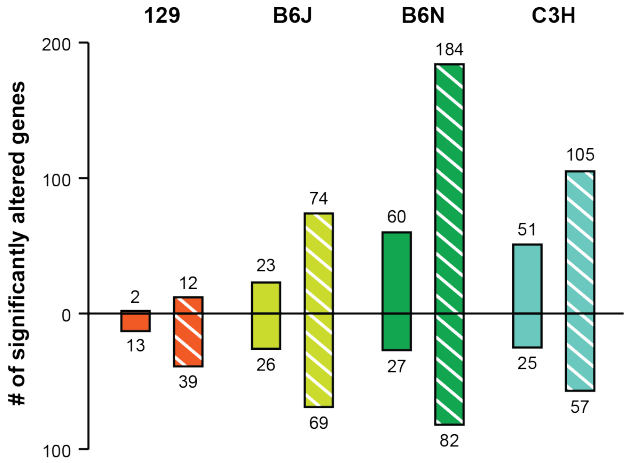

Figure 3.9 – Significantly altered genes in the livers of HFD treated mice. The number of significantly up- and down-regulated genes (y-axis) in each strain, according to conservative Bonferroni correction ($\alpha = 5\%$; filled bars) and less stringent FDR (FDR $< 1\%$; shaded bars).

B6N and C3H more genes are up-regulated than down-regulated in mice exposed to the HFD than in those exposed to the LFD (Figure 3.9).

To find out whether the individual genetic responses to the HFD induced NAFLD phenotype are enriched for genes involved in specific metabolic pathways, I examined the sets of significantly altered genes for overrepresentation of genes involved in the same metabolic pathways (KEGG) for each of the four strains separately. The KEGG pathways ›drug metabolism‹ (12.2-53.6 fold; p-value $= 4.99 \times 10^{-4}$-3.99×10^{-14}) and ›metabolism of xenobiotics by cytochrome P450‹ (13.8-60.9 fold; p-value $= 3.05 \times 10^{-4}$-5.01×10^{-13}) both were enriched in all four strains (Figure 3.10). Some strains showed also enrichment in closely related pathways including ›retinol metabolism‹ (B6J and B6N), ›glutathione metabolism‹, or ›linolenic acid metabolism‹ (129 and B6J). In strains B6J and C3H, but not 129 or B6J, genes involved in ›fatty acid metabolism‹ and ›PPAR signalling pathway‹ were also significantly overrepresented. In B6N, three more pathways related to fatty acid metabolism and PPAR signalling were enriched (Figure 3.10).

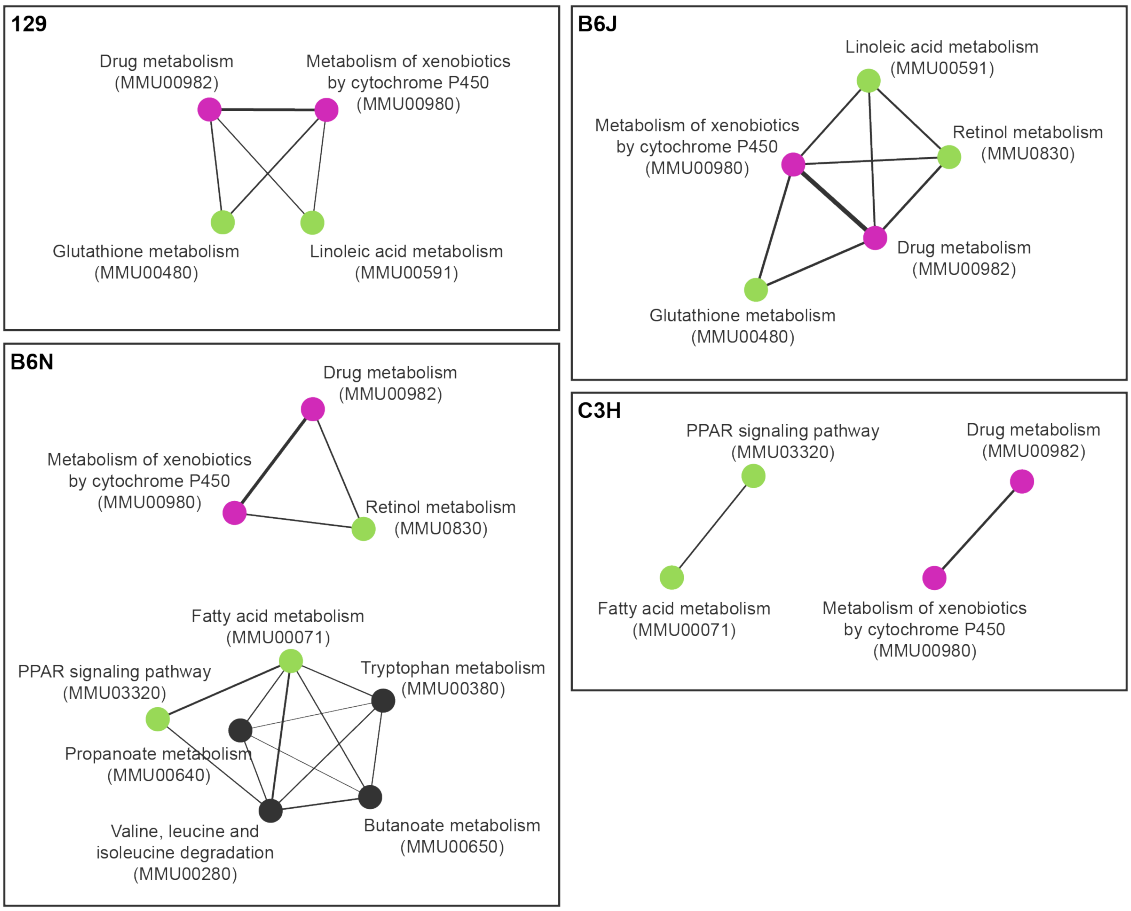

Figure 3.10 – Enrichment maps of significantly altered genes in the four strains. Circles indicate enriched pathways (FDR $< 1\%$) among the sets of differentially expressed genes. Edges between circles indicate the pairwise overlap of enriched genes within two pathways, with thick edges corresponding to greater overlap than thin edges. Some pathways show enrichment in all four strains (purple), some in two (green), and some are only enriched in one strain (black).

Replication of significant gene expression changes across strains

To determine which genes were similarly altered in more than one strain, I selected significantly expressed genes (Bonferroni adjusted p-value; $\alpha = 5\%$) with unadjusted p-values below 0.05 in the remaining strains (Methods 2.6.7); this way, I created sets of joint and disjoint gene expression changes.

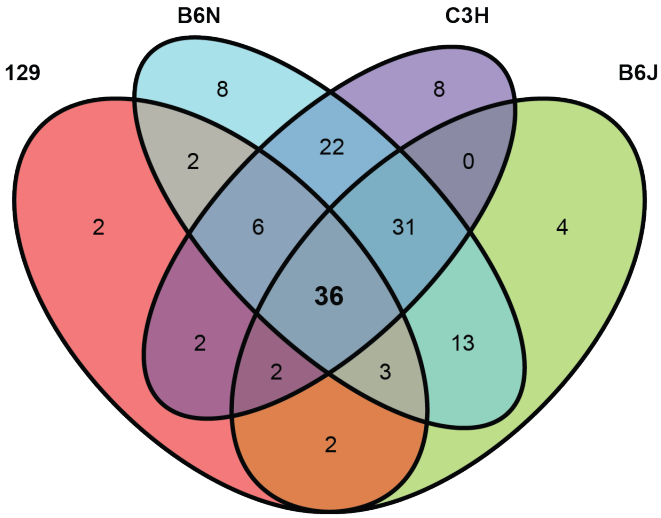

Figure 3.11 – Overlapping gene expression traits that are significantly associated with the HFD exposure. Out of 22,030 initially measured genes, 95 are significantly affected in at least one of the four models of NASH. Of these genes, 16 change significantly between HFD and LFD groups in all four strains.

Out of the 22,030 initially measured genes, a total of 141 genes were differentially expressed between the HFD and LFD groups in at least 1 out of 4 strains. Among these, the results of 36 genes replicated in the remaining strains, i.e. these genes were ›jointly affected‹ in all 4 mouse strains (Figure 3.11). The remaining gene expression traits were either shared between three or two, but not all strains. Out of 141 genes which were differentially expressed in 1 strain, 42 replicate in another 2 strains; 19 genes replicate in one more strain; finally, 22 genes did not replicate in any other strain, i.e. these genes are significantly affected in one strain but not in all the others.

Looking for over- or under-represented genes involved in the same metabolic pathways among the 36 genes whose expression was jointly altered in all four strains, I found that they were enriched for genes from three closely related metabolic pathways (KEGG): ›metabolism of xenobiotics by cytochrome P450‹ (33.1 fold, p-value $= 1.33 \times 10^{-9}$), ›drug metabolism‹ (32.8 fold, p-value $= 6.46 \times 10^{-11}$), and ›glutathione metabolism‹ (26.3 fold, p-value $= 2.61 \times 10^{-5}$); thereof, ›metabolism of xenobiotics by cytochrome P450‹ and ›drug metabolism‹ were enriched among

the individual lists of significantly affected genes in all four strains (see Figure 3.10).

Except for the cytochromes Cyp3a44, Cyp3a11, and Cyp3a41a, 33 out of 36 jointly affected genes changed to the same direction in all four strains (Figure 3.2). While Cyp3a44, Cyp3a11, and Cyp3a41a were down-regulated in strains 129, B6J and B6N, their expression was stimulated by the HFD induced NAFLD phenotype in C3H.

Table 3.2 – 36 genes that are significantly affected across all four strains.

Symbol	Name	Log_2 fold change 129 B6J B6N C3H
1810055G02Rik	RIKEN cDNA 1810055G02 gene	
9030619P08Rik	RIKEN cDNA 9030619P08 gene	
Aldh3a2	aldehyde dehydrogenase family 3, subfamily A2	
Dio1	deiodinase, iodothyronine, type I; similar to Dio1 protein	
Ech1	enoyl coenzyme A hydratase 1, peroxisomal	
Fabp2	fatty acid binding protein 2, intestinal	
Gpd2	glycerol phosphate dehydrogenase 2, mitochondrial	
Mfsd2a	major facilitator superfamily domain containing 2	
Mgll	monoglyceride lipase	
Paqr9	progestin and adipoQ receptor family member IX	
Pgm3	phosphoglucomutase 3	
Serpina7	serine (or cysteine) peptidase inhibitor, clade A (alpha-1 antiproteinase, antitrypsin), member 7	
Slc10a2	solute carrier family 10, member 2	
Stap1	signal transducing adaptor family member 1; similar to stem cell adaptor protein STAP-1	
Vnn1	vanin 1	
Acmsd	amino carboxymuconate semialdehyde decarboxylase	
Akr1c19	aldo-keto reductase family 1, member C19	
Car14	carbonic anhydrase 14	
Csad	cysteine sulfinic acid decarboxylase	
Cth	cystathionase (cystathionine gamma-lyase)	
Cyp2a5	cytochrome P450, family 2, subfamily a, polypeptide 21, pseudogene; cytochrome P450, family 2, subfamily a, polypeptide 5	
Ddc	dopa decarboxylase	
Ethe1	ethylmalonic encephalopathy 1	
Etnppl	ethanolamine phosphate phospholyase	
Gm2a	GM2 ganglioside activator protein	
Gm3601	predicted gene 3601	
Gsta2	glutathione S-transferase, alpha 2 (Yc2)	
Gsta4	glutathione S-transferase, alpha 4	
Gstm1	glutathione S-transferase, mu 1	
Gstm3	glutathione S-transferase, mu 3	
Gstm6	glutathione S-transferase, mu 6	
Slc13a2	solute carrier family 13 (sodium-dependent dicarboxylate transporter), member 2	
Urad	ureidoimidazoline (2-oxo-4-hydroxy-4-carboxy-5) decarboxylase	
Cyp3a11	cytochrome P450, family 3, subfamily a, polypeptide 11	
Cyp3a41a	cytochrome P450, family 3, subfamily a, polypeptide 41A; cytochrome P450, family 3, subfamily a, polypeptide 41B	
Cyp3a44	cytochrome P450, family 3, subfamily a, polypeptide 44	

Genes with significant results that replicate in all four strains. Genes involved in ›drug metabolism‹ and ›metabolism of xenobiotics by cytochrome p450‹ were significantly overrepresented (green).

Log_2 fold change

-2 0 2

3.3 Discussion

NAFLD and T2DM are closely related, with NAFLD often seen as an early manifestation of diabetes in the liver. Along with obesity and IFG, NAFLD is assumed to be a key factor of the metabolic syndrome, a collection of risk factors linked to T2DM. Targher et al. reported that in their study cohort, 70% of people with diabetes had also NAFLD [25]. It is clear that both genetic and environmental factors contribute to the disease's progress. In the NHGRI-EBI GWAS Catalog, nine NAFLD susceptibility loci are listed (www.ebi.ac.uk/gwas; state as of 07/2015). However, the disease's pathophysiology is not fully understood and the molecular mechanisms of NAFLD as well as its link to T2DM remain to be revealed.

A common approach to study the mechanisms of human diseases are functional studies in animal models, in particular mouse models. Several models in different mouse strains have been established for the study of NAFLD. For example, in 129, B6J, B6N, and C3H mice, HFD feeding results in phenotypes very similar to NAFLD. However, results obtained in one model are often irreproducible in other models. Besides different experimental conditions, the different genetic constitutions of strains is the main reason for that. In a collaborative study, comparing the HFD induced NAFLD phenotypes of the genetically heterogenous strains 129, B6J, B6N, and C3H under similar conditions, revealed slight differences in their phenotypes [132].

The key to understand these differences lies clearly in their unique molecular constitution. In this chapter, I took a first step to a systematic characterization of different mouse strains for NAFLD research based on their liver transcript signatures. Whole genome mRNA expression profiling in 72 liver samples of four genetically heterozygous inbred mouse strains (129, B6J, B6N, C3H), which are commonly used as models of NAFLD, enabled me to systematically assess the concordances and discordances of the genetic responses to HFD induced NAFLD across these strains.

HFD exposure causes significant gains of body weight and fat mass

After 21 days of HFD exposure, whole body mass and whole body fat mass was significantly increased in all four strains as compared to baseline levels (Figure 3.2, A-B). In comparison to the other three strains, B6J mice on the HFD gained less body weight and fat mass during the study. In B6J, but not the other strains, LFD fed mice displayed a slight reduction (1%) in their terminal body weights (Figure 3.2, A-B). Except for the strain B6J, the plasma insulin levels were significantly increased in the HFD groups as compared to the corresponding LFD controls (Figure 3.2, D). In strain B6J, and even more in strain B6N, the levels of circulating glucose were increased in the HFD group (Figure 3.2, E).

In all four strains, the gain of body weight that is parallelled by an increase of whole body fat mass reflects an increase of adipogenesis and lipogenesis in response to the HFD that appears to be smaller in B6J than in the other strains. Both adipogenesis and lipogenesis are insulin-dependent processes [143]. It is known that B6J mice are glucose intolerant, featuring decreased glucose-stimulated insulin secretion [144]. Toye et al. showed that the reason for that is a loss-of-function mutation in the gene coding for Nicotine amide-Nucleotide Transhydrogenase (Nnt), an enzyme involved in mitochondrial energy metabolism. Deletion and lower expression of the Nnt gene in B6J causes a relative decrease in insulin secretion and impaired glucose tolerance in comparison to other strains, where the gene expression of Nnt is higher [144]. Assuming that insulin stimulated adipogenesis is responsible for the weight gain under HFD exposure, it is likely that an impaired insulin secretion in B6J mice because of the Nnt mutation is responsible for the smaller terminal body weight and whole body fat mass among these mice.

HFD exposure manifests in different grades of hepatic steatosis

Hepatic Triacylglycerol (TAG) levels were raised in all four strains after 21 days of HFD exposure (Figure 3.2, C), clearly indicating increased lipid storage in their livers (›hepatic steatosis‹) – which is a hallmark of NAFLD. The bar-plot of the terminal

TAG levels roughly resemble the corresponding bar-plots of the whole body weight and whole body fat mass (Figure 3.2, A-C), suggesting a direct relationship between weight gain and the degree of lipid storage in the liver. In addition to differences in terminal levels of TAG, histological staining revealed that the appearance of hepatic steatosis differed among strains; while in strains 129 and C3H, the lipid vesicles in the liver were generally large, resembling a form of ›macrovesicular steatosis‹, B6J and B6N stored hepatic TAG in rather small lipid vesicles, which is comparable to ›microvesicular steatosis‹ (Figure 3.3).

Considering that the liver is insulin responsive and that hepatic fatty acid metabolism is affected by insulin action, I was surprised that, despite their low insulin secretion, HFD fed B6J mice showed similar increases of terminal TAG levels and signs of hepatic steatosis. There are mainly two sources of fatty acids for TAG synthesis in the liver: first, an increased de-novo lipogenesis in liver; and second, an increased uptake of circulating Nonesterified fatty acids (NEFAs) by the liver. Recently, Vatner et al. showed that with more than 60%, the greater part of hepatic TAG attributes to the esterification of circulating NEFAs taken up by the liver rather than fatty acids that are newly synthesized in de novo lipogenesis, accounting for less than 20% of hepatic TAG [145]. The authors further showed that, in contrast to de novo lipogenesis, esterification of available fatty acids is primarily dependent on substrate availability and not hepatic insulin action [145]. Such an insulin independent mechanism leading to TAG accumulation in liver would explain why, in comparison to the remaining three strains, B6J mice displayed similar increases in hepatic lipid storage despite smaller raises in insulin levels after 21 days of HFD exposure (Figure 3.2, D).

Pairwise correlations of gene expression changes are small across the four strains

After examining the phenotypic features of the HFD induced NAFLD phenotypes in the individual strains, I focussed on the genomic responses in their livers. To estimate the overall similarity of their genetic responses, I calculated Spearman's correlation coefficient on the $\log_2$ fold changes of all 22,030 measured genes for each pairwise comparison between strains: 129×B6J, 129×B6N, 129×C3H, B6J×B6N,

B6J×C3H, and B6N×C3H. Correlating the fold changes of all 22,030 measured genes, I found small but significant correlations (Spearman's rho 0.02-0.22; p-value < 0.01) for all six pairwise comparisons (Figure 3.4). Considering the close genetic relationship of the two C57/BL substrains B6J and B6N, I observed surprisingly small correlations between them.

Many points in the middle of the scatterplots that lie close to the origin indicate that many of the 22,030 expression changes between the HFD and LFD groups are negligible (i.e. their expression is likely to be not affected by the HFD induced NAFLD phenotype) and therefore irrelevant in our setting; hence, I assumed that correlating all gene expression changes (including those that do not change with the HFD induced NAFLD phenotype) underestimates the true similarity between the genomic responses.

There is a clear concordance among biologically relevant genes across strains

To obtain more realistic estimates, I constrained the comparison to genes that are ›biologically relevant‹ in the genetic response to the HFD induced NAFLD phenotype. To this end, I pursued two different strategies: first, I constrained the individual datasets to genes with a minimal absolute fold change of 1.3 between HFD and LFD groups and re-calculated the pairwise correlations (Spearman's correlation coefficient). Second, I calculated the weighted sum over the ranked gene expression changes for each pairwise comparison between the four strains.

Thresholding constrained the individual datasets to 561, 329, 436, and 341 genes in 129, B6J, B6N, and C3H, respectively (Table 2.2). Correlating the $\log_2$ fold changes of these biologically relevant genes across strains, the Spearman correlation coefficients became greater for all pairwise comparisons (Spearman's rho 0.50-0.87). Except for the comparisons of 129×C3H and B6J×C3H, the scatter-plots resemble almost diagonal patterns (Figure 3.5), indicating that changes of genes with linear fold changes greater than 1.3 are highly concordant across these strains.

In contrast to choosing an arbitrary threshold, the weighted sum approach dynamically choses an optimal weighting factor for each comparison by resampling. This

weighting parameter defines how many top- and bottom-ranked genes are considered for the calculation of the similarity between two strains, and how much weight each single rank contributes to the total sum (Methods 2.6.5); hence, the more similar the gene expression changes are between two studies, the more genes are considered for the calculation and the total weighted sum becomes larger. In our setting, the weighting parameters identified in the resampling procedures were identical for the six pairwise comparisons. In each case, the 500 top- and bottom-ranked gene expression changes were considered for the calculation of the corresponding weighted sums, suggesting that the genomic responses of all four strains are generally similar (Table 3.1).

Both varying correlation coefficients between the constrained datasets and differing weighted sums of the ranked gene expression changes suggest closer similarity between some strains than others. The two C57/BL substrains B6J and B6N achieve the highest and most significant correlation (Spearman's rho = 0.87) and the greatest total weighted sum (weighted sum of the top and bottom 500 genes, 1,734); thus, in terms of their genetic responses to the HFD induced NAFLD, the strains B6J and B6N seem to be the most similar among all four strains. In line with that, contrasting their $\log_2$ fold changes reveals an almost diagonal pattern (Figure 3.5), with few genes responding in both strains but changing to different directions in the individual strains. Considering their common parental strain (C57/BL), it is not surprising that B6J and B6N are closest in terms of their genomic responses in the liver in response to the HFD induced NAFLD phenotype. In contrast to that, the constrained fold changes in 129 and C3H correlate weakly (Spearman's rho = 0.21), and the weighted sum of their ranked gene expression changes is smaller (711) than those of the remaining comparisons (Table 3.1). It appears that many genes with greater fold changes in strain 129 are much less affected in strain C3H, and vice versa (Figure 3.5); moreover, many genes change to opposite directions in 129 and C3H, which explains the small correlation between these two strains. Similarly, genes with such contrary effects lie at the opposite ends of the ranked lists and reduce the total score of the weighted sum approach. Based on these results, it appears that, among all four strains, 129 and C3H have the least in common in terms of their genomic responses to the HFD induced NAFLD.

While the results for the comparisons of B6J×B6N and 129×C3H were in line, the results for the remaining comparison are slightly different for the correlation and the weighted sum approach. Correlation coefficients between the constrained gene expression changes suggest that the NAFLD related gene expression changes in the liver of strains B6J, B6N, and 129 are more similar as compared to the genomic response in C3H (Figure 3.5). Clustering the pairwise distances between the $\log_2$ fold changes (hierarchical clustering, Ward's method; Manhattan distance) emphasizes this observation, with B6J and B6N clustering closely together, 129 clustering nearby, and C3H being more distant to the other three strains (Figure 3.6). In contrast to that, calculating the weighted sums of the 500 top- and bottom-ranked gene expression changes suggests that the genomic responses in the liver of strains B6J and B6N are more similar to C3H than to 129. In particular, the strains B6N and C3H achieve the second highest sum among all six comparisons (weighted sum 1,631), indicating that they share a considerable overlap among the 500 top- and bottom-ranked gene expression changes, which is not evident from the correlation results.

However, it is difficult to directly compare the results from the correlation analysis with those of the weighted sum approach. For instance, other than the correlation approach that works on the constrained datasets of different sizes, the weighted sum approach initially considers the gene expression changes of all 22,030 measured genes to determine an optimal weighting parameter; as a result, in any case the 500 top- and bottom-ranked gene expression changes (i.e. 1,000 in total) are considered to calculate the weighted sums between the strains. Another factor relating to different results may be the choice of fold change cut-off used for the correlation analysis. Because a generally valid fold change cutoff that discriminates responding from non-responding genes does not exist, the choice of threshold (here: 1.3) is always arbitrary and biases the results either positively or negatively. Also, the correlation is calculated from the $\log_2$ fold changes, whereas the ranking uses information about their statistical significance ($-\log_{10}$-transformed p-values). Lastly, the weighted sum approach is likely to be not as sensible to different orderings of the effects as is the correlation.

Genes with greater fold changes are more concordantly affected across strains than genes with smaller fold changes

Correlating the constrained datasets and the weighted sum approach both consider only the general similarity between the genetic responses. Moreover, both approaches determine the pairwise similarity based on the extremes (genes with fold changes > 1.3; top- and bottom-ranked gene expression changes); hence, patterns such as correlation trends and local overlaps between strains cannot be considered by these approaches.

Because of that, I applied another rank-based measure, the RRHO (Methods 2.6.6). Just like the weighted sum approach, the RRHO works on the lists of ranked gene expression changes and determines the significance of the over- or underrepresentation of shared gene expression changes between the two studies from the hypergeometric distribution for all subsets (i.e. gene expression changes up to a certain rank). Using this approach has the benefit that it considers also overlaps between sets of unequal size comparable to non-linear correlation and locally limited overlaps (e.g., great overlap in the middle of the lists, while the top ranks are different). Visualization of the hypergeometric p-values ($-\log_{10}$-transformed) using heat-maps allows the convenient identification of such patterns.

The results of the RRHO revealed significant overlaps of different sizes across all pairwise comparisons of inbred strains. The comparisons of B6J×B6N, 129×B6J, and B6N×C3H all reveal significant overlaps over the complete ranked list of 22,030 gene expression changes, indicating substantial similarities among their genomic responses. For all six comparisons, the most significant overlap, i.e. the highest concordance between genetic responses, is found at the extremes (Figure 3.7, lower left and upper right corners) between the top and bottom ranks. The subsets with the most significant p-values are generally bigger for the top ranks (Figure 3.7, lower left corners; Figure 3.11, upper panel) than for the bottom ranks (Figure 3.7, upper right corner; Figure 3.11, lower panel), suggesting that the similarities among up-regulated genes (i.e. genes which are more expressed in HFD than LFD mice) are greater than for down-regulated genes across the strains. Comparing B6J×B6N and B6N×C3H revealed the most significant overlaps between these strains.

In case of the comparisons of B6J×C3H and in particular 129×B6N and 129×C3H, the p-values for comparisons of greater subsets (i.e. greater ranks) become quickly insignificant, indicating less substantial similarity across their genomic responses. These results basically reconfirm my findings from the correlation and weighted sum approach.

Although some strains show only overlap among the most extreme gene expression changes, assuming that genes with greater fold changes ranked at the top or bottom of the lists are biologically more relevant than genes with smaller fold changes ranked somewhere in between, these significant overlaps between the top and bottom ranks found for all comparisons indicate a – more or less general – common genomic response to the HFD induced NAFLD in the liver of all four inbred strains.

The individual genetic responses are enriched for genes involved in the same metabolic pathways

Assessing the overall similarities of genetic responses across strains suggested that all strains have some expression changes in common. In particular, genes which display the greatest changes in their expression between the HFD and LFD groups seemed to be commonly affected by the HFD induced NAFLD phenotype in all four inbred strains.

I defined the set of differentially expressed genes in response to the HFD induced NAFLD by selecting genes with linear fold changes greater than 1.3 and whose differential expression between the HFD and LFD groups was statistically significant after Bonferroni correction ($\alpha = 5\%$) (Figure 3.9, closed bars) for each strain separately. In terms of the number of significantly up- and down-regulated genes, the genetic response to the HFD induced NAFLD differed across strains. While in B6N 20% of genes were differentially affected by NAFLD, the fractions were notably smaller in strains B6J (15%), C3H (15%) and 129 (3%). Such differences may be mainly caused by true biological variation or undesired batch effects. Although I cannot exclude with certainty that the latter caused these differences, regarding the study design and my analysis strategy there are some considerations on why these differences reflect the

genetic variation among the four inbred mouse strains: first, all experiments were done in the same lab, all mice were held under the same standardized conditions using identical protocols, and gene expression profiling measurements were done using the same platform (Affymetrix® GeneChip® Mouse Gene 1.0 ST), minimizing the risk for unwanted batch effects; second, all mice received the same diets, thus the differences in the number of differentially expressed genes are likely to be not diet related; lastly, except for strain C3H, the sample sizes were similar among strains and I used the same statistical methods, excluding these factors as potential sources of bias. In addition, despite the numerical discrepancies of differentially affected genes, the individual sets were enriched for genes with similar metabolic functions (Figure 3.10), in particular ›drug metabolism‹ and ›metabolism of xenobiotics by cytochrome p450‹. Cytochrome P450 (CYP) monooxygenases catalyze various endogenous and exogenous compounds, particularly drugs and other xenobiotics, but also fatty acids and steroids [146]; hence, overrepresentation of members of the CYP family among differentially expressed genes in all four strains could be related to the HFD feeding and may be important for the genetic adaptions in the HFD induced NAFLD.

All four strains share major parts of their genetic responses to HFD induced NAFLD

To determine joint and disjoint gene expression changes, I assessed the individual sets of differentially expressed genes for replication among strains. Notably, out of the 141 genes that were significantly altered in at least 1 of 4 strains (Bonferroni, $\alpha = 5\%$), the results of 84% replicated in at least 1 more strain, and almost 26% replicated in all 4 strains. The results of 16% of 141 genes did not replicate in any other strain (Figure 3.11). Unsurprisingly, I found a significant enrichment of the ›drug metabolism‹ and ›metabolism of xenobiotics by cytochrome p450‹ pathways among the genes that replicate across all four strains, suggesting an important role of these pathways in the genetic adaption to the HFD induced NAFLD in strains 129, B6J, B6N, and C3H. Moreover, 33 of the 36 jointly affected genes were consistently up- or down-regulated in all 4 strains in response to the HFD, indicating high concordance

across the genetic responses. I find that interesting, as it may relate to a conserved genetic response in NAFLD.

In all of the four strains, the gene Vanin-1 (VNN1), which encodes the enzyme pantetheinase, was strongly induced in mice with NAFLD (Table 3.2). This is in line with results from another study in B6J mice, where the HFD both induced NAFLD and resulted in significant overexpression of VNN1 [147]. Pantetheinase is an ubiquitous, membrane bound enzyme [148] that recycles pantothenic acid (vitamin B5); furthermore, under physiological conditions pantetheinase is the primary source of cysteamine, a potent anti-oxidant [148]. Correspondingly, an induction of VNN1 expression might act as a counter-mechanism in response to increased oxidative stress in mice with NAFLD, for example caused by increased fatty acid oxidation in their steatotic livers [149].

In line with a potentially increased oxidative stress level in the livers of mice with NAFLD, five genes coding for Glutathione S-Transferase (GST) (GSTa2, GSTa4, GSTm1, GSTm3, GSTm6) and a sixth one coding for an aldo-keto reductase (Akr1c19) were concertedly down-regulated in the HFD groups of all strains (Table 3.2). Their down-regulation suggests an decreased conjugation of glutathione, another important anti-oxidant, potentially leading to an impaired defense to reactive oxygen species in HFD induced NAFLD. Accordingly, Aleksunes and Manautou showed that differential expression of some GST genes associates with changes in the redox state in conjunction with oxidative stress [150].

Three genes coding for enzymes from the same CYP subfamily (CYP3a) were significantly up-regulated in C3H and at the same time down-regulated in 129, B6J, and B6N in response to the HFD: CYP3a11, CYP3a41a, and CYP3a44 (Table 3.2). CYPs are regulated through the activation of various nuclear receptors, notably the pregnane X receptor, the aryl hydrocarbon receptor, and the constitutive androstane receptor. From all cytochromes, CYP3a is the predominant CYP subfamily and the major drug-metabolizing enzyme expressed in liver. The results of multiple studies in rat suggest that their gene expression and enzymatic activity decreases with steatosis and NAFLD [151–153]. In contrast to that, Baumgardner et al. showed that NAFLD induced by overfeeding with a HFD containing much high-polyunsaturated fat in rats resulted in the overexpression of certain CYP3a isoforms [154]. Results from

two other studies in rats demonstrated a temporal pattern in the regulation of several CYPs during NAFLD progression, showing that the gene expression of CYP3a generally decreased after 2 weeks, increased between 2 and 8 weeks, and decreased again after 12 weeks [151, 152]. However, the results from both genetic and nutritional mouse models for NAFLD are inconsistent: while in many genetic mouse models of obesity and diabetes no alterations of CYP3a expression were found, in mouse models where NAFLD is diet induced changes of CYP3a expression could be observed [154]. Here, I can exclude dietary factors as the source for different CYP regulation, since the diets used in our setting was the same for all four strains.

Taken together, I showed that in four genetically heterogenous mouse strains for the study of HFD induced NAFLD (129, B6J, B6N, and C3H), the expression of many genes was equally affected indicating for conserved, genotype-independent genetic adaptions to diet induced NAFLD. In particular, these genotype-independent adaptions in response to hepatic lipid accumulation included various genes coding for proteins (GSTs, VNN1) which are involved in the response to oxidative stress. Hence, the defenses against reactive oxygen species appears to be similarly impaired by the HFD induced NAFLD phenotype in all four models. Given that most genes involved in these genotype-independent genetic adaptions have orthologs in human, they present promising candidates for translational functional studies on the molecular mechanisms of NAFLD's pathogenesis.

Chapter 4

Comparative metabolomics in obese diabetic humans and mice: how well does the monogenetic db/db model mimic the metabolic alterations of type 2 diabetes?

While in the previous chapter, I compared high-troughput transcriptomics data to determine the within-species reproducibility of findings obtained in different mouse models for the study of NAFLD, in this chapter I focus on the cross-species comparison of metabolic profiles measured in mice and humans to study how well the findings in the model correlate with the findings in humans.

To this end, I adapted the meta-analysis workflow established on transcriptomics data presented in Chapter 3. It is important to note that as of today, there is no established workflow for the meta-analysis of results across different species. The primary reason for that is that current meta-analysis methods are of limited use for this kind of analyis. For example, commonly applied meta-analysis approaches comparing effect-sizes such as fixed effects or random effects models would be biased by the different experimental conditions in the two studies. Similarly, approaches which combine p-values from the individual studies into meta-p-values (e.g. Fisher's P, Stouffer's Z) would be driven by the study with the greater statistical power. And

finally, approaches which compare sets of meaningful results are obviously biased by the selection of results (by a certain statistical test).

Here I present the first steps to a systematic metabolic characterization of mouse models to provide a reliable basis for knowledge transfer to human. My work was the basis of a reasearch proposal which was successfully approved for funding to characterize two more mouse models for T2DM research (not presented in this thesis). Moreover, in the context of a poster talk, I presented my results to an international audience on the International Conference on Systems Biology in 2014. A publication is currently under preparation/submitted/under revision and is going to be published in 2016.

4.1 Research Design

Our study is based on 666 serum samples from 45 obese diabetic humans (newly diagnosed, without any previous anti-diabetic drug treatment) and 621 healthy humans (390 lean, 231 obese), as well as 40 plasma samples from 20 db/db and 20 wt mice. Targeted and non-targeted metabolomics were applied to measure a broad spectrum of metabolites from all major metabolic pathways, including amino acids (46), carbohydrates (7), cofactors and vitamins (5), metabolites related to energy metabolism (3), lipids (189), nucleotides (5), and peptides (6). A total of 319 metabolite measures could be detected in both murine plasma and human serum. These measures correspond to a panel of 287 unique metabolites (see Methods 2.5.3).

Using these data, I determined the effect of obesity and diabetes on individual metabolite levels within mouse and human in a differential analysis. To this end, I calculated linear regression models on the metabolite levels measured in BKS.Cg-Dock7m+/+ Leprdb/J (db/db) and Dock7m+/+ (wt) mice, and obese diabetic (od) and lean healthy (lh) humans. Based on these results, I compared the metabolic changes in mice and humans using correlation and rank-based statistics. Moreover, I assessed the metabolite associations for joint and species-specific effects, which might be relevant for the transfer of results from the model to human.

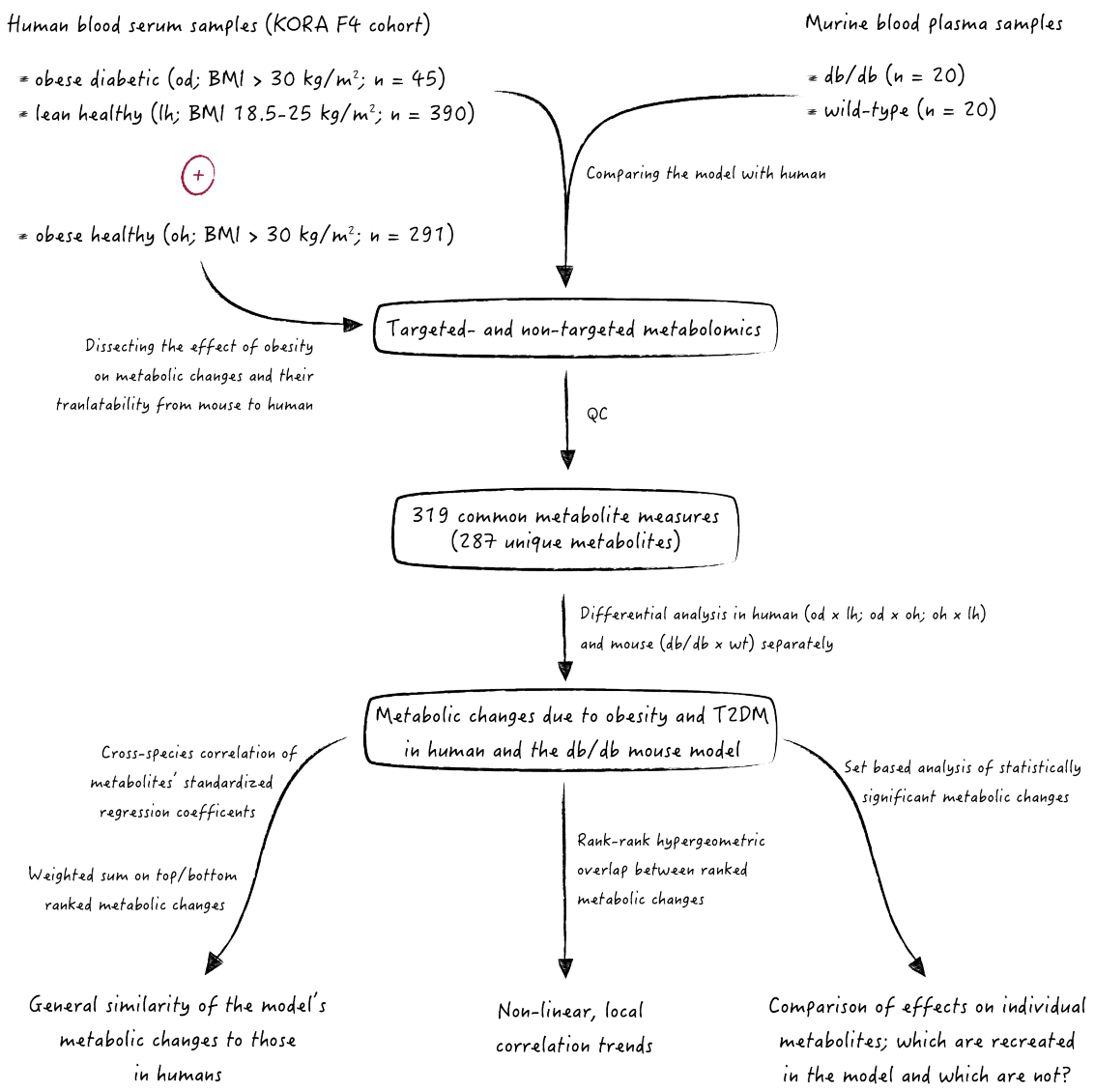

Figure 4.1 – Schematic representation of the analysis workflow for the cross-species comparison of metabolic changes in response to obesity and T2DM in humans and db/db mice.

To get additional evidence about the potential reasons for joint and species-specific metabolic changes and to characterize these in greater detail, I did another differential analysis using additional human samples from healthy obese participants. Calculating linear regression models on samples from obese diabetic (od) and obese healthy (oh), and obese healthy (oh) and lean healthy (lh), I determined the individual effects of obesity and T2DM on metabolite levels.

The schematic workflow of the characterization of metabolic traits in serum of obese diabetic humans and plasma of db/db mice and the cross-species comparison of these traits is given in Figure 4.1.

4.2 Results

4.2.1 Metabolic signals of obesity and T2DM in human serum and murine plasma

Here, it is important to note that diabetic db/db mice are inherently heavier than their wt controls; hence, to make the results from both species better comparable, I contrasted data from obese diabetic to lean healthy humans. To determine the effect of obesity and T2DM on metabolite levels in human serum and the corresponding db/db phenotype in murine plasma samples, I calculated the linear regression models for both studies separately, including age and sex (human) or the time of sacrifice (mouse) as covariates (see Methods 2.6.2). As a result, I obtained the estimated effect size, the effect's direction (i.e. whether the metabolite's level is increased or decreased in the diabetic group), and the effect's respective statistical significance for each of the 319 metabolites.

Table 4.1 – Significant metabolic traits in human and mouse

	Significant changes		Up		Down	
Contrasted study groups	**Bonferroni**	**FDR**	**Bonferroni**	**FDR**	**Bonferroni**	**FDR**
od×lh	96	139	51	75	44	64
db/db×wt	111	149	54	73	57	76
od×oh	80	-	43	-	37	-
oh×lh	21	-	13	-	8	-

The number of significant metabolic changes for od×lh, od×oh, and oh×lh (human), and db/db×wt (mouse) according to the strict Bonferroni criterion ($\alpha = 5\%$) or the less conservative FDR criterion (FDR $< 1\%$).

Contrasting samples from obese diabetic ($n = 45$, BMI $\geq 30\,\mathrm{kg\,m^{-2}}$) and lean healthy ($n = 390$, BMI 18.5-25.0 $\mathrm{kg\,m^{-2}}$) subjects, I determined the metabolic traits associated with obesity and T2DM in human serum. Almost half (48%; 152/319) of the 319 investigated metabolites showed significantly different levels (FDR $< 1\%$); 105 metabolites (33%; 105/319) achieved significance after conservative correction for multiple testing according to Bonferroni ($\alpha = 5\%$, Table 4.1). The top 50 results for the comparison of od×lh are shown in Table 4.2. Among the metabolites with significant concentration differences were 99 lipids, 31 amino acids, all 8 carbohydrates, 4 nucleotides, 3 peptides, 2 cofactors or vitamins, and 1 xenobiotic metabolite. In addition, there were 4 so-called ›unknown‹ metabolites. These unknown metabolites represent well-defined signatures in the metabolomics experiments that could not be annotated with a chemical structure yet.

Analogously, to identify metabolic traits associated with the db/db mutation in the murine db/db model of T2DM, I calculated the linear regression models on samples from diabetic db/db mutant (n = 20) and wild-type mice (n = 20). I found statistic-

Table 4.2 – Top 10 metabolites whose levels change between obese diabetic and healthy lean humans.

Metabolite	Effect	se	P-value	Bonferroni	FDR
Amino acid					
Glu	0.21	0.03	1.45×10^{-15}	4.71×10^{-13}	7.85×10^{-14}
Carbohydrate					
H1	0.10	0.01	2.52×10^{-35}	8.19×10^{-33}	8.19×10^{-33}
glucose	0.13	0.01	7.85×10^{-33}	2.55×10^{-30}	1.28×10^{-30}
mannose	0.14	0.02	4.04×10^{-17}	1.31×10^{-14}	3.29×10^{-15}
Lipid					
lysoPC a C17:0	−0.18	0.02	6.75×10^{-18}	2.19×10^{-15}	7.31×10^{-16}
lysoPC a C18:2	−0.18	0.02	2.92×10^{-16}	9.50×10^{-14}	1.90×10^{-14}
PC ae C34:3	−0.14	0.02	4.48×10^{-15}	1.46×10^{-12}	2.08×10^{-13}
PC ae C36:2	−0.14	0.02	7.10×10^{-15}	2.31×10^{-12}	2.88×10^{-13}
PC ae C42:3	−0.12	0.01	1.35×10^{-14}	4.39×10^{-12}	4.52×10^{-13}
lysoPC a C18:1	−0.14	0.02	1.39×10^{-14}	4.52×10^{-12}	4.52×10^{-13}

Metabolites listed by metabolic pathways, sorted by p-values.

Table 4.3 – Top 10 metabolites affected by the db/db mutant in mouse.

Metabolite	Effect	se	P-value	Bonferroni	FDR
Amino acid					
trans-4-hydroxyproline	−0.82	0.06	6.93×10^{-17}	2.22×10^{-14}	1.11×10^{-14}
Gly	−0.29	0.02	1.34×10^{-15}	4.30×10^{-13}	8.59×10^{-14}
glycine	−0.56	0.05	4.91×10^{-14}	1.57×10^{-11}	1.97×10^{-12}
Carbohydrate					
H1	0.38	0.02	2.98×10^{-24}	9.53×10^{-22}	9.53×10^{-22}
Lipid					
PC aa C38:3	0.44	0.03	1.79×10^{-16}	5.74×10^{-14}	1.91×10^{-14}
C10	0.24	0.02	8.77×10^{-16}	2.81×10^{-13}	7.02×10^{-14}
PC aa C38:4	0.29	0.02	9.49×10^{-15}	3.04×10^{-12}	4.34×10^{-13}
PC ae C34:1	−0.25	0.02	5.74×10^{-14}	1.84×10^{-11}	2.04×10^{-12}
PC aa C36:2	0.19	0.02	1.26×10^{-13}	4.02×10^{-11}	4.02×10^{-12}
Peptide					
pro-hydroxy-pro	−0.41	0.03	2.55×10^{-15}	8.14×10^{-13}	1.36×10^{-13}

Metabolites listed by metabolic pathways, sorted by p-values.

ally significant differences in the levels of 50% (160/319) of all measured metabolites (FDR < 1%); 119 metabolites met the more stringent Bonferroni criterion (Table 4.1). Refer to Table 4.3 for the top 50 metabolic changes in the db/db mouse model. The significantly affected metabolites in mouse included 97 lipids, 39 amino acids, 4 cofactors or vitamins, 3 carbohydrates, 3 peptides, 2 nucleotides, 2 energy related metabolites, and 9 unknown metabolites.

4.2.2 Global accordance of metabolic signals of obesity and T2DM in humans and mice

Cross-species correlation between the metabolic changes in human and mouse

To estimate how well the metabolic traits associated to the artificial disease phenotype caused by the db/db mutation in the mouse model correspond to those as-

sociated with human T2DM, I quantified the overall similarity of the effects of obesity and T2DM on metabolite levels in human and mouse. To this end, I calculated the Spearman correlation of the standardized regression coefficients resulting from the separate differential analyses for all 319 metabolite measures (see Methods 2.6.2).

Table 4.4 – Spearman correlation across metabolic changes associated with obesity and T2DM in human and mouse.

Metabolic pathway (n)	Spearman's rho	p-value
All (319)	0.10	0.08
All, w/o H1 and glucose (317)	0.08	0.15
Amino acid (58)	0.47	0.00023
Carbohydrate (8)	0.60	0.13
Carbohydrate, w/o H1 and glucose (6)	0.03	1
Cofactors and vitamins (5)	−0.50	0.45
Energy (3)	−1.00	0.33
Lipid (208)	−0.05	0.43
Nucleotide (5)	0.00	1
Peptide (6)	0.20	0.71
Unknown (24)	0.02	0.91
Xenobiotics (2)	-	-

Spearman's rho and their corresponding p-values of the cross-species comparison between effects of obesity and T2DM in human and the db/db mutant in the mouse model.

The overall correlation across all metabolites was small and non-significant (Spearman's rho = 0.097; p-value = 0.08; Table 4.4). In line with that, the standardized effects do not show a clear clustering as to represent a straight line (Figure 4.2). When I excluded the effects of glucose and H1, which both show high cross-species correlation by the definition of the disease model, from the comparison, the already small correlation between metabolic traits in human and mouse became even smaller (Table 4.4).

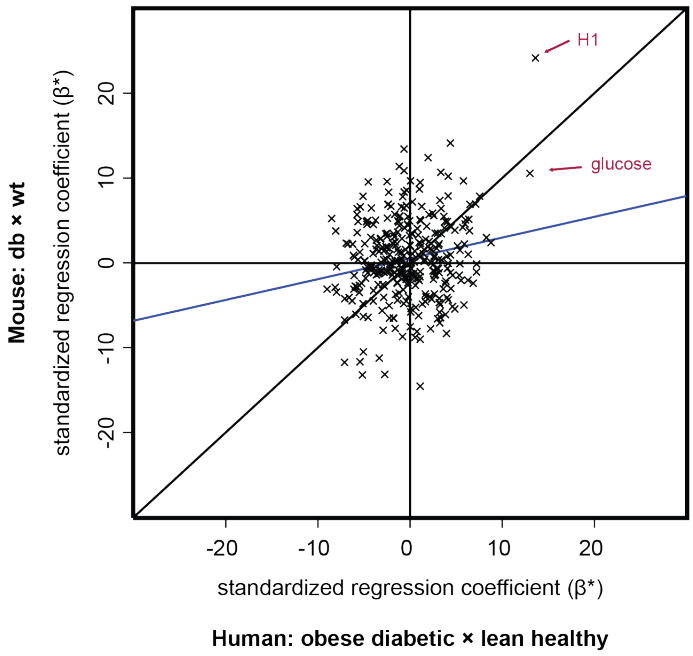

Figure 4.2 – Overall correlation of metabolic traits of obesity and T2DM in humans and the murine db/db model. Scatterplot of the standardized effect estimates (β^*) across the 319 metabolite measures in human (x-axis) and mouse (y-axis). Both glucose measures (H1 and glucose) are strongly correlated. The regression line is depicted in blue.

Global similarity of the metabolic signatures in terms of the weighted-sum rank-based statistic

To assess whether the similarity among metabolites whose levels are strongly affected by obesity and T2DM in either species is higher than that over the whole panel of metabolic changes, I determined the overlap between the ranked lists of differentially abundant metabolites. To this end, I calculated the weighted sum over the overlap of ranked metabolic changes in human and mouse (Methods 2.6.5). Depending on the choice of the weighting parameter α, more or less of the top- and bottom-ranked metabolites were considered for the comparison of two studies; the greater the choice of α, the more metabolites are compared and used to calculate the weighted sum. Using a resampling strategy, I empirically determined an ›optimal‹ α from a predefined set of possible choices of α for the comparison of the ranked lists between human and mouse. Here, optimality was measured by the pAUC score, which measures the separability between weighted sums calculated on resamples

and randomized data; the α that achieved the best separability (i.e. the greatest pAUC) was assumed to be optimal. I defined a set of possible α so that 5 to 150 top- and bottom-ranked effects were considered for the calculation of the weighted sum. Again, I excluded the highly correlated and top ranked measures of H1 and glucose to avoid an overestimation of the overlap.

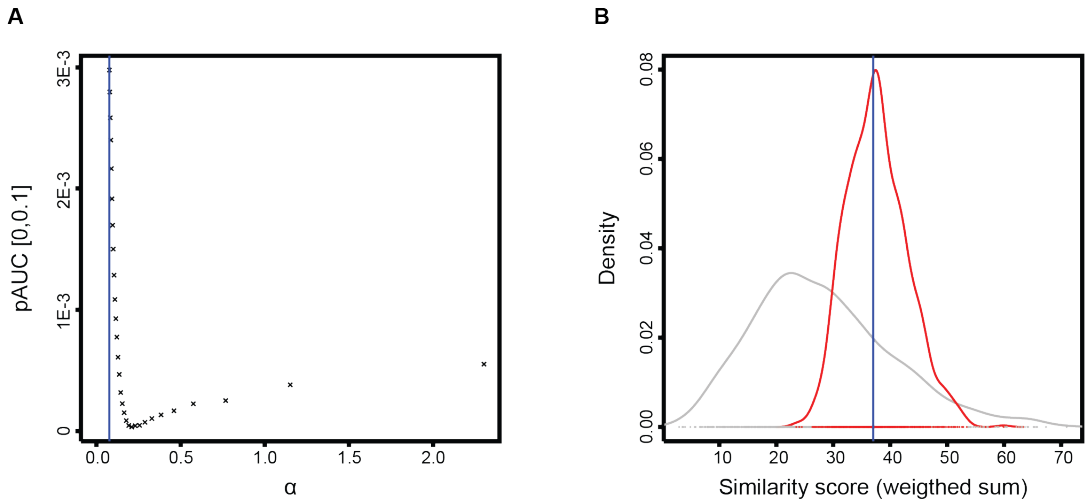

Figure 4.3 – Optimal tuning parameter α for the comparison of the ranked metabolic changes between od and lh humans with those between db/db and wt mice. (A) For 30 different choices of the regularization parameter α (x-axis), the pAUC-score (y-axis) was calculated, measuring the separation of scores calculated on 1,000 resamples of the original datasets (signal) and 1,000 resamples of the datasets with shuffled class labels (noise). The vertical line (blue) marks the α providing the best separation (greatest pAUC). (B) Similarity-score distributions of signal (red) and noise (grey) for chosen α. The vertical line (blue) marks the actual similarity-score, i.e. the weighted sum of the overlap between the 150 top and bottom ranked metabolic alterations humans and the db/db mouse model.

In line with the overall small correlation, in terms of the weighted sum there was no significant overlap between the ranked lists of metabolic traits of T2DM and obesity in human and the db/db mutant in mouse, irrespective of the choice of α, i.e. irrespective of how many metabolites were considered to determine the similarity score. Among the 10 top- and bottom-ranked metabolites (i.e. metabolites whose levels are most increased or decreased in od or db/db) in either species, glycine was the only metabolite which human and mouse had in common. The corresponding weighted sum was almost 0 (p-value = 0.267).

Resampling resulted in an optimal choice of $\alpha = 0.077$ (Figure 4.3), corresponding to the 150 top- and bottom-ranked metabolites. However, the corresponding weighted sum based on the 150 top- and bottom-ranked effects was not significant (p-value = 0.96).

Patterns of local accordance between the metabolic signatures

Correlation analysis and the weighted sum approach both asess the overall accordance of metabolic changes. Clearly, mouse models imitate some but not all characteristics of human disease phenotypes; hence it is likely that not all disease related changes in metabolite levels are reflected in the model. To identify possible partial overlaps between metabolic changes that link to obesity and T2DM in human and to the db/db mutant in the mouse model, I focussed on whether there are groups of metabolic traits such as metabolites within the same metabolic pathways, which show better concordance across species than others, in the next steps.

To dissect the overall similarity of metabolic traits by predefined metabolic pathways, I calculated the Spearman correlation for each of the nine measured metabolite classes (›Amino acid‹, ›Carbohydrate‹, ›Cofactors and vitamins‹, ›Energy‹, ›Lipid‹, ›Nucleotide‹, ›Peptide‹, ›Xenobiotics‹, ›Unknown‹) separately. Correlations across changes in metabolite levels stratified by pathways revealed a clear positive and significant correlation of the disease effects on amino acid metabolites (Table 4.4). For the remaining investigated metabolite classes, there was no significant linear relationship between the effects on metabolite levels in human and the mouse model. However, the strong but non-significant positive correlation of changes in carbohydrates between both species was clearly driven by the changes in H1 and glucose.

In addition, to determine possible pathway independent overlaps, I calculated the RRHO on the ranked effects (without H1 and glucose) on metabolite levels in human and mouse. The RRHO determines for all pairwise comparisons of subsets of the

ranked lists (i.e. each rank-rank combination) the significance of their overlap using the hypergeometric distribution.

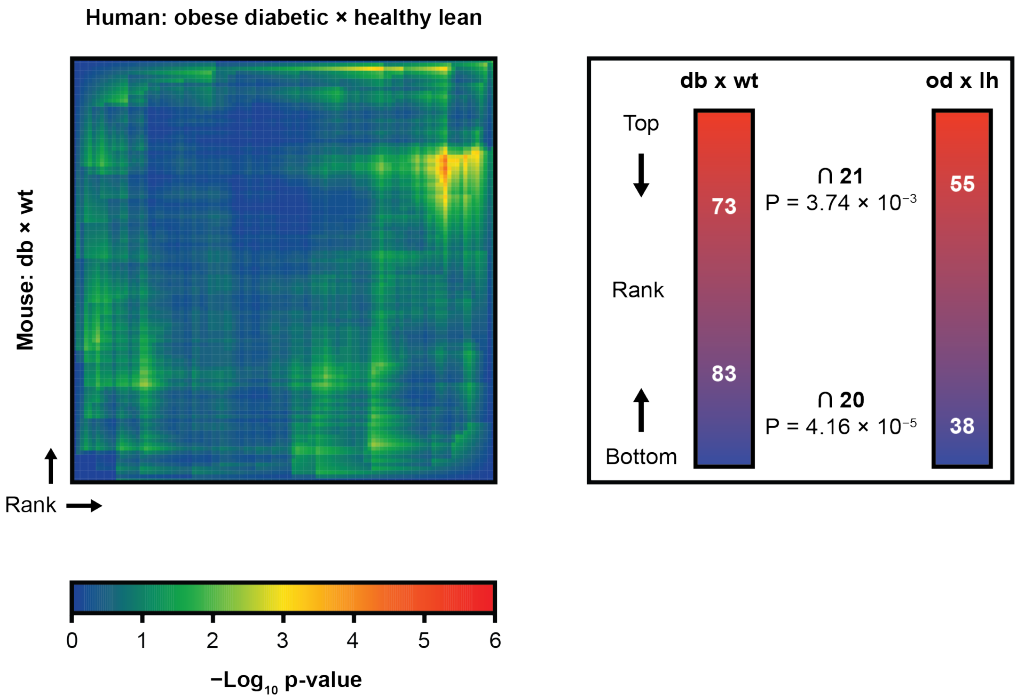

Figure 4.4 – Local overlaps between metabolic changes between od and lh humans and between db/db and wt mice. Left: Heatmap visualizing the hypergeometric p-values ($-log_{10}$). Each pixel corresponds to the p-value for the overlap between metabolic changes up to a certain rank in the human study (x-axis) and the db/db mouse model (y-axis). Here, pixels in the lower left area correspond to overlaps between traits with positive effect, and those in the upper right area to overlaps between traits with negative effect in both studies. Right: Rank-threshold pairs with the most significant overrepresentation of common metabolic changes.

In line with the overall small correlations, the effect of obesity and T2DM on metabolite levels in humans and the db/db mutant in mice did not show significant overlap over the complete ranked lists, but rather between the top- and bottom-ranked effects, i.e. the metabolites whose abundance was most different between diabetic and healthy subjects (Figure 4.4). In particular, among metabolites whose levels were raised in obese and diabetic humans and mice, the most significant overlap (overlap 21; p-value $= 3.74 \times 10^{-3}$) was found for the top 55 and 73 effects in human and

Table 4.5 – The 21 metabolites whose levels are raised in diabetic humans and mice identified by the RRHO approach.

Metabolite	Rank human	Rank mouse
Amino acid		
2-hydroxybutyrate (AHB)	3	20
3-(4-hydroxyphenyl)lactate	6	23
3-methyl-2-oxobutyrate	8	25
tyrosine	9	73
isoleucine	10	47
Tyr	13	49
3-methyl-2-oxovalerate	17	9
valine	18	68
leucine	24	72
Phe	28	67
4-methyl-2-oxopentanoate	33	7
Val	38	57
alpha-hydroxyisovalerate	44	55
tryptophan	46	70
Carbohydrate		
erythronate*	14	60
fructose	35	17
Cofactors and vitamins		
pantothenate	52	6
Lipid		
PC aa C38:3	32	1
dihomo-linolenate (20:3n3 or n6)	51	34
docosapentaenoate (DPA; 22:5n3)	55	21
Peptide		
gamma-glutamylphenylalanine	47	43

For metabolites raised in T2DM, human and mouse show the most significant overlap between ranks 73 and 55, respectively. Shown are the common 21 metabolites between these sets.

mouse. Notably, 67% (14/21) of these metabolites were amino acids or amino acid degradation products (Table 4.5).

Table 4.6 – The 20 metabolites whose levels are decreased in diabetic humans and mice identified by the RRHO approach.

Metabolite	Rank human	Rank mouse
Amino acid		
histidine	283	277
Gly	285	316
glycine	311	314
Lipid		
PC ae C34:0	281	311
PC ae C32:2	282	293
PC ae C42:2	286	238
PC ae C34:1	288	313
PC ae C40:4	290	256
PC ae C36:3	291	244
PC ae C44:5	296	247
SM (OH) C22:2	298	290
PC ae C44:6	299	246
PC ae C38:2	302	252
PC ae C42:5	305	273
PC ae C36:1	306	265
PC ae C40:5	309	268
PC ae C34:2	310	300
PC ae C42:3	313	255
PC ae C34:3	315	248
lysoPC a C17:0	317	251

For metabolites decreased in T2DM, human and mouse show the most significant overlap between the lowest 83 and 38 ranks, respectively. Shown are the common 20 metabolites between these sets.

I found an overlap of similar size (overlap 20; p-value = 4.16×10^{-5}) between the bottom 38 and 83 metabolites with decreased levels in obese and diabetic humans and mice (Figure 4.4). Here, except for the amino acids histidine and glycine, 85% (17/20) of the overlap accounted to lipids (Table 4.6).

4.2.3 Joint and distinct metabolic changes

To further dissect the similarities and differences between effects obesity and T2DM on metabolite levels in human and mouse, I determined statistically significant effects in either study and compared these sets on the metabolite level. Using this strategy, I was able to consider metabolites whose levels are affected in both studies, but whose levels change to opposite directions. These are metabolites whose levels increase in one and decrease in the other study in response to obesity and diabetes.

Note that in the following analysis the reported numbers refer to the 287 unique metabolites.

Jointly affected metabolites in human and mouse

According to my selection criterion (FDR $< 1\%$; Bonferroni, $\alpha = 5\%$ in at least one of both studies; see Methods 2.6.7), the levels of 23% (66/287) of metabolites were significantly different between both od and lh humans, and db/db and wt mice (irrespective of the direction of the effect): 39 lipids, 20 amino acids, 3 carbohydrates, 2 nucleotides, 1 cofactor or vitamin, and 1 peptide (Figure 4.5; Figure 4.6, A).

Asking whether the effects of obesity and T2DM on metabolite levels in certain metabolic pathways agreed better between human and mouse than in others revealed a significant overrepresentation of metabolites from the amino acid pathway class (odds ratio = 3.54; p-value = 2.14×10^{-4}). Metabolites from other pathways were not significantly enriched among metabolites whose levels are significantly affected in human and mouse.

Jointly affected metabolites whose levels change to the same directions in human and mouse

Taking the direction of the effect into account, out of 66 metabolites that are jointly affected in both species, 59% (39/66) changed in the same direction between both

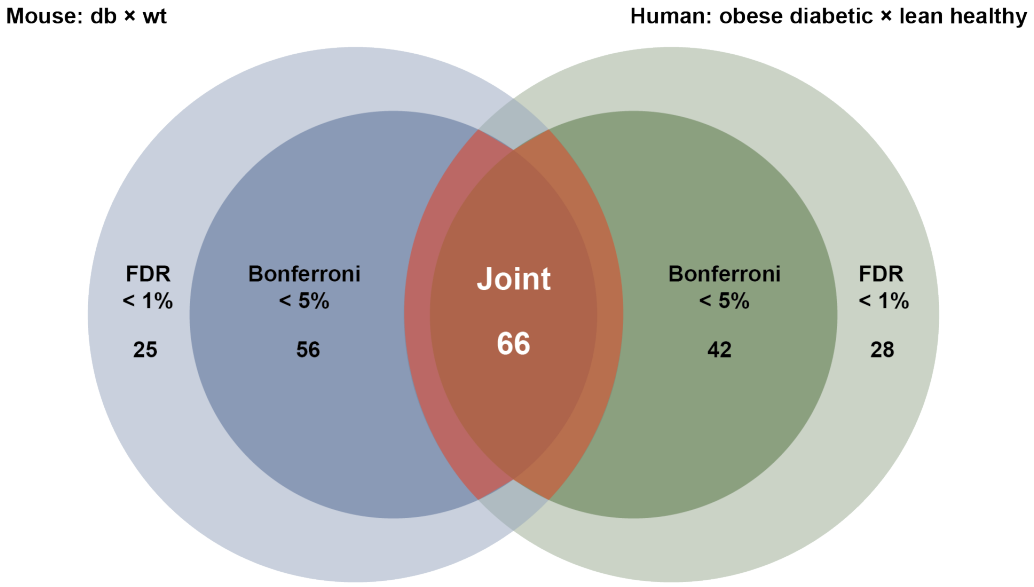

Figure 4.5 – Overlap between significant metabolic changes. Based on my selection criterion (Methods, 2.6.7), I identified 66 metabolic changes which are significantly affected by the disease phenotype in both humans and mice (red). The remaining changes with effects achieving significance according to the conservative Bonferroni criterion ($\alpha = 5\%$) are considered species-specific (dark blue, dark green).

obese diabetic and lean healthy humans and mice (Figure 4.6, A). Compared to lean controls, the levels of all carbohydrates were higher in the blood of obese diabetic mice and humans (Table 4.7). For 80% (16/20) of jointly affected amino acids, I observed concordant effects in humans and mice. Thereof, the levels of 11 amino acids including the 3 BCAAs valine, leucine, and isoleucine, several alpha-ketoacids, phenylalanine, and tyrosine were increased in obese diabetic humans and mice. The remaining 5 amino acids glycine, serine, histidine, asparagine, and serotonin were less abundant in obese diabetic humans and mice as compared to lean controls (Table 4.7).

In contrast to carbohydrates and amino acids, the levels of less than half (46%; 18/39) of the jointly affected lipids were concordantly increased or decreased in both species, but changed to opposite directions (Figure 4.6, A). Of these 18 concordantly affected lipids, the levels of 15 were lower in obese diabetic humans and mice than in their corresponding lean controls (Table 4.7). In contrast to that, the two long chain fatty acids dihomo-linolenate (20:3) and docosapentaenoate (22:5) and the diacyl-

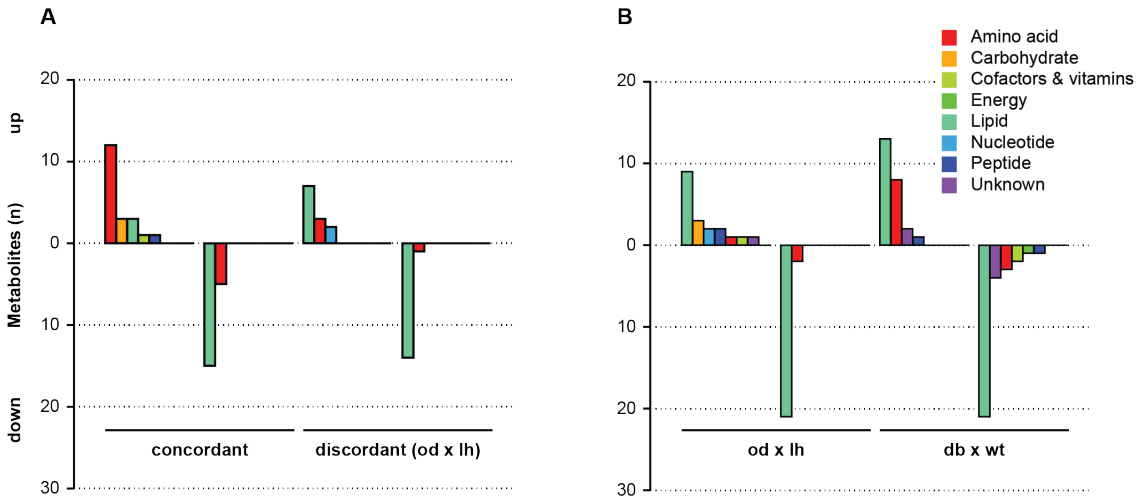

Figure 4.6 – Joint and species-specific metabolic traits with significant effects in human and mouse. (A) Concordant (left) and discordant (right) metabolic traits separated direction of effect (y-axis) and metabolic pathways (colors). The number of positive and negative discordant effects in mouse correspond to the inverted values in human shown here (right). (B) Species-specific metabolic traits with significant effect in human (left) and mouse (right).

Phosphatidylcholine (PC) PC aa C38:3 were more abundant in obese diabetics as compared to healthy subjects.

The levels of both pantothenate and gamma-glutamylphenylalanine were greater in the diabetic than in the control groups in either species (Table 4.7).

Table 4.7 – Metabolites whose levels are similarly affected and which change to the same direction.

	Human			Mouse		
Metabolite	**Effect**	**se**	**P-value**	**Effect**	**se**	**P-value**
Amino acid						
2-hydroxybutyrate (AHB)	0.19	0.03	2.67×10^{-13}	0.38	0.05	2.62×10^{-9}
Gly	−0.09	0.02	3.40×10^{-7}	−0.29	0.02	1.34×10^{-15}
glycine	−0.13	0.02	4.80×10^{-12}	−0.56	0.05	4.91×10^{-14}
serine	−0.08	0.02	6.57×10^{-6}	−0.26	0.04	1.60×10^{-7}
histidine	−0.05	0.01	4.95×10^{-7}	−0.09	0.02	2.54×10^{-5}
Tyr	0.08	0.01	3.79×10^{-9}	0.14	0.03	1.22×10^{-5}
tyrosine	0.08	0.01	3.18×10^{-10}	0.08	0.02	5.64×10^{-4}
Phe	0.05	0.01	1.15×10^{-5}	0.09	0.02	1.50×10^{-4}
3-(4-hydroxyphenyl)lactate	0.15	0.02	4.65×10^{-12}	0.25	0.04	3.48×10^{-8}
Serotonin	−0.10	0.03	8.57×10^{-5}	−1.03	0.32	2.29×10^{-3}
isoleucine	0.07	0.01	4.83×10^{-10}	0.11	0.02	9.24×10^{-6}
leucine	0.05	0.01	1.62×10^{-6}	0.13	0.03	4.50×10^{-4}
Val	0.06	0.01	6.02×10^{-5}	0.16	0.03	2.19×10^{-5}
valine	0.05	0.01	2.14×10^{-8}	0.13	0.03	1.69×10^{-4}
3-methyl-2-oxobutyrate	0.08	0.01	2.25×10^{-10}	0.30	0.04	3.91×10^{-8}
3-methyl-2-oxovalerate	0.08	0.01	1.38×10^{-8}	0.31	0.03	1.18×10^{-11}
4-methyl-2-oxopentanoate	0.06	0.01	4.18×10^{-5}	0.34	0.03	2.65×10^{-12}
alpha-hydroxyisovalerate	0.12	0.03	1.55×10^{-4}	0.16	0.03	1.92×10^{-5}
asparagine	−0.05	0.02	2.58×10^{-3}	−0.32	0.06	1.98×10^{-6}
Carbohydrate						
erythronate*	0.10	0.02	5.25×10^{-9}	0.14	0.03	4.95×10^{-5}
fructose	0.15	0.04	4.45×10^{-5}	0.55	0.07	1.96×10^{-9}
glucose	0.13	0.01	7.85×10^{-33}	0.31	0.03	1.05×10^{-12}
H1	0.10	0.01	2.52×10^{-35}	0.38	0.02	2.98×10^{-24}
Cofactors and vitamins						
pantothenate	0.08	0.02	9.59×10^{-4}	0.32	0.03	7.55×10^{-13}

Table 4.7 – Metabolites whose levels are similarly affected and which change to the same direction, continued.

	Human			Mouse		
Metabolite	**Effect**	**se**	**P-value**	**Effect**	**se**	**P-value**
Lipid						
docosapentaenoate (DPA; 22:5n3)	0.09	0.03	1.31×10^{-3}	0.31	0.04	9.33×10^{-9}
dihomo-linolenate (20:3n3 or n6)	0.07	0.02	8.27×10^{-4}	0.24	0.04	1.82×10^{-7}
lysoPC a C17:0	−0.18	0.02	6.75×10^{-18}	−0.06	0.02	3.62×10^{-3}
PC aa C38:3	0.07	0.02	1.55×10^{-5}	0.44	0.03	1.79×10^{-16}
PC ae C32:1	−0.06	0.01	7.67×10^{-5}	−0.10	0.02	6.41×10^{-5}
PC ae C32:2	−0.07	0.01	5.66×10^{-7}	−0.14	0.02	2.19×10^{-7}
PC ae C34:0	−0.09	0.02	5.85×10^{-7}	−0.26	0.03	1.20×10^{-12}
PC ae C34:1	−0.08	0.01	9.14×10^{-8}	−0.25	0.02	5.74×10^{-14}
PC ae C34:2	−0.12	0.02	5.07×10^{-12}	−0.14	0.02	6.08×10^{-8}
PC ae C40:5	−0.08	0.01	5.56×10^{-12}	−0.09	0.02	1.46×10^{-4}
PC ae C42:5	−0.08	0.01	7.63×10^{-10}	−0.06	0.01	6.73×10^{-5}
PC ae C36:1	−0.10	0.01	1.05×10^{-10}	−0.08	0.02	2.22×10^{-4}
PC ae C38:2	−0.10	0.02	2.29×10^{-9}	−0.07	0.02	3.59×10^{-3}
PC ae C40:4	−0.07	0.01	6.38×10^{-8}	−0.08	0.02	1.24×10^{-3}
PC ae C42:3	−0.12	0.01	1.35×10^{-14}	−0.09	0.03	1.42×10^{-3}
PC aa C36:0	−0.07	0.02	3.59×10^{-3}	−0.17	0.02	1.59×10^{-9}
SM (OH) C22:2	−0.10	0.02	8.25×10^{-9}	−0.15	0.03	4.89×10^{-7}
SM C24:1	−0.05	0.01	8.93×10^{-4}	−0.26	0.02	1.75×10^{-13}
Peptide						
gamma-glutamylphenylalanine	0.06	0.02	2.86×10^{-4}	0.15	0.03	3.62×10^{-6}

Jointly affected metabolites whose levels change to the opposite directions in human and mouse

Although jointly affected in both species, the levels of 40% (27/66) of these metabolites were increased in od versus lh humans but decreased in db/db versus wt mice or vice versa (Figure 4.6, A). Except for 4 metabolites from the amino acid pathway class (alanine, lysine, kynurenine, cysteine-glutathione disulfide) and the 2 nucleotides N1-methyladenosine and pseudouridine, these metabolites comprised solely lipids (Table 4.8). Among the 21 discordantly affected lipids, the levels of 2 fatty acids and 4 acylcarnitines were higher in obese diabetic humans and lower in db/db mice as compared to their respective lean healthy control groups. In contrast, all 11 glycerophospholipids and glyerco 3-phosphate (G3P) were lower in obese diabetic humans and higher in db/db mice as compared to their controls (Table 4.8).

Table 4.8 – Metabolites whose levels are similarly affected and which change to the opposite directions in human and mouse.

	Human			Mouse		
Metabolite	**Effect**	**se**	**P-value**	**Effect**	**se**	**P-value**
Amino acid						
alanine	0.07	0.02	4.19×10^{-5}	−0.18	0.04	9.80×10^{-5}
cysteine-glutathione disulfide	−0.17	0.04	3.06×10^{-6}	0.14	0.03	2.20×10^{-5}
lysine	0.05	0.01	1.16×10^{-3}	−0.10	0.02	1.67×10^{-5}
kynurenine	0.09	0.02	1.01×10^{-8}	−0.15	0.03	1.53×10^{-5}
Lipid						
acetylcarnitine	0.08	0.02	1.41×10^{-4}	−0.19	0.03	4.62×10^{-7}
C2	0.07	0.02	1.49×10^{-3}	−0.21	0.04	1.08×10^{-6}
carnitine	0.03	0.01	2.97×10^{-3}	−0.30	0.05	9.94×10^{-8}
hexanoylcarnitine	0.10	0.03	9.82×10^{-4}	−0.28	0.04	1.40×10^{-7}
C6 (C4:1-DC)	0.07	0.02	1.41×10^{-3}	−0.24	0.03	2.21×10^{-8}
propionylcarnitine	0.07	0.02	1.63×10^{-3}	−0.17	0.04	3.70×10^{-5}

Table 4.8 – Metabolites whose levels are similarly affected and which change to the opposite directions in human and mouse, continued.

	Human			Mouse		
Metabolite	**Effect**	**se**	**P-value**	**Effect**	**se**	**P-value**
Lipid						
glycerol 3-phosphate (G3P)	−0.10	0.02	7.89×10^{-5}	0.13	0.03	6.19×10^{-5}
eicosenoate (20:1n9 or 11)	0.14	0.03	5.46×10^{-6}	−0.21	0.04	8.78×10^{-6}
10-nonadecenoate (19:1n9)	0.12	0.03	7.06×10^{-5}	−0.18	0.04	2.20×10^{-4}
lysoPC a C18:0	−0.08	0.02	7.28×10^{-6}	0.18	0.02	1.62×10^{-11}
lysoPC a C18:2	−0.18	0.02	2.92×10^{-16}	0.16	0.03	7.15×10^{-6}
lysoPC a C20:4	−0.08	0.02	2.51×10^{-5}	0.08	0.03	4.80×10^{-3}
PC aa C32:3	−0.07	0.01	5.31×10^{-6}	0.11	0.02	1.53×10^{-5}
PC aa C42:0	−0.11	0.02	1.61×10^{-8}	0.13	0.02	1.74×10^{-6}
PC ae C40:2	−0.07	0.02	3.80×10^{-6}	0.09	0.02	5.86×10^{-5}
PC ae C40:3	−0.07	0.01	1.82×10^{-8}	0.14	0.02	1.90×10^{-7}
PC ae C36:2	−0.14	0.02	7.10×10^{-15}	0.07	0.02	5.89×10^{-4}
PC ae C44:4	−0.09	0.02	1.81×10^{-8}	0.07	0.02	1.05×10^{-3}
PC ae C38:0	−0.07	0.02	2.02×10^{-4}	0.13	0.03	1.33×10^{-5}
PC ae C38:3	−0.06	0.01	3.09×10^{-5}	0.13	0.02	1.53×10^{-7}
SM C16:0	−0.06	0.01	4.81×10^{-7}	0.15	0.02	2.18×10^{-9}
X - 10419|palmitoyl sphingomyelin	−0.09	0.02	1.09×10^{-7}	0.15	0.02	9.53×10^{-8}
SM (OH) C14:1	−0.10	0.02	2.88×10^{-8}	0.10	0.02	2.09×10^{-5}
7-alpha-hydroxy-3-oxo-4-cholestenoate (7-Hoca)	0.09	0.02	1.68×10^{-6}	−0.22	0.04	3.57×10^{-6}
Nucleotide						
N1-methyladenosine	0.04	0.01	1.23×10^{-5}	−0.06	0.02	4.58×10^{-3}
pseudouridine	0.05	0.01	9.09×10^{-5}	−0.19	0.02	5.11×10^{-10}

Distinct changes in metabolite levels in humans and mice

In addition to the 66 shared metabolic alterations in humans and mice, the levels of 42 metabolites (15%, 42/287) changed between od and lh humans but not the db/db mouse model (›human specific‹ alterations), and those of 56 metabolites

(20%, 56/287) changed in the db/db mouse model but not between od and lh humans (›mouse specific‹ alterations; Figure 4.6, B). The human specific changes in metabolite levels encompassed 71% lipids, some carbohydrates, amino acids, nucleotides, peptides, 1 cofactor or vitamin, and 1 unknown metabolite (Figure 4.6, B, left). The mouse-specific metabolic alterations comprised mainly lipids (60%) and amino acids (21%) (Figure 4.6, B, right).

Please refer to Tables 4.9 and 4.10 for the top 10 human and mouse specific metabolites.

Table 4.9 – Top 10 changes of metabolite levels specific to the human cohort.

	Human			Mouse		
Metabolite	**Effect**	**se**	**P-value**	**Effect**	**se**	**P-value**
Amino acid						
Glu	0.21	0.03	1.45×10^{-15}	0.12	0.04	5.10×10^{-3}
Carbohydrate						
mannose	0.14	0.02	4.04×10^{-17}	0.06	0.02	2.29×10^{-2}
lactate	0.11	0.01	2.67×10^{-12}	−0.03	0.03	2.86×10^{-1}
Cofactors and vitamins						
O-methylascorbate*	0.10	0.01	2.57×10^{-11}	−0.09	0.04	2.14×10^{-2}
Lipid						
PC ae C34:3	−0.14	0.02	4.48×10^{-15}	−0.07	0.02	6.46×10^{-3}
lysoPC a C18:1	−0.14	0.02	1.39×10^{-14}	−0.01	0.03	6.50×10^{-1}
PC ae C42:4	−0.11	0.02	1.46×10^{-11}	0.05	0.02	2.58×10^{-2}
glycerophosphorylcholine (GPC)	−0.16	0.02	4.97×10^{-11}	0.09	0.04	3.33×10^{-2}
glycerol	0.14	0.02	6.93×10^{-10}	0.02	0.02	3.24×10^{-1}
Nucleotide						
urate	0.09	0.01	2.44×10^{-12}	−0.01	0.04	8.83×10^{-1}

Top 10 metabolites with changes specific to the human cohort, listed by pathways and sorted by p-values.

Within each pathway class, I determined whether the fraction of jointly affected metabolites was greater than the fraction of species specific changes. As a result, I found that amino acid metabolites were significantly overrepresented among joint changes (odds ratio = 2.72; p-value = 7.71×10^{-3}) as compared to species specific

Table 4.10 – Top 10 changes of metabolite levels specific to the db/db mouse model.

	Mouse			Human		
Metabolite	**Effect**	**se**	**P-value**	**Effect**	**se**	**P-value**
Amino acid						
trans-4-hydroxyproline	−0.82	0.06	6.93×10^{-17}	0.03	0.03	2.75×10^{-1}
pipecolate	−0.27	0.03	7.16×10^{-11}	0.03	0.03	2.71×10^{-1}
Cofactors and vitamins						
alpha-tocopherol	0.31	0.03	4.55×10^{-13}	−0.01	0.02	5.13×10^{-1}
Lipid						
C10	0.24	0.02	8.77×10^{-16}	−0.02	0.03	5.11×10^{-1}
PC aa C38:4	0.29	0.02	9.49×10^{-15}	0.03	0.02	5.13×10^{-2}
PC aa C36:2	0.19	0.02	1.26×10^{-13}	−0.01	0.01	2.41×10^{-1}
PC aa C36:3	0.24	0.02	1.14×10^{-11}	0.00	0.01	9.60×10^{-1}
PC aa C28:1	0.24	0.03	1.45×10^{-11}	−0.04	0.02	1.28×10^{-2}
PC aa C40:6	0.23	0.02	1.95×10^{-11}	0.02	0.02	2.74×10^{-1}
Peptide						
pro-hydroxy-pro	−0.41	0.03	2.55×10^{-15}	−0.06	0.02	6.15×10^{-3}

Top 10 metabolites with changes specific to the db/db mouse model. Listed by pathways, sorted by p-values.

ones. I did not find significant enrichments of joint or species specific changes within the remaining eight pathways classes.

4.2.4 Dissecting the effect of obesity on metabolic signals in the db/db mouse model

In the murine db/db model of T2DM, it is not possible to distinguish between effects primarily related to obesity and effects primarily related to T2DM. The reason for that is the inherent weight difference between diabetic db/db and healthy wt mice. In contrast to that, such a differentiation can be made in human using two different case-control settings. Using samples from obese healthy (oh) and lean healthy (lh) subjects, I determined the individual effect of obesity in the absence of T2DM on metabolite levels; similarly, using samples from obese diabetic (od) and

obese healthy (oh) individuals, I estimated the individual effect of T2DM in the absence of obesity on metabolite levels. Comparing these effects to the changes linked to the db/db knockout in the mouse model of T2DM, I can make assumptions about whether individual changes are primarily driven by the obesity phenotype of the model or mainly T2DM related.

Metabolic signals of T2DM in the human cohort that are independent of weight differences

To identify the metabolic traits that associate to T2DM without the presence of obesity, I did a weight-matched differential analysis contrasting serum samples from od (n = 45) and oh (n = 231) subjects. Calculating the regression models on the metabolite levels measured in these samples revealed significant differences for 13% (41/319) metabolites (FDR < 1%); the levels of 22 metabolites (7%; 22/319) were significantly altered according to conservative Bonferroni correction ($\alpha = 5\%$) in response to T2DM irrespective of weight differences: 14 lipids, 5 carbohydrates, 1 amino acid, 1 energy related metabolite, and 1 unknown. See Table 4.11 for the top 10 metabolites whose levels are significantly different between case and control samples.

Metabolic signals of obesity in the absence of diabetes in the human cohort

Similarly, to examine the isolated effect of obesity in the disease trait (i.e. the effect of obesity on the concentrations of metabolites without the presence of T2DM), I calculated the linear regression models on samples from obese healthy (n = 231) and lean healthy humans (n = 390). Here, 41% (130/319) of measured metabolites showed significant changes in their levels (FDR < 1%); according to Bonferroni adjusted p-value ($\alpha = 5\%$), 28% (88/319) of the investigated metabolites displayed significant alterations with increased body weight (Table 4.1). Lipids (61%; 79/130) and amino acids (25%; 32/130) thereby account for the greatest fraction of significantly altered metabolites. The remaining changes include 5 peptides, 4 carbohydrates,

Table 4.11 – Top 10 metabolites whose levels are significantly altered between od and oh humans.

Metabolite	Effect	se	p-value	Bonferroni	FDR
Amino acid					
2-hydroxybutyrate (AHB)	0.15	0.03	1.24×10^{-8}	4.02×10^{-6}	1.34×10^{-6}
Carbohydrate					
H1	0.09	0.01	2.14×10^{-26}	6.97×10^{-24}	6.97×10^{-24}
glucose	0.11	0.01	7.69×10^{-19}	2.50×10^{-16}	1.25×10^{-16}
mannose	0.09	0.02	3.96×10^{-6}	1.29×10^{-3}	1.61×10^{-4}
Energy					
citrate	0.08	0.02	3.34×10^{-6}	1.09×10^{-3}	1.55×10^{-4}
Lipid					
PC ae C36:2	−0.09	0.02	1.27×10^{-7}	4.12×10^{-5}	1.03×10^{-5}
glycerol	0.11	0.02	5.49×10^{-7}	1.78×10^{-4}	3.57×10^{-5}
eicosenoate (20:1n9 or 11)	0.14	0.03	2.26×10^{-6}	7.33×10^{-4}	1.22×10^{-4}
PC ae C34:2	−0.08	0.02	5.16×10^{-6}	1.68×10^{-3}	1.86×10^{-4}
stearate (18:0)	0.07	0.01	6.14×10^{-6}	1.99×10^{-3}	1.89×10^{-4}

Metabolites listed by metabolic pathways, sorted by p-values.

4 nucleotides, 2 cofactors or vitamins, 1 energy related metabolite and 3 unknown metabolites. The top 10 results are shown in Table 4.12.

Figure 4.7 shows the estimated effect sizes (standardized regression coefficients, Equation 2.3) for all pairwise group comparisons and the corresponding box plots of metabolite levels within the groups for selected metabolites.

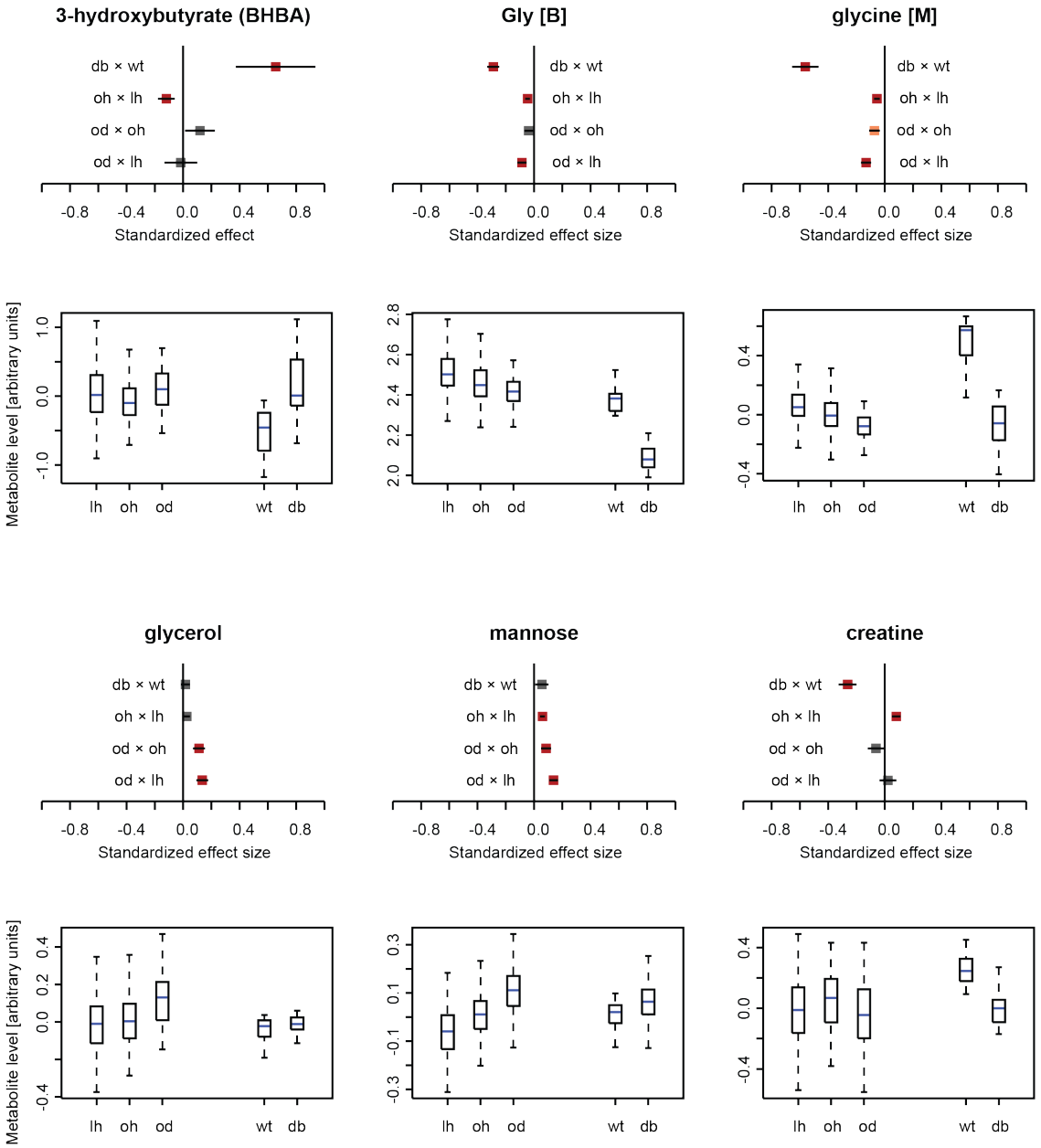

Figure 4.7 – Estimated effect sizes for selected metabolites Upper panels: Forrest plots of the estimated effect sizes for the different pairwise comparisons between od, oh, and lh humans as well as the db/db mouse model. Lower panels: Box plots of metabolite levels within the individual study groups.

Table 4.12 – Top 10 metabolites whose levels are significantly altered between oh and lh humans.

Metabolite	Effect	se	p-value	Bonferroni	FDR
Amino acid					
tyrosine	0.06	0.01	7.08×10^{-20}	2.30×10^{-17}	6.57×10^{-18}
Glu	0.13	0.01	8.08×10^{-20}	2.63×10^{-17}	6.57×10^{-18}
isoleucine	0.05	0.01	9.12×10^{-18}	2.96×10^{-15}	4.94×10^{-16}
phenylalanine	0.04	0.00	1.36×10^{-17}	4.43×10^{-15}	6.33×10^{-16}
valine	0.04	0.00	4.08×10^{-17}	1.33×10^{-14}	1.33×10^{-15}
Lipid					
lysoPC a C18:2	−0.11	0.01	1.31×10^{-24}	4.24×10^{-22}	4.24×10^{-22}
lysoPC a C18:1	−0.09	0.01	3.07×10^{-22}	9.97×10^{-20}	4.98×10^{-20}
PC aa C38:3	0.07	0.01	5.12×10^{-18}	1.66×10^{-15}	3.33×10^{-16}
PC ae C42:3	−0.07	0.01	2.95×10^{-17}	9.60×10^{-15}	1.20×10^{-15}
Nucleotide					
urate	0.05	0.01	3.75×10^{-17}	1.22×10^{-14}	1.33×10^{-15}

Metabolites listed by metabolic pathways, sorted by p-values.

Overall similarity between the individual effects of obesity and diabetes in human, and the effects of the db/db mutant in mice

Changes in metabolite levels between od and oh humans, i.e. changes that are associated with T2DM but not obesity did not significantly correlate with changes in the same metabolites in the db/db mouse model (Table 4.4; Figure 4.8, A). In contrast to that, the metabolic alterations between oh and lh humans, i.e. changes of metabolite levels that are associated with obesity but not T2DM, correlate slightly but significantly with the changes between db/db and wt mice (Table 4.4; Figure 4.8, B).

Apparently, the effect of T2DM determined between obese diabetic and obese healthy humans is smaller on most metabolites as compared to the effect of obesity determined between obese healthy and lean healthy individuals (Figure 4.8).

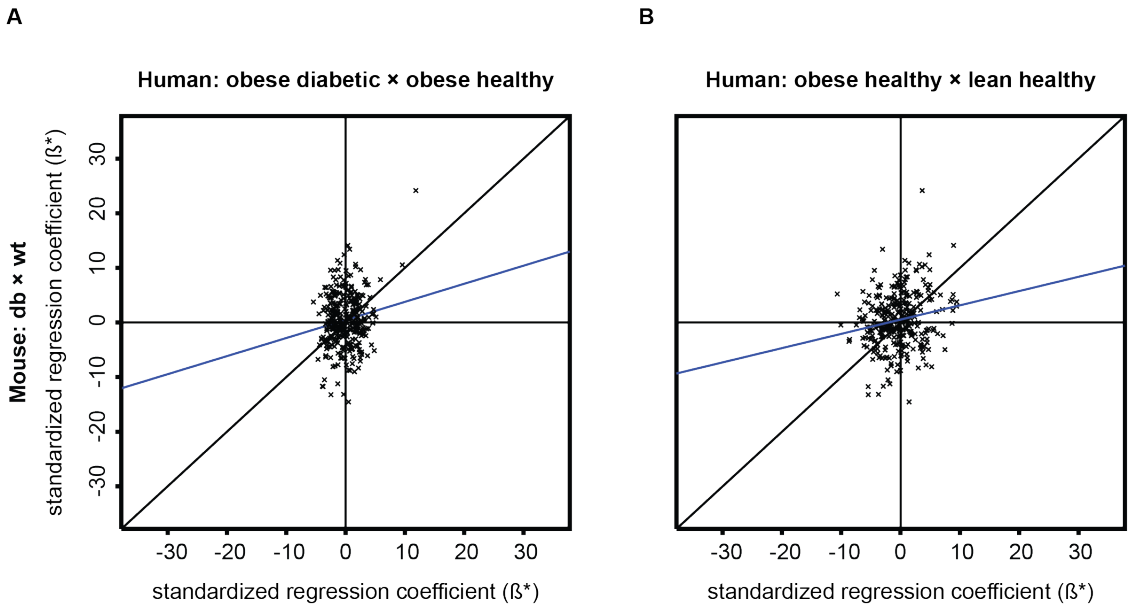

Figure 4.8 – Correlation between metabolic changes associated to obesity or T2DM in human and the db/db mutation in mouse. (A) Scatter-plot of the effect of T2DM on individual metabolite levels between od and oh humans and that of the db/db mutant in the mouse model. (B) Similar representation for the effect of obesity, contrasting the changes between oh and lh human samples to those between db/db and wt mice. Regression lines depicted in blue.

To further assess the overall similarities between the individual effects of T2DM and obesity and the mouse model, I calculated the weighted sums on their ranked lists of metabolic changes for the two pairwise comparisons. Here, I used 30 different choices for the tuning parameter α, which determines how many metabolites are considered for the weighted sum, covering the 5 to 150 top- and bottom-ranked metabolic changes each for the individual comparisons. H1 and glucose were excluded from this analysis.

There was no significant similarity between the ranked lists of metabolic changes between obese diabetic and obese healthy humans and that of the mouse model. Resampling resulted in an optimal $\alpha = 0.1$, corresponding to a weighted sum of 22.7 (p-value = 0.608) among the 115 top and bottom ranked metabolites.

For the comparison of metabolic changes between obese healthy and lean healthy humans and changes in the db/db model, the optimal separation of signal and random scores was achieved for $\alpha = 2.203$, i.e. the weighted sum was computed on the 5 top

and bottom ranks. The corresponding weighted sum was marginal and insignificant (p-value = 0.063); the only shared metabolite among the 5 top and bottom ranked effects was PC aa C38:3.

Local overlap between metabolic changes linked to T2DM or obesity in human and the db/db mutant in mouse

For metabolic traits mainly related to T2DM determined between weight-matched obese diabetics and obese healthy humans, I find small overlap among the top and bottom ranked metabolic traits in both studies (Figure 4.9, A). The most significant overlap (p-value = 1.09×10^{-3}) between top ranked metabolic effects, i.e. metabolites whose levels are increased in obese diabetic versus obese healthy humans and in db/db versus wt mice, includes 5 metabolites: the carbohydrate fructose, amino acid degradation products 2-hydroxybutyrate (AHB), 3-(4-hydroxyphenyl)lactate, 3-methyl-2-oxobutyrate, and the lipid docosapentaenoate (DPA; 22:5n3). The overlap with the smallest p-value among bottom ranked metabolic effects is slightly bigger (overlap 14; p-value = 1.05×10^{-4}); with the exception of the two amino acids glycine and histidine, this overlap contains only lipids, mainly acyl-alkyl PCs (PC ae).

In line with the higher correlations between effects (Table 4.4; Figure 4.8, B), the metabolic traits linked to obesity (oh×lh) show greater overlap with metabolic changes in the db/db mouse model (Figure 4.9, B) as compared to effects linked to obesity and T2DM (od×lh) or T2DM (od×oh). Among the 79 and 121 top ranked metabolic changes in human and mouse, 46 metabolites do significantly overlap (p-value = 2.20×10^{-5}); of the metabolites whose levels decrease between obese healthy and lean healthy humans and between db/db and wt mice, 69 overlap significantly (p-value = 1.15×10^{-3}).

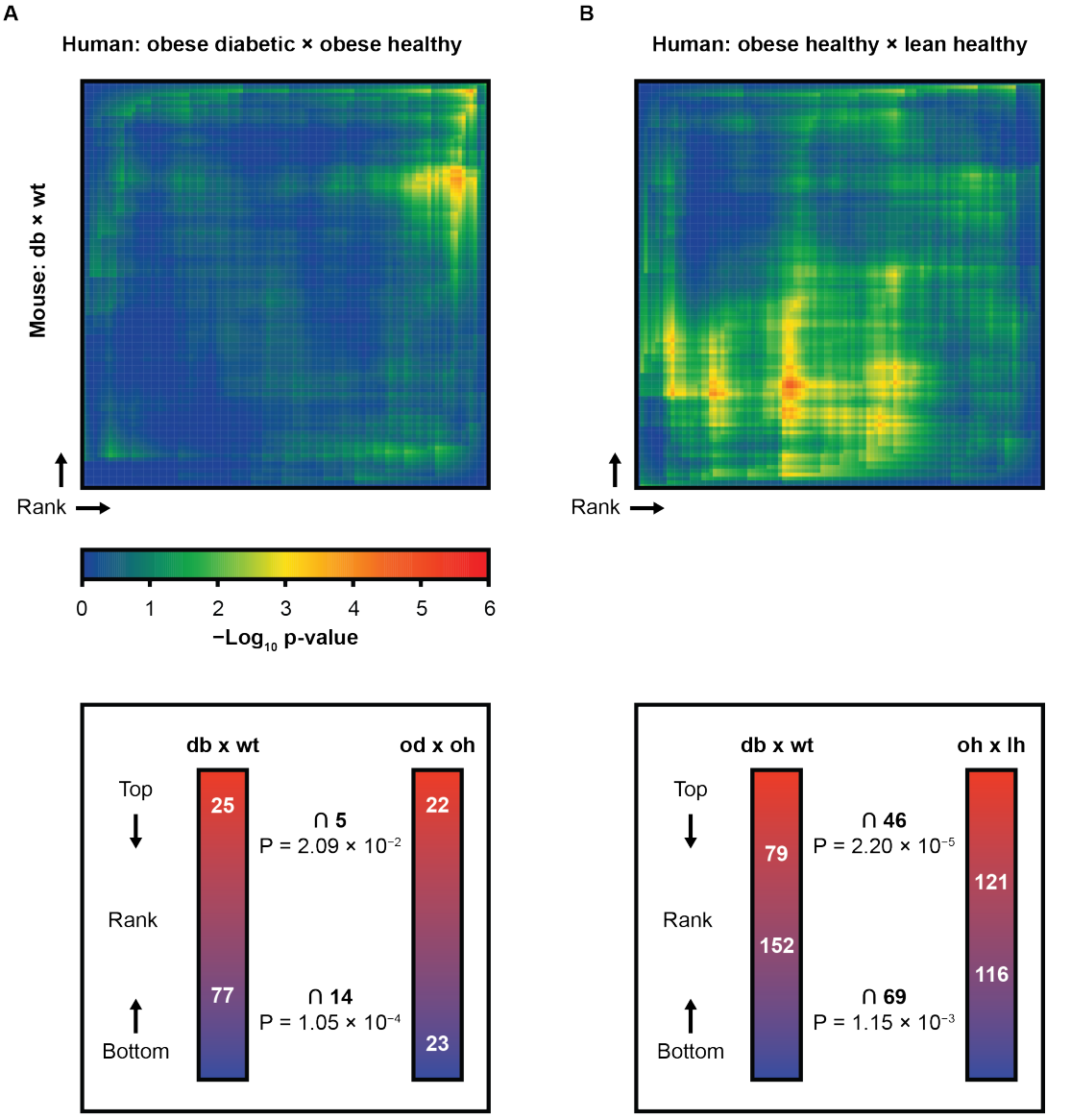

Figure 4.9 – Local overlaps between metabolic traits in mouse and those of T2DM or obesity. (A) Heatmap of the hypergeometric P-Values for the overlap of metabolic traits of T2DM in humans and those of db/db mice for all rank-threshold combinations in human (x-axis) and mouse (y-axis). The corresponding rank-combinations with the most significant overlaps (smallest hypergeometric P-Value) between top and bottom ranked metabolic traits are shown below. (B) Similar visualizations for metabolic traits of obesity in human and those in the murine db/db model.

4.3 Discussion

The db/db mouse model is one of the most commonly used animal models in diabetes research and preclinical drug testing. Although phenotypically well described, a systematic characterization on the molecular level is still missing.

In this chapter, I took a first step to metabolically characterize the murine db/db model of T2DM. To this end, I adapted the meta-analysis workflow for the comparative analysis of genomic responses in four mouse models of NAFLD (Chapter 3). This enabled me to systematically compare the alterations of the blood metabolomes in db/db mice with alterations in human T2DM. Along with the identified similarities and differences in the metabolic alterations between the two species in response to T2DM, my research provides a profound basis to extrapolate results from the model to the human setting.

My study was based on plasma samples from 20 BKS.Cg-Dock7m+/+ Leprdb/J (db/db) and 20 Dock7m+/+ (wt) mice, and serum samples from 45 non-treated, obese diabetic (od) and 390 lean healthy (lh) humans. A second control group of 291 obese healthy (oh) humans additionally enabled me to dissect metabolic effects that are mainly driven by obesity, which is prevalent in the animal model. Targeted- and non-targeted metabolomics were combined to identify 319 shared blood metabolic features corresponding to 287 unique metabolites from all major pathways detected in the blood of both humans and mice.

The db/db mouse model mimics some but not all metabolic aspects of human diabetes

I found a weak overall similarity in changes between obese diabetic and lean healthy humans and db/db and wt mice; both the cross-species correlation between the standardized effects (Figure 4.2; Table 4.4), as well as the weighted sum over the ranked effects on the 319 measured metabolite levels were small and statistically insignificant. However, when I separately assessed the changes of metabolites from the same metabolic pathways, I found an improved cross-species correlation and large

fractions of metabolites changing to the same direction in some cases. In particular, metabolites involved in carbohydrate and amino acid metabolism seemed to be similarly affected in both human and mouse. In contrast to that, the effects on metabolites from other pathways were rather uncorrelated; in fact, many of them changed to the opposite direction in humans and mice (Table 4.4). In contrast to the missing correlation among changes in lipids, when I searched for partial overlaps between the metabolic changes irrespective of an a priori stratification by metabolic pathways, I found many lipids similarly decreased in obese diabetic humans and db/db mice; it therefore seems that at least some metabolites involved in the lipid metabolism are concordantly affected by obesity and T2DM in both species. Generally, the metabolic changes appear to be most similar among metabolites with the greatest differences (increase or decrease) of their blood levels between obese diabetic and lean healthy humans and mice (Figure 4.4). In other words, many metabolites which are largely affected by the disease in human are also affected in mouse, indicating that the db/db model mimics at least some (important) metabolic aspects of T2DM. In line with that, I found 66 metabolites which were significantly altered in both species (Figure 4.5).

Comparable studies which systematically compared omics data across species are still sparse. In a study from 2013, Seok et al. correlated the expression changes of 5,554 genes that were significantly altered in response to human inflammatory diseases with those in different mouse models. While the transcriptomic responses within the human conditions (trauma, burns, and endotoxemia) correlated well with each other, their cross-species correlations between humans and the corresponding mouse models were marginal and insignificant. Likewise, the correlations of gene expression changes in activated or suppressed pathways in human between species were small [112]. The authors found, moreover, that the genomic responses in the mouse models differed not only from the human conditions, but also from one another. Based on their findings, the authors concluded that the results from mouse models, developed to mimic human inflammatory diseases, do not translate directly to the human conditions [112]. Claiming that mice fell short as models for human diseases, their study unsurprisingly gained a lot of attention both from the scientific community [111, 155, 156] and the mass media [157]. ›The New York Times‹ claimed in response to the work of Seok et al. that mouse models had been totally

misleading for at least three major killers – sepsis, burns, and trauma. In this article, they further wrote that years and billions of dollars had been wasted following false leads [157]. However, shortly after the first publication of their results, criticism was expressed that the methods used to compare the genomic responses in human with those in the models were strongly biased. Hence, another group reanalysed the same data and came to a different conclusion [129]. Takao and Miyakawa found that the investigated mouse models do indeed mimic some aspects of the transcriptomic responses in inflammatory conditions observed in humans [129]. Other than Seok et al., in the reanalysis of the data the authors selected only genes which changed both in the human disease conditions and the corresponding mouse models, excluding those genes which do not respond in the mouse models, which would otherwise produce noise in the correlation analysis. Opposed to the findings of the earlier publication [112], Takao and Miyakawa found significant correlations between the gene expression changes in humans and mice. Moreover, without the biased inclusion of genes that respond only in humans, the authors showed that many pathways were commonly regulated in response to the disease conditions in human and the corresponding mouse models [129].

Another study applied NMR based metabolomics on urine samples from diabetic humans, db/db mice, and ZDF rats, and studied these metabolic profiles for similar changes across species [130]. Of around 40 metabolites measured in each species, the authors found 29 metabolites that were changed in the urine of diabetic humans and db/db mice [130]. Despite the expected glycosuria and several changes in energy metabolism, most of the investigated nucleotides were similarly changed in humans and mice. Based on their results, the authors claimed that these metabolic processes are similarly perturbed in both species, making them interesting targets for biomarker studies in these models [130].

Changes in amino acid and carbohydrate metabolism are more closely represented by the model than those in lipid pathways

Unsurprisingly, the changes in measured carbohydrates in db/db mice were very similar to those in obese human diabetics, indicated by a clear positive but stat-

istically insignificant correlation between the effects in this pathway (Table 4.4). Here, the strong correlation is mainly driven by the glucose measures (H1 and glucose), which are surrogate markers of the hyperglycemic conditions prevalent in the diabetic groups of both species (Figure 2.1). If I exclude these two measures, the correlation of the remaining carbohydrates almost vanishes (Spearman's rho = 0.03; p-value = 1). However, because of the small number of measured carbohydrates (8), the statistical power is low and might explain the small and insignificant correlations. Irrespective of statistical significance, the blood levels of all measured carbohydrates change to the same direction in obese diabetic humans and db/db mice.

In addition to the increased glucose concentrations which basically reconfirm the hyperglycemic conditions in both species, I found increased levels of circulating fructose both in obese diabetic humans and db/db mice (Table 4.7). Increased fructose levels in human diabetics are often associated with an increased intake of fructose-sweetened beverages [158, 159]. Analogously, the higher dietary intake of db/db than control mice because of the disrupted leptin signalling axis in the knockout might explain increased fructose levels in db/db mice, although both groups received the same food. Irrespective of the causal reasons for its increased concentrations, elevated blood fructose is known to be associated both with insulin resistance and T2DM. Most importantly, in contrast to glucose, fructose uptake and turnover is insulin-independent and can be steadily metabolized in glycolysis. Moreover, fructose is involved in de-novo lipogenesis which can contribute to insulin resistance by increasing fatty acid release [158, 160].

Interestingly, the levels of mannose were significantly increased in obese diabetic versus lean healthy humans, but not in db/db mice; moreover, mannose was significantly increased between obese diabetic and obese healthy and between obese healthy and lean healthy humans, suggesting that both T2DM and obesity affect mannose levels individually (Figure 4.7). Consistent with this hypothesis, Kalhan et al. described increased levels of mannose in non-diabetic humans with NAFLD or NASH as compared to healthy controls [161]. Based on their results, the authors claimed that mannose – and other hexoses other than glucose – constitute independent risk factors for T2DM [161]. The reasons for increased mannose levels in diabetics, however, are unknown. An immoderate consumption of mannitol sweetened food

such as candy and chewing gums by obese people could be a reasonable explanation; hence, since in our setting db/db and wt mice received the same standardized, mannitol-free food, I would not expect a difference in mannose levels between these two groups.

Many amino acid metabolites behaved very similar in obese diabetic humans and db/db mice, indicated by a significant cross-species correlation (Spearman's rho = 0.47; p-value < 0.001) and a great fraction of significant changes in the same direction in humans and mice (approximately 83%). Of all pathway classes, amino acid metabolites were significantly overrepresented among shared changes. In addition, of all significantly altered amino acid metabolites, the fraction of shared changes was significantly greater than the fraction of changes unique to human or mouse. Many of the joint changes in amino acid metabolites I found in our study are already known to be markers of obesity, insulin resistance, or T2DM. In particular, increased concentrations of α-hydroxyisovalerate, branched-chain amino acids, branched-chain keto acids, tyrosine and phenylalanine, as well as decreased concentrations of glycine and serine were associated with these risk factors in human [79, 81, 82, 84, 85, 162] and rodents [163].

In contrast to carbohydrates and amino acid metabolites, the changes in lipid metabolites appeared to be more distinct within both species. I found almost no correlation in the changes of the many lipids measured in human and murine blood (Table 4.4). Considering the diversity of lipid species, it is likely that the unspecific classification is responsible for the small correlation, concealing similarities between lipid subspecies. In line with that, a subset of 17 lipids – mainly acyl-alkyl PCs – was significantly overrepresented among metabolites whose levels were decreased in both obese diabetic humans and mice as compared to their corresponding controls (Figure 4.4; Table 4.6). Similar decreases of these PCs in both species are likely to be the result of an increased turnover induced by elevated insulin levels in diabetic subjects [164]. Alteration in single other lipids, for example the eicosanoid progenitors dihomo-linolenate and docosapentaenoate, implicate pro-inflammatory reactions in both species.

Many lipids and metabolites from other pathways are uniquely affected in humans and mice

Most lipids did not jointly change in response to obesity and T2DM in both species. And even of the 39 lipids whose blood levels were significantly altered in both species, more than half displayed decreased levels in obese diabetic humans but increased levels in db/db mice relative to the corresponding controls, or vice versa (Figure 4.6). For example, the levels of several acylcarnitines including acetylcarnitine, propionyl-, butyryl- and hexanoyl-carnitine were generally higher in obese diabetic humans, while in db/db mice their levels were lower. A potential reason for these differences may be related to mitochondrial fatty acid oxidation. While in people with T2DM, raising insulin resistance leads to decreases in the capacity of mitochondrial fatty acid oxidation [165–167], it was shown that the gene transcription of key enzymes linked to mitochondrial fatty acid oxidation activity was enhanced in several rodent models of T2DM – including the db/db mouse model [166].

As one of the top hits in the human cohort, the levels of glycerol were significantly increased in obese diabetic versus lean healthy humans ($\beta = 0.14 \pm 0.02$; p-value $= 6.93 \times 10^{-10}$). However, in the db/db mouse model, I did not observe a change of glycerol (Table 4.2). Inspecting the individual effects in humans I found similarly significant effects between the obese diabetic and obese healthy groups, but not between the obese and lean healthy groups (Figure 4.7); here the interaction term of BMI and T2DM has significantly more effect on glycerol levels than both terms individually (p-value $= 4.00 \times 10^{-3}$), suggesting that the combination of obesity and T2DM is decisive for changing glycerol levels in human. The levels of circulating glycerol are indirectly regulated by insulin, as it inhibits lipolysis of triacylglycerols in adipocytes. HAGEN et al. showed that in states of decreased insulin sensitivity, lipolysis increases, which in turn leads to raised glycerol levels [168]. In the liver, glycerol can be converted to glucose in gluconeogenesis. Although I do not implicate a causal connection between altered glycerol levels with the disease physiology, considering its crucial role in connecting lipolysis with endogenous glucose metabolism, the different results for glycerol could indicate crucial differences in human and the db/db mouse model's disease physiology.

With the exception of some acyl-alkyl PCs, I found that most of the measured phospholipids (diacyl-, acyl-alkyl-, and lyso-phospholipids) changed differentially with obesity and T2DM in humans and the db/db mouse model. PCs are major integral components of the lipoproteins including High Density Lipoprotein (HDL), Low Density Lipoprotein (LDL), and Very Low Density Lipoprotein (VLDL). Marai and Kuksis revealed already in the late 1960 differences in the PC profiles of healthy humans and rodents [169]. They showed that especially the fractions of unsaturated phospholipids in plasma differ between these species. While the fraction of monoene PCs in humans was twice as high as in rats, the fraction of hexaene PCs in humans was three times smaller in humans than in rats [169]. Recently, Wiesner et al. showed that concentrations of circulating PC correlate with lipoprotein concentrations [170]. It is known that the proportions of these blood lipoproteins differ between human and rodents. While in rodents, the majority of cholesterol is carried in HDL, in humans the preferred carrier of cholesterol is LDL. In humans, the levels of HDL are typically decreased in obesity, insulin resistance, or T2DM [171]; opposite to that, I observed increased HDL concentrations in db/db mice, which is in line with results from others [172]. Taken together, it appears that many different changes in phospholipids within humans and the db/db mouse model mirrors their distinct lipoprotein metabolism.

Some metabolites from the few other pathways measured by our approach showed largely different alterations in obese diabetic humans and db/db mice. For instance, alpha-tocopherol (vitamin E) was massively increased in db/db versus wt mice, while its levels did not change in the human cohort. Vitamin E is a fat-soluble antioxidant which prevents damage by reactive oxygen species. Because oxidative stress is thought to be a crucial part of T2DM pathophysiology, vitamin E was the subject to many studies. Some suggested that vitamin E supplementation improves insulin sensitivity [173], delays the onset of T2DM, and slows down its progression [174]. Gulec et al. concluded vitamin E supplementation might have been beneficial in preventing fatty acid induced liver damage [175]. Results from other studies, however, suggest that there is no effect of vitamin E supplementation on insulin sensitivity in patients with T2DM [176]. Sesso et al. found that vitamin E treatment did not reduce the risk for cardiovascular disease, one of the major complications of T2DM [177]. Clearly, it is possible that the increased levels of vitamin E in the mouse

model are in fact just an artifact of the specific setting of the model. The standardized food used in the animal model contained 2% vitamin mix including vitamin E; hence, the increased levels of alpha-tocopherol in db/db mice might simply reflect their increased food intake in comparison to wt controls, resulting from impaired leptin signalling in db/db mice. This hypothesis could be tested using another diet that does not contain vitamin E for the db/db mouse model. Another potential reason for the different responses of alpha-tocopherol between the two species is the more severe state of T2DM and worse metabolic control in db/db mice as compared to patients with newly diagnosed T2DM as they are in the cohort. Consistent with this hypothesis, Muis et al. showed in patients with new-onset T1DM that levels of alpha-tocopherol significantly decrease with improved metabolic control and insulin treatment during the first three months; after six months, however, the levels returned to the baseline [178]. Irrespective of the potential causes for the increased levels of alpha-tocopherol in db/db mice, considering previous findings on its potential role in T2DM, I strongly suggest to consider these differences when extrapolating the results from the db/db model to humans that did not receive vitamin E supplementation.

The inherent obesity phenotype in the murine model needs to be considered when translating the metabolic changes to human

Given the large weight differences between obese diabetic and lean healthy humans and between db/db and wt mice, I wondered to what extend the observed metabolic changes reflect weight differences rather than the impact of T2DM. I found that the overall correlation between the metabolic changes in humans and the db/db mouse model was better for obesity related effects between obese healthy and lean healthy humans than for T2DM related effects between obese diabetic and obese healthy humans (Figure 4.8). Moreover, the partial overlaps of the ranked effects linked to obesity between human and the mouse model were greater than those for the effects linked to T2DM. Hence, it seemed that many of the metabolic alterations which are mimicked by the db/db model are primarily linked to the obesity phenotype rather than T2DM per se. This observation was not unexpected, because the db/db

mouse is explicitly a model for obesity linked T2DM. However, in human studies data is usually adjusted for confounding by weight differences between participants; in the db/db model, such an adjustment is not possible as the diabetes phenotype is inherently linked to the db/db knockout induced obesity phenotype. Hence, to reliably translate results from the unadjusted data from the db/db model to human, information about the individual effects of T2DM and obesity on metabolites is crucial.

For example, as one of the top hits among commonly changed metabolites, the levels of circulating glycine were greatly diminished in both species (Table 4.7); based on these results, I expected that the effect on glycine levels in the human cohort are well reflected by the db/db model. However, inspecting the effects on glycine between the obese diabetic and obese healthy groups and between the obese healthy and lean healthy groups, I found that obesity and T2DM distinctly affect the levels of glycine (Figure 4.7). In particular, the effect of T2DM on glycine levels appears to be smaller and less significant than that of obesity. In the db/db mouse model, the standardized effect on glycine levels is almost three times higher than that in humans (Figure 4.7). I have two considerations on this result: first, obesity may be the main driver of the observed decrease of glycine. This would implicate that the metabolic change in the db/db mouse model mainly reflects the bold weight difference between db/db and wt mice, putting the result in another perspective. My second consideration is that both obesity and T2DM act on glycine levels in combination rather than independently. In line with this hypothesis, I found that the interaction term of BMI and T2DM is significantly stronger associated with the changes in glycine than both terms individually ($P < 2.97 \times 10^{-2}$).

Another interesting example was creatine. The levels of circulating creatine were strongly decreased in db/db versus wt mice. In the human cohort, however, the blood levels of creatine were only slightly and insignificantly smaller in obese diabetic as compared to obese healthy controls; but between obese healthy and lean healthy humans, I found a significant positive effect on creatine levels, i.e. an effect that is opposed to the one observed in the db/db mouse model (Figure 4.7). Creatine is primarily transported to and metabolized in muscle tissue. Decreased circulating creatine in db/db mice may therefore reflect the small proportion of lean to fat body mass as compared to wild type controls. Similarly, increased levels of creatine in

obese healthy humans to the other two groups may account to a higher proportion of muscle mass in these people compared to obese diabetic or lean healthy volunteers. It is known that the BMI overestimates the fraction of fat mass in people with a high fraction of lean mass [179] and in general I expect obese healthy people to have greater muscle mass than obese diabetic people with an equal BMI. Decreased levels of creatine in db/db mice may also reflect a higher transport rate because of increased insulin secretion in these animals. Previous studies in animals have shown that insulin increases creatine uptake from the blood by an augmentation of sodium-dependent creatine transport, however, only under supraphysiological insulin concentrations [180].

I found significantly higher levels of 3-hydroxybutyrate (BHBA) in db/db mice but not in obese diabetic humans relative to the corresponding other two groups; between obese healthy and lean healthy humans, however, I found significantly decreased levels of BHBA (Figure 4.7). In addition, the individual effects have significantly greater impact on the levels of BHBA than the interaction of BMI and T2DM. These data suggest that the effect on BHBA in the human cohort is mainly obesity-related and different from that of the db/db knockout in the mouse model. Usually, small amounts of BHBA are formed during fat burning from acetyl-CoA in ketogenesis. Smaller levels of BHBA in obese humans could be therefore explained by decreased rates of fatty acid oxidation and ketogenesis in these people. One reason for that could be that obese people usually have a higher dietary intake i.e., the diet mostly covers their energy needs making the oxidation of stored lipids unnecessary. Another reason might be that obese people tend to be less physically active than lean humans. In particular, endurance sports such as running, cycling and swimming stimulates fat burning and therefore ketogenesis. High levels of circulating BHBA, however, are typically observed in people with T1DM or long term T2DM, where insufficient insulin secretion creates a persistent state of excess fat burning; hence, the greatly increased BHBA levels in db/db mice implicate an advanced state of T2DM, more severe than that in obese diabetic individuals with newly diagnosed T2DM in our cohort. Translating results in pathways related to fatty acid oxidation and ketogenesis from the db/db model to humans might therefore be biased towards a more severe disease progress in mice.

Taken together and in line with data from other studies, the application of metabolomics and the cross-species comparison of the results provide detailed definitions of clinical phenotypes. Clearly, just as the models do not recreate the full spectrum of diseases, they do not mimic the complete panel of molecular perturbations. Instead, partial concordance and discordance of metabolites likely point to commonly affected pathways and species specific alterations, indicating where the transfer of results is reliable and where it is not.

Chapter 5

Conclusion and Outlook

Type 2 Diabetes Mellitus (T2DM) is one of the most prevalent metabolic diseases world wide with its clinical complications imposing major human and financial burden on societies. The etiology of T2DM is rather complex, involving interactions between various genetic and environmental factors. Accordingly, the underlying pathogenic mechanisms are not fully understood and treatment options are still not optimal. Functional studies aiming at the investigation of the disease's causes or aiming at preclinical testing of antidiabetic drugs are primarily performed in animal models. Here, the laboratory mouse is widely considered the model organism of choice. However, in general, many findings obtained in animal models fail to replicate across strains or species, questioning their use in studying human diseases. One possible reason for the problems in reproducing and transferring results from these studies is – although they are usually well characterized on the phenotypic level – that for many models little is known about their underying molecular constitutions.

Recent developments in biotechnology led to an increasingly common application of system-wide and data-driven methods in diverse research areas. These large-scale screening methods – collectively referred to as ›omics‹ – simultaneously measure thousands of molecules from individual biological samples and thereby provide systems-level readouts of cells, tissues, or even whole organisms.

In this thesis, I took a first step towards a comprehensive investigation of the comparability of popular mouse models in T2DM and their human disease counterpart on a molecular level. To this end, I developed a generic meta-analysis workflow which allows to systematically study universal and species-specific molecular characteristics across different mouse models, or across mouse models and the corresponding human diseases based on high-throughput omics data.

In Chapter 3, I applied my workflow on liver mRNA transcriptomics data from four genetically heterogeneous mouse strains for the study of Non-Alcoholic Fatty-Liver Disease (NAFLD). Here, I could show how the small differences in the models' phenotypes are reflected in their liver transcript signatures. A major outcome of this comparative meta-analysis was that considerable parts of the genes that are significantly differentially expressed in response to the High Fat Diet (HFD) induced NAFLD phenotype are equally affected in all four genetically different strains. Moreover, among the common genomic response in the four mouse models of NAFLD, genes involved in inflammatory pathways were significantly enriched, implicating functional relevance of these genes in the disease's etiology. Since most of these genes have orthologs in humans, this strain-independent genomic response to HFD induced NAFLD might as well have functional relevance for the disease progression in humans. Accordingly, findings related to these genes and pathways obtained in one of the four models might be more likely to be transferrable to human than findings related to other genes which are less conserved across the four strains. Apart from the shared features revealed by my meta-analysis, strain-specific gene expression changes are equally important for the comprehensive molecular characterization of the strains and for ultimately judging the comparability and transferability of results across models and species. For example, small differences on the molecular level, i.e. unique expression changes of single genes, might lead to new explanations for the irreproducibility of results (e.g. drug candidates which do not replicate across models) even if the phenotypes of the models are very similar.

In Chapter 4, I adapted my workflow for the comparative analysis of blood metabolic signatures measured in the popular BKS.Cg-Dock7m+/+ Leprdb/J (db/db) mouse model for T2DM and corresponding signatures from human patients. The goal of this study was to estimate the cross-species translatability of findings obtained in this model to humans. Surprisingly, I found that the changes in blood metabolite

concentrations in the model only weakly correlated with the human data, indicating few similarities between the metabolic signature of diabetes in the db/db mouse model and human T2DM on a first glance. However, detailed inspection of the accordance of metabolites from different metabolic classes or pathways showed good correlations for the changes in carbohydrates and amino acids. In contrast, most lipids were differentially affected in the mouse model and humans, many of them being uniquely affected in one species but not the other. Taken together, my results suggest that while the db/db model mimicks metabolic aspects observed in human diabetics related to changes in carbohydrate and amino acid metabolsism, the value of the db/db model appears to be very limited for the study of disease related changes in lipid metabolism. It is important to note that the diabetes phenotype in the db/db model is strongly connected to an extreme obesity phenotype which is hardly comparable to obese humans and therefore likely to be reflected in a different molecular constitution as well. In line with that, comparing the metabolic signature of the db/db model to the signatures determined between lean diabetic and lean healthy people and between obese healthy and lean healthy people, I found that numerous effects in the model reflect rather obesity than diabetes per se.

Both, the within-species comparison of genomic responses across mouse models of NAFLD as well as the cross-species comparison of metabolic signatures in the db/db mouse model of T2DM and humans demonstrated how much such comparative studies contribute to a broader understanding of these models. Detailed knowledge about similarities and strain- or species-specific differences on the molecular level provides a more reliable basis for the interpretation of findings and their transfer to the human setting than information about phenotypic characteristics alone. In addition, it enables researchers to make better choices based on facts when searching the optimal model for working a certain scientific question.

The workflow for comparative, omics based analyses proposed in my thesis is a first step towards closing the gap which is still existent between the phenotypic descriptions of animal models and our knowledge about their molecular constitutions. Growing numbers of publicly available omics data sets from soundly described functional experiments and growing availability of computational tools for comparative studies of these datasets such as the one described here (further approaches are needed to find the optimal solution), will lead to more comprehensive descrip-

tions of animal models and finally to better informed selections of models and more replicable experiments. In addition, given the many biological layers involved in disease processes, similar analyses on data on other molecules (e.g. proteins) or measured in other tissues enable deep characterizations that are even more holistic.

Another point I want to make is that molecular characterizations do not only enable more reliable conclusion from the own research, but they might also help to interpret results from other labs and to explain why findings obtained from the same models are inconsistent across labs. Results are always achieved under the lab's very specific conditions, which are likely to be different from those of other labs. As a result, analysis of the same models in different labs almost certainly reveals different results, suggesting that the findings from the experiments are not replicable or even contradictory. From the phenotypic descriptions it is almost impossible to explain the varation of data between labs. Knowledge about the models' molecular constitutions, however, would significantly restrict the scope of potential explanations for these variations. If more labs would systematically characterize their models on the molecular level, I'm convinced that in many cases the interpretation of formerly irreproducible results would be eventually possible.

The voices of critics claiming that research has to shift back to the human system because of the rather small success rates of animal experiments have become louder in the last years. However, since functional studies and drug testing are not doable in humans for practical and ethical reasons, it should be clear to everyone that currently there is no alternative to animal studies in biomedical research. Although cumbersome and having small scientific impact at first view, I'm convinced that systematic characterizations of models' molecular constitutions as presented in this thesis provide reliable bases for knowledge transfer and are the key to higher success rates in animal research.

Bibliography

[1] Thomas Willis. Pharmaceutice Rationalis, 1975.

[2] World Health Organization and International Diabetes Federation. Definition and diagnosis of diabetes mellitus and intermediate hyperglycaemia. Technical report, World Health Organization/International Diabetes Federation, 2006. URL `http://www.who.int/diabetes/publications/diagnosis_diabetes2006/en/`.

[3] International Diabetes Federation. *IDF Diabetes Atlas - 6th edition (2014 update)*. International Diabetes Federation, Brussels, Belgium, 6th edition, 2014. URL `http://www.idf.org/diabetesatlas`.

[4] World Health Organization. WHO | Global status report on noncommunicable diseases 2014. Technical report, World Health Organization, 2014. URL `http://www.who.int/nmh/publications/ncd-status-report-2014/en/`.

[5] Goodarz Danaei, Mariel M Finucane, Yuan Lu, Gitanjali M Singh, Melanie J Cowan, Christopher J Paciorek, John K Lin, Farshad Farzadfar, Young-Ho Khang, Gretchen A Stevens, Mayuree Rao, Mohammed K Ali, Leanne M Riley, Carolyn A Robinson, and Majid Ezzati. National, regional, and global trends in fasting plasma glucose and diabetes prevalence since 1980: systematic analysis of health examination surveys and epidemiological studies with 370 country-years and $2 \cdot 7$ million participants. *Lancet*, 378(9785):31–40, July 2011. ISSN 1474-547X. doi: 10.1016/S0140-6736(11)60679-X. URL `http://www.thelancet.com/journals/a/article/PIIS0140-6736(11)60679-X/fulltext`.

[6] K G M M Alberti, P Zimmet, and J Shaw. International Diabetes Federation: a consensus on Type 2 diabetes prevention. *Diabetic medicine : a journal of the British Diabetic Association*, 24(5):451–63, May 2007. ISSN 0742-3071. doi: 10.1111/j.1464-5491.2007.02157.x. URL `http://www.ncbi.nlm.nih.gov/pubmed/17470191`.

[7] K Gu, C C Cowie, and M I Harris. Mortality in adults with and without diabetes in a national cohort of the U.S. population, 1971-1993. *Diabetes care*, 21(7):1138–45, July 1998. ISSN 0149-5992. URL `http://www.ncbi.nlm.nih.gov/pubmed/9653609`.

[8] M. J. Fowler. Microvascular and Macrovascular Complications of Diabetes. *Clinical Diabetes*, 26(2):77–82, April 2008. ISSN 0891-8929. doi: 10.2337/diaclin.26.2.77. URL `http://clinical.diabetesjournals.org/content/26/2/77.full`.

[9] WHO. World Health Organisation. Definition, Diagnosis and Classification of Diabetes Mellitus and its Complications. Part 1: Diagnosis and Classification of Diabetes Mellitus. Report of a WHO consultation. Technical report, WHO, Geneva, 1999.

[10] American Diabetes Association. Diagnosis and classification of diabetes mellitus. *Diabetes care*, 37 Suppl 1(Supplement_1):S81–90, January 2014. ISSN 1935-5548. doi: 10.2337/dc14-S081. URL `http://care.diabetesjournals.org/content/37/Supplement_1/S81.full?sid=a0e00f80-b5a8-4cf1-aaef-740b3f9fd867`.

[11] Chase Romere, Clemens Duerrschmid, Juan Bournat, Petra Constable, Mahim Jain, Fan Xia, Pradip K. Saha, Maria Del Solar, Bokai Zhu, Brian York, Poonam Sarkar, David A. Rendon, M. Waleed Gaber, Scott A. LeMaire, Joseph S. Coselli, Dianna M. Milewicz, V. Reid Sutton, Nancy F. Butte, David D. Moore, and Atul R. Chopra. Asprosin, a Fasting-Induced Glucogenic Protein Hormone. *Cell*, 165(3):566–579, 2016. ISSN 10974172. doi: 10.1016/j.cell.2016.02.063.

[12] G Roglic, S Resnikoff, K Strong, and N Unwin. Definition and diagnosis of diabetes mellitus and intermediate hyperglycaemia. *Geneva, Switzerland: World*

Health ..., 2006. URL http://www.who.int/diabetes/publications/diagnosis_diabetes2006/en/http://scholar.google.com/scholar?hl=en&btnG=Search&q=intitle:Definition+and+diagnosis+of+diabetes+mellitus+and+intermediate+hyperglycaemia#0.

[13] Glucose tolerance tests: What exactly do they involve?, October 2013. URL http://www.ncbi.nlm.nih.gov/books/PMH0072515/.

[14] Leonid Poretsky, editor. *Principles of Diabetes Mellitus*. Springer US, Boston, MA, 2010. ISBN 978-0-387-09840-1. doi: 10.1007/978-0-387-09841-8. URL http://www.springerlink.com/index/10.1007/978-0-387-09841-8.

[15] J. M. Chan, E. B. Rimm, G. A. Colditz, M. J. Stampfer, and W. C. Willett. Obesity, Fat Distribution, and Weight Gain as Risk Factors for Clinical Diabetes in Men. *Diabetes Care*, 17(9):961–969, September 1994. ISSN 0149-5992. doi: 10.2337/diacare.17.9.961. URL http://care.diabetesjournals.org/content/17/9/961.

[16] Youfa Wang, Eric B Rimm, Meir J Stampfer, Walter C Willett, and Frank B Hu. Comparison of abdominal adiposity and overall obesity in predicting risk of type 2 diabetes among men. *The American journal of clinical nutrition*, 81 (3):555–63, March 2005. ISSN 0002-9165. URL http://www.ncbi.nlm.nih.gov/pubmed/15755822.

[17] Beverley Balkau, Céline Lange, Leopold Fezeu, Jean Tichet, Blandine de Lauzon-Guillain, Sebastien Czernichow, Frederic Fumeron, Philippe Froguel, Martine Vaxillaire, Stephane Cauchi, Pierre Ducimetière, and Eveline Eschwège. Predicting diabetes: clinical, biological, and genetic approaches: data from the Epidemiological Study on the Insulin Resistance Syndrome (DESIR). *Diabetes care*, 31(10):2056–61, October 2008. ISSN 1935-5548. doi: 10.2337/dc08-0368. URL http://www.pubmedcentral.nih.gov/articlerender.fcgi?artid=2551654&tool=pmcentrez&rendertype=abstract.

[18] L O Ohlson, B Larsson, K Svärdsudd, L Welin, H Eriksson, L Wilhelmsen, P Björntorp, and G Tibblin. The influence of body fat distribution on the incidence of diabetes mellitus. 13.5 years of follow-up of the participants in

the study of men born in 1913. *Diabetes*, 34(10):1055–8, October 1985. ISSN 0012-1797. URL http://www.ncbi.nlm.nih.gov/pubmed/4043554.

[19] David W Dunstan, Jo Salmon, Neville Owen, Timothy Armstrong, Paul Z Zimmet, Timothy A Welborn, Adrian J Cameron, Terence Dwyer, Damien Jolley, and Jonathan E Shaw. Physical activity and television viewing in relation to risk of undiagnosed abnormal glucose metabolism in adults. *Diabetes care*, 27(11):2603–9, November 2004. ISSN 0149-5992. URL http://www.ncbi.nlm.nih.gov/pubmed/15504993.

[20] M Chen, R N Bergman, and D Porte. Insulin resistance and beta-cell dysfunction in aging: the importance of dietary carbohydrate. *The Journal of clinical endocrinology and metabolism*, 67(5):951–7, November 1988. ISSN 0021-972X. doi: 10.1210/jcem-67-5-951. URL http://www.ncbi.nlm.nih.gov/pubmed/3053750.

[21] Catherine Kim, Katherine M Newton, and Robert H Knopp. Gestational diabetes and the incidence of type 2 diabetes: a systematic review. *Diabetes care*, 25(10):1862–8, October 2002. ISSN 0149-5992. URL http://www.ncbi.nlm.nih.gov/pubmed/12351492.

[22] Naga Chalasani, Zobair Younossi, Joel E Lavine, Anna Mae Diehl, Elizabeth M Brunt, Kenneth Cusi, Michael Charlton, and Arun J Sanyal. The diagnosis and management of non-alcoholic fatty liver disease: practice Guideline by the American Association for the Study of Liver Diseases, American College of Gastroenterology, and the American Gastroenterological Association. *Hepatology (Baltimore, Md.)*, 55(6):2005–23, June 2012. ISSN 1527-3350. doi: 10.1002/hep.25762. URL http://www.ncbi.nlm.nih.gov/pubmed/22488764.

[23] Varman T Samuel, Zhen-Xiang Liu, Xianqin Qu, Benjamin D Elder, Stefan Bilz, Douglas Befroy, Anthony J Romanelli, and Gerald I Shulman. Mechanism of hepatic insulin resistance in non-alcoholic fatty liver disease. *The Journal of biological chemistry*, 279(31):32345–53, July 2004. ISSN 0021-9258. doi: 10.1074/jbc.M313478200. URL http://www.jbc.org/content/279/31/32345.short.

[24] Melania Gaggini, Mariangela Morelli, Emma Buzzigoli, Ralph A DeFronzo, Elisabetta Bugianesi, and Amalia Gastaldelli. Non-alcoholic fatty liver disease (NAFLD) and its connection with insulin resistance, dyslipidemia, atherosclerosis and coronary heart disease. *Nutrients*, 5(5):1544–60, May 2013. ISSN 2072-6643. doi: 10.3390/nu5051544. URL http://www.pubmedcentral.nih.gov/articlerender.fcgi?artid=3708335&tool=pmcentrez&rendertype=abstract.

[25] G. Targher, L. Bertolini, R. Padovani, S. Rodella, R. Tessari, L. Zenari, C. Day, and G. Arcaro. Prevalence of Nonalcoholic Fatty Liver Disease and Its Association With Cardiovascular Disease Among Type 2 Diabetic Patients. *Diabetes Care*, 30(5):1212–1218, February 2007. ISSN 0149-5992. doi: 10.2337/dc06-2247. URL http://www.ncbi.nlm.nih.gov/pubmed/17277038.

[26] F B Hu, R M van Dam, and S Liu. Diet and risk of Type II diabetes: the role of types of fat and carbohydrate. *Diabetologia*, 44(7):805–17, July 2001. ISSN 0012-186X. doi: 10.1007/s001250100547. URL http://www.ncbi.nlm.nih.gov/pubmed/11508264.

[27] F B Hu, J E Manson, M J Stampfer, G Colditz, S Liu, C G Solomon, and W C Willett. Diet, lifestyle, and the risk of type 2 diabetes mellitus in women. *The New England journal of medicine*, 345(11):790–7, September 2001. ISSN 0028-4793. doi: 10.1056/NEJMoa010492. URL http://www.ncbi.nlm.nih.gov/pubmed/11556298.

[28] Emmanuel Somm, Valérie M Schwitzgebel, Audrey Toulotte, Christopher R Cederroth, Christophe Combescure, Serge Nef, Michel L Aubert, and Petra S Hüppi. Perinatal exposure to bisphenol a alters early adipogenesis in the rat. *Environmental health perspectives*, 117(10):1549–55, October 2009. ISSN 1552-9924. doi: 10.1289/ehp.11342. URL http://www.pubmedcentral.nih.gov/articlerender.fcgi?artid=2790509&tool=pmcentrez&rendertype=abstract.

[29] Frederick S Vom Saal, Susan C Nagel, Benjamin L Coe, Brittany M Angle, and Julia A Taylor. The estrogenic endocrine disrupting chemical bisphenol A (BPA) and obesity. *Molecular and cellular endocrinology*, 354(1-2):74–84, May 2012. ISSN 1872-8057. doi: 10.1016/j.mce.2012.

01.001. URL http://www.pubmedcentral.nih.gov/articlerender.fcgi?artid=3306519&tool=pmcentrez&rendertype=abstract.

[30] Frédéric Guénard, Yves Deshaies, Katherine Cianflone, John G Kral, Picard Marceau, and Marie-Claude Vohl. Differential methylation in glucoregulatory genes of offspring born before vs. after maternal gastrointestinal bypass surgery. *Proceedings of the National Academy of Sciences of the United States of America*, 110(28):11439–44, July 2013. ISSN 1091-6490. doi: 10.1073/pnas.1216959110. URL http://www.pnas.org/content/110/28/11439.abstract.

[31] Anette-G Ziegler, Maike Wallner, Imme Kaiser, Michaela Rossbauer, Minna H Harsunen, Lorenz Lachmann, Jörg Maier, Christiane Winkler, and Sandra Hummel. Long-term protective effect of lactation on the development of type 2 diabetes in women with recent gestational diabetes mellitus. *Diabetes*, 61 (12):3167–71, December 2012. ISSN 1939-327X. doi: 10.2337/db12-0393. URL http://diabetes.diabetesjournals.org/content/early/2012/10/11/db12-0393.abstract.

[32] M Diamant, E E Blaak, and W M de Vos. Do nutrient-gut-microbiota interactions play a role in human obesity, insulin resistance and type 2 diabetes? *Obesity reviews : an official journal of the International Association for the Study of Obesity*, 12(4):272–81, April 2011. ISSN 1467-789X. doi: 10.1111/j.1467-789X.2010.00797.x. URL http://www.ncbi.nlm.nih.gov/pubmed/20804522.

[33] I. M Stratton. Association of glycaemia with macrovascular and microvascular complications of type 2 diabetes (UKPDS 35): prospective observational study. *BMJ*, 321(7258):405–412, August 2000. ISSN 09598138. doi: 10.1136/bmj.321.7258.405. URL http://www.bmj.com/content/321/7258/405.

[34] Ernest Adeghate, Peter Schattner, and Earl Dunn. An update on the etiology and epidemiology of diabetes mellitus. *Annals of the New York Academy of Sciences*, 1084:1–29, November 2006. ISSN 0077-8923. doi: 10.1196/annals.1372.029. URL http://www.ncbi.nlm.nih.gov/pubmed/17151290.

[35] S C Elbein, S J Hasstedt, K Wegner, and S E Kahn. Heritability of pancreatic beta-cell function among nondiabetic members of Caucasian familial type 2 diabetic kindreds. *The Journal of clinical endocrinology and metabolism*, 84 (4):1398–403, April 1999. ISSN 0021-972X. doi: 10.1210/jcem.84.4.5604. URL `http://www.ncbi.nlm.nih.gov/pubmed/10199785`.

[36] Eleftheria Zeggini, Michael N Weedon, Cecilia M Lindgren, Timothy M Frayling, Katherine S Elliott, Hana Lango, Nicholas J Timpson, John R B Perry, Nigel W Rayner, Rachel M Freathy, Jeffrey C Barrett, Beverley Shields, Andrew P Morris, Sian Ellard, Christopher J Groves, Lorna W Harries, Jonathan L Marchini, Katharine R Owen, Beatrice Knight, Lon R Cardon, Mark Walker, Graham A Hitman, Andrew D Morris, Alex S F Doney, Mark I McCarthy, and Andrew T Hattersley. Replication of genome-wide association signals in UK samples reveals risk loci for type 2 diabetes. *Science (New York, N.Y.)*, 316(5829):1336–41, June 2007. ISSN 1095-9203. doi: 10.1126/science.1142364. URL `http://www.pubmedcentral.nih.gov/articlerender.fcgi?artid=3772310&tool=pmcentrez&rendertype=abstract`.

[37] Benjamin F Voight, Laura J Scott, Valgerdur Steinthorsdottir, Andrew P Morris, Christian Dina, Ryan P Welch, Eleftheria Zeggini, Cornelia Huth, Yurii S Aulchenko, Gudmar Thorleifsson, Laura J McCulloch, Teresa Ferreira, Harald Grallert, Najaf Amin, Guanming Wu, Cristen J Willer, Soumya Raychaudhuri, Steve A McCarroll, Claudia Langenberg, Oliver M Hofmann, Josée Dupuis, Lu Qi, Ayellet V Segrè, Mandy van Hoek, Pau Navarro, Kristin Ardlie, Beverley Balkau, Rafn Benediktsson, Amanda J Bennett, Roza Blagieva, Eric Boerwinkle, Lori L Bonnycastle, Kristina Bengtsson Boström, Bert Bravenboer, Suzannah Bumpstead, Noisël P Burtt, Guillaume Charpentier, Peter S Chines, Marilyn Cornelis, David J Couper, Gabe Crawford, Alex S F Doney, Katherine S Elliott, Amanda L Elliott, Michael R Erdos, Caroline S Fox, Christopher S Franklin, Martha Ganser, Christian Gieger, Niels Grarup, Todd Green, Simon Griffin, Christopher J Groves, Candace Guiducci, Samy Hadjadj, Neelam Hassanali, Christian Herder, Bo Isomaa, Anne U Jackson, Paul R V Johnson, Torben Jø rgensen, Wen H L Kao, Norman Klopp, Augustine Kong, Peter Kraft, Johanna Kuusisto, Torsten Lauritzen, Man Li, Aloysius Lieverse, Cecilia M Lindgren, Valeriya Lyssenko,

Michel Marre, Thomas Meitinger, Kristian Midthjell, Mario A Morken, Narisu Narisu, Peter Nilsson, Katharine R Owen, Felicity Payne, John R B Perry, Ann-Kristin Petersen, Carl Platou, Christine Proença, Inga Prokopenko, Wolfgang Rathmann, N William Rayner, Neil R Robertson, Ghislain Rocheleau, Michael Roden, Michael J Sampson, Richa Saxena, Beverley M Shields, Peter Shrader, Gunnar Sigurdsson, Thomas Sparsø, Klaus Strassburger, Heather M Stringham, Qi Sun, Amy J Swift, Barbara Thorand, Jean Tichet, Tiinamaija Tuomi, Rob M van Dam, Timon W van Haeften, Thijs van Herpt, Jana V van Vliet-Ostaptchouk, G Bragi Walters, Michael N Weedon, Cisca Wijmenga, Jacqueline Witteman, Richard N Bergman, Stephane Cauchi, Francis S Collins, Anna L Gloyn, Ulf Gyllensten, Torben Hansen, Winston A Hide, Graham A Hitman, Albert Hofman, David J Hunter, Kristian Hveem, Markku Laakso, Karen L Mohlke, Andrew D Morris, Colin N A Palmer, Peter P Pramstaller, Igor Rudan, Eric Sijbrands, Lincoln D Stein, Jaakko Tuomilehto, Andre Uitterlinden, Mark Walker, Nicholas J Wareham, Richard M Watanabe, Gonçalo R Abecasis, Bernhard O Boehm, Harry Campbell, Mark J Daly, Andrew T Hattersley, Frank B Hu, James B Meigs, James S Pankow, Oluf Pedersen, H-Erich Wichmann, Inês Barroso, Jose C Florez, Timothy M Frayling, Leif Groop, Rob Sladek, Unnur Thorsteinsdottir, James F Wilson, Thomas Illig, Philippe Froguel, Cornelia M van Duijn, Kari Stefansson, David Altshuler, Michael Boehnke, and Mark I McCarthy. Twelve type 2 diabetes susceptibility loci identified through large-scale association analysis. *Nature genetics*, 42(7):579–89, July 2010. ISSN 1546-1718. doi: 10.1038/ng.609. URL `http://www.pubmedcentral.nih.gov/articlerender.fcgi?artid=3080658&tool=pmcentrez&rendertype=abstract`.

[38] Jaspal S Kooner, Danish Saleheen, Xueling Sim, Joban Sehmi, Weihua Zhang, Philippe Frossard, Latonya F Been, Kee-Seng Chia, Antigone S Dimas, Neelam Hassanali, Tazeen Jafar, Jeremy B M Jowett, Xinzhong Li, Venkatesan Radha, Simon D Rees, Fumihiko Takeuchi, Robin Young, Tin Aung, Abdul Basit, Manickam Chidambaram, Debashish Das, Elin Grundberg, Asa K Hedman, Zafar I Hydrie, Muhammed Islam, Chiea-Chuen Khor, Sudhir Kowlessur, Malene M Kristensen, Samuel Liju, Wei-Yen Lim, David R Matthews, Jianjun Liu, Andrew P Morris, Alexandra C Nica, Janani M Pinidiyapathirage,

Inga Prokopenko, Asif Rasheed, Maria Samuel, Nabi Shah, A Samad Shera, Kerrin S Small, Chen Suo, Ananda R Wickremasinghe, Tien Yin Wong, Mingyu Yang, Fan Zhang, Goncalo R Abecasis, Anthony H Barnett, Mark Caulfield, Panos Deloukas, Timothy M Frayling, Philippe Froguel, Norihiro Kato, Prasad Katulanda, M Ann Kelly, Junbin Liang, Viswanathan Mohan, Dharambir K Sanghera, James Scott, Mark Seielstad, Paul Z Zimmet, Paul Elliott, Yik Ying Teo, Mark I McCarthy, John Danesh, E Shyong Tai, and John C Chambers. Genome-wide association study in individuals of South Asian ancestry identifies six new type 2 diabetes susceptibility loci. *Nature genetics*, 43(10):984–9, October 2011. ISSN 1546-1718. doi: 10.1038/ng.921. URL `http://www.pubmedcentral.nih.gov/articlerender.fcgi?artid=3773920&tool=pmcentrez&rendertype=abstract`.

[39] Andrew P Morris, Benjamin F Voight, Tanya M Teslovich, Teresa Ferreira, Ayellet V Segrè, Valgerdur Steinthorsdottir, Rona J Strawbridge, Hassan Khan, Harald Grallert, Anubha Mahajan, Inga Prokopenko, Hyun Min Kang, Christian Dina, Tonu Esko, Ross M Fraser, Stavroula Kanoni, Ashish Kumar, Vasiliki Lagou, Claudia Langenberg, Jian'an Luan, Cecilia M Lindgren, Martina Müller-Nurasyid, Sonali Pechlivanis, N William Rayner, Laura J Scott, Steven Wiltshire, Loic Yengo, Leena Kinnunen, Elizabeth J Rossin, Soumya Raychaudhuri, Andrew D Johnson, Antigone S Dimas, Ruth J F Loos, Sailaja Vedantam, Han Chen, Jose C Florez, Caroline Fox, Ching-Ti Liu, Denis Rybin, David J Couper, Wen Hong L Kao, Man Li, Marilyn C Cornelis, Peter Kraft, Qi Sun, Rob M van Dam, Heather M Stringham, Peter S Chines, Krista Fischer, Pierre Fontanillas, Oddgeir L Holmen, Sarah E Hunt, Anne U Jackson, Augustine Kong, Robert Lawrence, Julia Meyer, John R B Perry, Carl G P Platou, Simon Potter, Emil Rehnberg, Neil Robertson, Suthesh Sivapalaratnam, Alena Stančáková, Kathleen Stirrups, Gudmar Thorleifsson, Emmi Tikkanen, Andrew R Wood, Peter Almgren, Mustafa Atalay, Rafn Benediktsson, Lori L Bonnycastle, Noël Burtt, Jason Carey, Guillaume Charpentier, Andrew T Crenshaw, Alex S F Doney, Mozhgan Dorkhan, Sarah Edkins, Valur Emilsson, Elodie Eury, Tom Forsen, Karl Gertow, Bruna Gigante, George B Grant, Christopher J Groves, Candace Guiducci, Christian Herder, Astradur B Hreidarsson, Jennie Hui, Alan James, Anna Jonsson,

Wolfgang Rathmann, Norman Klopp, Jasmina Kravic, Kaarel Krjutškov, Cordelia Langford, Karin Leander, Eero Lindholm, Stéphane Lobbens, Satu Männistö, Ghazala Mirza, Thomas W Mühleisen, Bill Musk, Melissa Parkin, Loukianos Rallidis, Jouko Saramies, Bengt Sennblad, Sonia Shah, Gunnar Sigurðsson, Angela Silveira, Gerald Steinbach, Barbara Thorand, Joseph Trakalo, Fabrizio Veglia, Roman Wennauer, Wendy Winckler, Delilah Zabaneh, Harry Campbell, Cornelia van Duijn, Andre G Uitterlinden, Albert Hofman, Eric Sijbrands, Goncalo R Abecasis, Katharine R Owen, Eleftheria Zeggini, Mieke D Trip, Nita G Forouhi, Ann-Christine Syvänen, Johan G Eriksson, Leena Peltonen, Markus M Nöthen, Beverley Balkau, Colin N A Palmer, Valeriya Lyssenko, Tiinamaija Tuomi, Bo Isomaa, David J Hunter, Lu Qi, Alan R Shuldiner, Michael Roden, Ines Barroso, Tom Wilsgaard, John Beilby, Kees Hovingh, Jackie F Price, James F Wilson, Rainer Rauramaa, Timo A Lakka, Lars Lind, George Dedoussis, Inger Njø lstad, Nancy L Pedersen, Kay-Tee Khaw, Nicholas J Wareham, Sirkka M Keinanen-Kiukaanniemi, Timo E Saaristo, Eeva Korpi-Hyövälti, Juha Saltevo, Markku Laakso, Johanna Kuusisto, Andres Metspalu, Francis S Collins, Karen L Mohlke, Richard N Bergman, Jaakko Tuomilehto, Bernhard O Boehm, Christian Gieger, Kristian Hveem, Stephane Cauchi, Philippe Froguel, Damiano Baldassarre, Elena Tremoli, Steve E Humphries, Danish Saleheen, John Danesh, Erik Ingelsson, Samuli Ripatti, Veikko Salomaa, Raimund Erbel, Karl-Heinz Jöckel, Susanne Moebus, Annette Peters, Thomas Illig, Ulf de Faire, Anders Hamsten, Andrew D Morris, Peter J Donnelly, Timothy M Frayling, Andrew T Hattersley, Eric Boerwinkle, Olle Melander, Sekar Kathiresan, Peter M Nilsson, Panos Deloukas, Unnur Thorsteinsdottir, Leif C Groop, Kari Stefansson, Frank Hu, James S Pankow, Josée Dupuis, James B Meigs, David Altshuler, Michael Boehnke, and Mark I McCarthy. Large-scale association analysis provides insights into the genetic architecture and pathophysiology of type 2 diabetes. *Nature genetics*, 44(9):981–90, September 2012. ISSN 1546-1718. doi: 10.1038/ng.2383. URL `http://www.pubmedcentral.nih.gov/articlerender.fcgi?artid=3442244&tool=pmcentrez&rendertype=abstract`.

[40] R B Tattersall. Mild familial diabetes with dominant inheritance. *The Quarterly journal of medicine*, 43(170):339–57, April 1974. ISSN 0033-5622.

URL http://www.ncbi.nlm.nih.gov/pubmed/4212169.

[41] Daphne Sl Gardner and E Shyong Tai. Clinical features and treatment of maturity onset diabetes of the young (MODY). *Diabetes, metabolic syndrome and obesity : targets and therapy*, 5: 101–8, January 2012. ISSN 1178-7007. doi: 10.2147/DMSO.S23353. URL http://www.pubmedcentral.nih.gov/articlerender.fcgi?artid=3363133&tool=pmcentrez&rendertype=abstract.

[42] Angela Galler, Thoralf Stange, Gabriele Müller, Andrea Näke, Christian Vogel, Thomas Kapellen, Heike Bartelt, Hildebrand Kunath, Rainer Koch, Wieland Kiess, and Ulrike Rothe. Incidence of childhood diabetes in children aged less than 15 years and its clinical and metabolic characteristics at the time of diagnosis: data from the Childhood Diabetes Registry of Saxony, Germany. *Hormone research in pædiatrics*, 74(4):285–91, January 2010. ISSN 1663-2826. doi: 10.1159/000303141. URL http://www.ncbi.nlm.nih.gov/pubmed/20516654.

[43] K F Eriksson and F Lindgärde. Prevention of type 2 (non-insulin-dependent) diabetes mellitus by diet and physical exercise. The 6-year Malmö feasibility study. *Diabetologia*, 34(12):891–8, December 1991. ISSN 0012-186X. URL http://www.ncbi.nlm.nih.gov/pubmed/1778354.

[44] X R Pan, G W Li, Y H Hu, J X Wang, W Y Yang, Z X An, Z X Hu, J Lin, J Z Xiao, H B Cao, P A Liu, X G Jiang, Y Y Jiang, J P Wang, H Zheng, H Zhang, P H Bennett, and B V Howard. Effects of diet and exercise in preventing NIDDM in people with impaired glucose tolerance. The Da Qing IGT and Diabetes Study. *Diabetes care*, 20(4):537–44, April 1997. ISSN 0149-5992. URL http://www.ncbi.nlm.nih.gov/pubmed/9096977.

[45] J Tuomilehto, J Lindström, J G Eriksson, T T Valle, H Hämäläinen, P Ilanne-Parikka, S Keinänen-Kiukaanniemi, M Laakso, A Louheranta, M Rastas, V Salminen, and M Uusitupa. Prevention of type 2 diabetes mellitus by changes in lifestyle among subjects with impaired glucose tolerance. *The New England journal of medicine*, 344(18):1343–50, May 2001. ISSN 0028-4793. doi: 10.1056/NEJM200105033441801. URL http://www.ncbi.nlm.nih.gov/pubmed/11333990.

[46] William C Knowler, Elizabeth Barrett-Connor, Sarah E Fowler, Richard F Hamman, John M Lachin, Elizabeth A Walker, and David M Nathan. Reduction in the incidence of type 2 diabetes with lifestyle intervention or metformin. *The New England journal of medicine*, 346(6):393–403, February 2002. ISSN 1533-4406. doi: 10.1056/NEJMoa012512. URL http://www.pubmedcentral.nih.gov/articlerender.fcgi?artid=1370926&tool=pmcentrez&rendertype=abstract.

[47] William C Knowler, Sarah E Fowler, Richard F Hamman, Costas A Christophi, Heather J Hoffman, Anne T Brenneman, Janet O Brown-Friday, Ronald Goldberg, Elizabeth Venditti, and David M Nathan. 10-year follow-up of diabetes incidence and weight loss in the Diabetes Prevention Program Outcomes Study. *Lancet*, 374(9702):1677–86, November 2009. ISSN 1474-547X. doi: 10.1016/S0140-6736(09)61457-4. URL http://www.pubmedcentral.nih.gov/articlerender.fcgi?artid=3135022&tool=pmcentrez&rendertype=abstract.

[48] Steven E Kahn, Mark E Cooper, and Stefano Del Prato. Pathophysiology and treatment of type 2 diabetes: perspectives on the past, present, and future. *Lancet*, 383(9922):1068–83, March 2014. ISSN 1474-547X. doi: 10.1016/S0140-6736(13)62154-6. URL http://www.thelancet.com/journals/a/article/PIIS0140-6736(13)62154-6/fulltext.

[49] Hans Hauner. The mode of action of thiazolidinediones. *Diabetes/metabolism research and reviews*, 18 Suppl 2:S10–5, January 2002. ISSN 1520-7552. URL http://www.ncbi.nlm.nih.gov/pubmed/11921433.

[50] UK Prospective Diabetes Study (UKPDS) Group. Intensive blood-glucose control with sulphonylureas or insulin compared with conventional treatment and risk of complications in patients with type 2 diabetes (UKPDS 33). UK Prospective Diabetes Study (UKPDS) Group. *Lancet*, 352(9131):837–53, September 1998. ISSN 0140-6736. URL http://www.ncbi.nlm.nih.gov/pubmed/9742976.

[51] Hertzel C Gerstein, Michael E Miller, Robert P Byington, David C Goff, J Thomas Bigger, John B Buse, William C Cushman, Saul Genuth, Faramarz Ismail-Beigi, Richard H Grimm, Jeffrey L Probstfield, Denise G Simons-

Morton, and William T Friedewald. Effects of intensive glucose lowering in type 2 diabetes. *The New England journal of medicine*, 358(24):2545–59, June 2008. ISSN 1533-4406. doi: 10.1056/NEJMoa0802743. URL http://www.ncbi.nlm.nih.gov/pubmed/18539917.

[52] Anushka Patel, Stephen MacMahon, John Chalmers, Bruce Neal, Laurent Billot, Mark Woodward, Michel Marre, Mark Cooper, Paul Glasziou, Diederick Grobbee, Pavel Hamet, Stephen Harrap, Simon Heller, Lisheng Liu, Giuseppe Mancia, Carl Erik Mogensen, Changyu Pan, Neil Poulter, Anthony Rodgers, Bryan Williams, Severine Bompoint, Bastiaan E de Galan, Rohina Joshi, and Florence Travert. Intensive blood glucose control and vascular outcomes in patients with type 2 diabetes. *The New England journal of medicine*, 358(24): 2560–72, June 2008. ISSN 1533-4406. doi: 10.1056/NEJMoa0802987. URL http://www.ncbi.nlm.nih.gov/pubmed/18539916.

[53] William Duckworth, Carlos Abraira, Thomas Moritz, Domenic Reda, Nicholas Emanuele, Peter D Reaven, Franklin J Zieve, Jennifer Marks, Stephen N Davis, Rodney Hayward, Stuart R Warren, Steven Goldman, Madeline McCarren, Mary Ellen Vitek, William G Henderson, and Grant D Huang. Glucose control and vascular complications in veterans with type 2 diabetes. *The New England journal of medicine*, 360(2):129–39, January 2009. ISSN 1533-4406. doi: 10.1056/NEJMoa0808431. URL http://www.ncbi.nlm.nih.gov/pubmed/19092145.

[54] Hertzel C Gerstein, Jackie Bosch, Gilles R Dagenais, Rafael Díaz, Hyejung Jung, Aldo P Maggioni, Janice Pogue, Jeffrey Probstfield, Ambady Ramachandran, Matthew C Riddle, Lars E Rydén, and Salim Yusuf. Basal insulin and cardiovascular and other outcomes in dysglycemia. *The New England journal of medicine*, 367(4):319–28, July 2012. ISSN 1533-4406. doi: 10.1056/NEJMoa1203858. URL http://www.ncbi.nlm.nih.gov/pubmed/22686416.

[55] RR Holman and SK Paul. 10-year follow-up of intensive glucose control in type 2 diabetes. *The New England journal of medicine*, 2008. URL http://www.nejm.org/doi/full/10.1056/NEJMoa0806470http://www.nejm.org/doi/full/10.1056/nejmoa0806470.

[56] Matthew C Riddle, Walter T Ambrosius, David J Brillon, John B Buse, Robert P Byington, Robert M Cohen, David C Goff, Saul Malozowski, Karen L Margolis, Jeffrey L Probstfield, Adrian Schnall, and Elizabeth R Seaquist. Epidemiologic relationships between A1C and all-cause mortality during a median 3.4-year follow-up of glycemic treatment in the ACCORD trial. *Diabetes care*, 33(5):983–90, May 2010. ISSN 1935-5548. doi: 10.2337/dc09-1278. URL http://www.pubmedcentral.nih.gov/articlerender.fcgi?artid=2858202&tool=pmcentrez&rendertype=abstract.

[57] Donna H Ryan, Mark A Espeland, Gary D Foster, Steven M Haffner, Van S Hubbard, Karen C Johnson, Steven E Kahn, William C Knowler, and Susan Z Yanovski. Look AHEAD (Action for Health in Diabetes): design and methods for a clinical trial of weight loss for the prevention of cardiovascular disease in type 2 diabetes. *Controlled clinical trials*, 24(5):610–28, October 2003. ISSN 0197-2456. URL http://www.ncbi.nlm.nih.gov/pubmed/14500058.

[58] RR Wing, P Bolin, and FL Brancati. Cardiovascular effects of intensive lifestyle intervention in type 2 diabetes. *The New England journal of medicine*, 2013. URL http://www.nejm.org/doi/full/10.1056/NEJMoa1212914http://www.ncbi.nlm.nih.gov/pubmed/23796131.

[59] Look AHEAD Research Group. Effect of a long-term behavioural weight loss intervention on nephropathy in overweight or obese adults with type 2 diabetes: a secondary analysis of the Look AHEAD. *The lancet. Diabetes & ...*, 2(10):801–9, October 2014. ISSN 2213-8595. doi: 10.1016/S2213-8587(14)70156-1. URL http://www.ncbi.nlm.nih.gov/pubmed/25127483.

[60] Rena R Wing. Long-term effects of a lifestyle intervention on weight and cardiovascular risk factors in individuals with type 2 diabetes mellitus: four-year results of the Look AHEAD trial. *Archives of internal medicine*, 170(17):1566–75, September 2010. ISSN 1538-3679. doi: 10.1001/archinternmed.2010.334. URL http://www.pubmedcentral.nih.gov/articlerender.fcgi?artid=3084497&tool=pmcentrez&rendertype=abstract.

[61] Mark A Espeland, Henry A Glick, Alain Bertoni, Frederick L Brancati, George A Bray, Jeanne M Clark, Jeffrey M Curtis, Caitlin Egan, Mary Evans, John P Foreyt, Siran Ghazarian, Edward W Gregg, Helen P Hazuda, James O

Hill, Don Hire, Edward S Horton, Van S Hubbard, John M Jakicic, Robert W Jeffery, Karen C Johnson, Steven E Kahn, Tina Killean, Abbas E Kitabchi, William C Knowler, Andrea Kriska, Cora E Lewis, Marsha Miller, Maria G Montez, Anne Murillo, David M Nathan, Ebenezer Nyenwe, Jennifer Patricio, Anne L Peters, Xavier Pi-Sunyer, Henry Pownall, J Bruce Redmon, Julia Rushing, Donna H Ryan, Monika Safford, Adam G Tsai, Thomas A Wadden, Rena R Wing, Susan Z Yanovski, and Ping Zhang. Impact of an intensive lifestyle intervention on use and cost of medical services among overweight and obese adults with type 2 diabetes: the action for health in diabetes. *Diabetes care*, 37(9):2548–56, September 2014. ISSN 1935-5548. doi: 10.2337/dc14-0093. URL `http://www.ncbi.nlm.nih.gov/pubmed/25147253`.

[62] Diego Botero and JI Wolfsdorf. Diabetes mellitus in children and adolescents. *Archives of Medical Research*, 36(3):281–90, 2005. ISSN 0188-4409. doi: 10.1016/j.arcmed.2004.12.002. URL `http://www.ncbi.nlm.nih.gov/pubmed/15925018http://www.sciencedirect.com/science/article/pii/S0188440904001808`.

[63] TODAY Study Group. Effects of metformin, metformin plus rosiglitazone, and metformin plus lifestyle on insulin sensitivity and β-cell function in TODAY. *Diabetes care*, 36(6):1749–57, June 2013. ISSN 1935-5548. doi: 10.2337/dc12-2393. URL `http://www.pubmedcentral.nih.gov/articlerender.fcgi?artid=3661836&tool=pmcentrez&rendertype=abstract`.

[64] Susanne Neschen, Markus Scheerer, Anett Seelig, Peter Huypens, Jürgen Schultheiss, Moya Wu, Wolfgang Wurst, Birgit Rathkolb, Karsten Suhre, Eckhard Wolf, Johannes Beckers, and Martin Hrabé de Angelis. Metformin supports the antidiabetic effect of a sodium glucose cotransporter 2 (SGLT2) inhibitor by suppressing endogenous glucose production in diabetic mice. *Diabetes*, July 2014. ISSN 1939-327X. doi: 10.2337/db14-0393. URL `http://www.ncbi.nlm.nih.gov/pubmed/25071027`.

[65] TODAY Study Group. A Clinical Trial to Maintain Glycemic Control in Youth with Type 2 Diabetes. *New England Journal of Medicine*, 366(24):2247–2256, 2012. ISSN 0028-4793. doi: 10.1056/NEJMoa1109333. URL `http://www.nejm.org/doi/full/10.1056/NEJMoa1109333`.

[66] David Russell-Jones and Rehman Khan. Insulin-associated weight gain in diabetes–causes, effects and coping strategies. *Diabetes, obesity & metabolism*, 9(6):799–812, November 2007. ISSN 1462-8902. doi: 10.1111/j.1463-1326.2006.00686.x. URL http://www.ncbi.nlm.nih.gov/pubmed/17924864.

[67] S Schäfer, K Kantartzis, J Machann, C Venter, A Niess, F Schick, F Machicao, H-U Häring, A Fritsche, and N Stefan. Lifestyle intervention in individuals with normal versus impaired glucose tolerance. *European journal of clinical investigation*, 37(7):535–43, July 2007. ISSN 0014-2972. doi: 10.1111/j.1365-2362.2007.01820.x. URL http://www.ncbi.nlm.nih.gov/pubmed/17576204.

[68] Richard Kahn and Mayer B Davidson. The reality of type 2 diabetes prevention. *Diabetes care*, 37(4):943–9, April 2014. ISSN 1935-5548. doi: 10.2337/dc13-1954. URL http://care.diabetesjournals.org/content/37/4/943.long.

[69] S S Deeb, L Fajas, M Nemoto, J Pihlajamäki, L Mykkänen, J Kuusisto, M Laakso, W Fujimoto, and J Auwerx. A Pro12Ala substitution in PPARgamma2 associated with decreased receptor activity, lower body mass index and improved insulin sensitivity. *Nature genetics*, 20(3):284–7, November 1998. ISSN 1061-4036. doi: 10.1038/3099. URL http://www.ncbi.nlm.nih.gov/pubmed/9806549.

[70] Richa Saxena, Benjamin F Voight, Valeriya Lyssenko, Noël P Burtt, Paul I W de Bakker, Hong Chen, Jeffrey J Roix, Sekar Kathiresan, Joel N Hirschhorn, Mark J Daly, Thomas E Hughes, Leif Groop, David Altshuler, Peter Almgren, Jose C Florez, Joanne Meyer, Kristin Ardlie, Kristina Bengtsson Boström, Bo Isomaa, Guillaume Lettre, Ulf Lindblad, Helen N Lyon, Olle Melander, Christopher Newton-Cheh, Peter Nilsson, Marju Orho-Melander, Lennart Rå stam, Elizabeth K Speliotes, Marja-Riitta Taskinen, Tiinamaija Tuomi, Candace Guiducci, Anna Berglund, Joyce Carlson, Lauren Gianniny, Rachel Hackett, Liselotte Hall, Johan Holmkvist, Esa Laurila, Marketa Sjögren, Maria Sterner, Aarti Surti, Margareta Svensson, Malin Svensson, Ryan Tewhey, Brendan Blumenstiel, Melissa Parkin, Matthew Defelice, Rachel Barry, Wendy Brodeur, Jody Camarata, Nancy Chia, Mary Fava,

John Gibbons, Bob Handsaker, Claire Healy, Kieu Nguyen, Casey Gates, Carrie Sougnez, Diane Gage, Marcia Nizzari, Stacey B Gabriel, Gung-Wei Chirn, Qicheng Ma, Hemang Parikh, Delwood Richardson, Darrell Ricke, and Shaun Purcell. Genome-wide association analysis identifies loci for type 2 diabetes and triglyceride levels. *Science (New York, N.Y.)*, 316(5829): 1331–6, June 2007. ISSN 1095-9203. doi: 10.1126/science.1142358. URL http://www.sciencemag.org/content/316/5829/1331.

[71] Jose C Florez, Alisa K Manning, Josée Dupuis, Jarred McAteer, Kathryn Irenze, Lauren Gianniny, Daniel B Mirel, Caroline S Fox, L Adrienne Cupples, and James B Meigs. A 100K genome-wide association scan for diabetes and related traits in the Framingham Heart Study: replication and integration with other genome-wide datasets. *Diabetes*, 56(12):3063–74, December 2007. ISSN 1939-327X. doi: 10.2337/db07-0451. URL http://www.ncbi.nlm.nih.gov/pubmed/17848626.

[72] Robert Sladek, Ghislain Rocheleau, Johan Rung, Christian Dina, Lishuang Shen, David Serre, Philippe Boutin, Daniel Vincent, Alexandre Belisle, Samy Hadjadj, Beverley Balkau, Barbara Heude, Guillaume Charpentier, Thomas J Hudson, Alexandre Montpetit, Alexey V Pshezhetsky, Marc Prentki, Barry I Posner, David J Balding, David Meyre, Constantin Polychronakos, and Philippe Froguel. A genome-wide association study identifies novel risk loci for type 2 diabetes. *Nature*, 445(7130):881–5, February 2007. ISSN 1476-4687. doi: 10.1038/nature05616. URL http://www.ncbi.nlm.nih.gov/pubmed/17293876.

[73] PR Burton, DG Clayton, and LR Cardon. Genome-wide association study of 14,000 cases of seven common diseases and 3,000 shared controls. *Nature*, 447(7145):661–78, June 2007. ISSN 1476-4687. doi: 10.1038/nature05911. URL http://dx.doi.org/10.1038/nature05911http://www.nature.com/nature/journal/v447/n7145/abs/nature05911.html.

[74] Laura J Scott, Karen L Mohlke, Lori L Bonnycastle, Cristen J Willer, Yun Li, William L Duren, Michael R Erdos, Heather M Stringham, Peter S Chines, Anne U Jackson, Ludmila Prokunina-Olsson, Chia-Jen Ding, Amy J Swift, Narisu Narisu, Tianle Hu, Randall Pruim, Rui Xiao, Xiao-Yi Li, Karen N Conneely, Nancy L Riebow, Andrew G Sprau, Maurine Tong, Peggy P White,

Kurt N Hetrick, Michael W Barnhart, Craig W Bark, Janet L Goldstein, Lee Watkins, Fang Xiang, Jouko Saramies, Thomas A Buchanan, Richard M Watanabe, Timo T Valle, Leena Kinnunen, Gonçalo R Abecasis, Elizabeth W Pugh, Kimberly F Doheny, Richard N Bergman, Jaakko Tuomilehto, Francis S Collins, and Michael Boehnke. A genome-wide association study of type 2 diabetes in Finns detects multiple susceptibility variants. *Science (New York, N.Y.)*, 316(5829):1341–5, June 2007. ISSN 1095-9203. doi: 10.1126/science.1142382. URL `http://www.pubmedcentral.nih.gov/articlerender.fcgi?artid=3214617&tool=pmcentrez&rendertype=abstract`.

[75] WG Feero. Genomics, type 2 diabetes, and obesity. *New England Journal of ...*, 2010. URL `http://www.nejm.org/doi/full/10.1056/NEJMra0906948http://www.nejm.org/doi/full/10.1056/nejmra0906948`.

[76] Robert A Scott, Vasiliki Lagou, Ryan P Welch, Eleanor Wheeler, May E Montasser, Jian'an Luan, Reedik Mägi, Rona J Strawbridge, Emil Rehnberg, Stefan Gustafsson, Stavroula Kanoni, Laura J Rasmussen-Torvik, Loïc Yengo, Cecile Lecoeur, Dmitry Shungin, Serena Sanna, Carlo Sidore, Paul C D Johnson, J Wouter Jukema, Toby Johnson, Anubha Mahajan, Niek Verweij, Gudmar Thorleifsson, Jouke-Jan Hottenga, Sonia Shah, Albert V Smith, Bengt Sennblad, Christian Gieger, Perttu Salo, Markus Perola, Nicholas J Timpson, David M Evans, Beate St Pourcain, Ying Wu, Jeanette S Andrews, Jennie Hui, Lawrence F Bielak, Wei Zhao, Momoko Horikoshi, Pau Navarro, Aaron Isaacs, Jeffrey R O'Connell, Kathleen Stirrups, Veronique Vitart, Caroline Hayward, Tõnu Esko, Evelin Mihailov, Ross M Fraser, Tove Fall, Benjamin F Voight, Soumya Raychaudhuri, Han Chen, Cecilia M Lindgren, Andrew P Morris, Nigel W Rayner, Neil Robertson, Denis Rybin, Ching-Ti Liu, Jacques S Beckmann, Sara M Willems, Peter S Chines, Anne U Jackson, Hyun Min Kang, Heather M Stringham, Kijoung Song, Toshiko Tanaka, John F Peden, Anuj Goel, Andrew A Hicks, Ping An, Martina Müller-Nurasyid, Anders Franco-Cereceda, Lasse Folkersen, Letizia Marullo, Hanneke Jansen, Albertine J Oldehinkel, Marcel Bruinenberg, James S Pankow, Kari E North, Nita G Forouhi, Ruth J F Loos, Sarah Edkins, Tibor V Varga, Göran Hallmans, Heikki Oksa, Mulas Antonella, Ramaiah Nagaraja, Stella Trompet, Ian Ford, Stephan J L Bakker, Augustine Kong, Meena Kumari,

Bruna Gigante, Christian Herder, Patricia B Munroe, Mark Caulfield, Jula Antti, Massimo Mangino, Kerrin Small, Iva Miljkovic, Yongmei Liu, Mustafa Atalay, Wieland Kiess, Alan L James, Fernando Rivadeneira, Andre G Uitterlinden, Colin N A Palmer, Alex S F Doney, Gonneke Willemsen, Johannes H Smit, Susan Campbell, Ozren Polasek, Lori L Bonnycastle, Serge Hercberg, Maria Dimitriou, Jennifer L Bolton, Gerard R Fowkes, Peter Kovacs, Jaana Lindström, Tatijana Zemunik, Stefania Bandinelli, Sarah H Wild, Hanneke V Basart, Wolfgang Rathmann, Harald Grallert, Winfried Maerz, Marcus E Kleber, Bernhard O Boehm, Annette Peters, Peter P Pramstaller, Michael A Province, Ingrid B Borecki, Nicholas D Hastie, Igor Rudan, Harry Campbell, Hugh Watkins, Martin Farrall, Michael Stumvoll, Luigi Ferrucci, Dawn M Waterworth, Richard N Bergman, Francis S Collins, Jaakko Tuomilehto, Richard M Watanabe, Eco J C de Geus, Brenda W Penninx, Albert Hofman, Ben A Oostra, Bruce M Psaty, Peter Vollenweider, James F Wilson, Alan F Wright, G Kees Hovingh, Andres Metspalu, Matti Uusitupa, Patrik K E Magnusson, Kirsten O Kyvik, Jaakko Kaprio, Jackie F Price, George V Dedoussis, Panos Deloukas, Pierre Meneton, Lars Lind, Michael Boehnke, Alan R Shuldiner, Cornelia M van Duijn, Andrew D Morris, Anke Toenjes, Patricia A Peyser, John P Beilby, Antje Körner, Johanna Kuusisto, Markku Laakso, Stefan R Bornstein, Peter E H Schwarz, Timo A Lakka, Rainer Rauramaa, Linda S Adair, George Davey Smith, Tim D Spector, Thomas Illig, Ulf de Faire, Anders Hamsten, Vilmundur Gudnason, Mika Kivimaki, Aroon Hingorani, Sirkka M Keinanen-Kiukaanniemi, Timo E Saaristo, Dorret I Boomsma, Kari Stefansson, Pim van der Harst, Josée Dupuis, Nancy L Pedersen, Naveed Sattar, Tamara B Harris, Francesco Cucca, Samuli Ripatti, Veikko Salomaa, Karen L Mohlke, Beverley Balkau, Philippe Froguel, Anneli Pouta, Marjo-Riitta Jarvelin, Nicholas J Wareham, Nabila Bouatia-Naji, Mark I McCarthy, Paul W Franks, James B Meigs, Tanya M Teslovich, Jose C Florez, Claudia Langenberg, Erik Ingelsson, Inga Prokopenko, and Inês Barroso. Large-scale association analyses identify new loci influencing glycemic traits and provide insight into the underlying biological pathways. *Nature genetics*, 44(9):991–1005, September 2012. ISSN 1546-1718. doi: 10.1038/ng.2385. URL `http://www.pubmedcentral.nih.gov/articlerender.fcgi?artid=3433394&tool=pmcentrez&rendertype=abstract`.

[77] Hon-Cheong So, Benjamin H K Yip, and Pak Chung Sham. Estimating the total number of susceptibility variants underlying complex diseases from genome-wide association studies. *PloS one*, 5(11): e13898, January 2010. ISSN 1932-6203. doi: 10.1371/journal.pone.0013898. URL http://www.pubmedcentral.nih.gov/articlerender.fcgi?artid=2984437&tool=pmcentrez&rendertype=abstract.

[78] Kyong Soo Park. The search for genetic risk factors of type 2 diabetes mellitus. *Diabetes & metabolism journal*, 35(1):12–22, February 2011. ISSN 2233-6087. doi: 10.4093/dmj.2011.35.1.12. URL http://synapse.koreamed.org/DOIx.php?id=10.4093/dmj.2011.35.1.12.

[79] Karsten Suhre, Christa Meisinger, Angela Döring, Elisabeth Altmaier, Petra Belcredi, Christian Gieger, David Chang, Michael V Milburn, Walter E Gall, Klaus M Weinberger, Hans-Werner Mewes, Martin Hrabé de Angelis, H-Erich Wichmann, Florian Kronenberg, Jerzy Adamski, and Thomas Illig. Metabolic footprint of diabetes: a multiplatform metabolomics study in an epidemiological setting. *PloS one*, 5(11):e13953, January 2010. ISSN 1932-6203. doi: 10.1371/journal.pone.0013953. URL http://dx.plos.org/10.1371/journal.pone.0013953http://www.pubmedcentral.nih.gov/articlerender.fcgi?artid=2978704&tool=pmcentrez&rendertype=abstracthttp://www.plosone.org/article/info:doi/10.1371/journal.pone.0013953#s1.

[80] Oliver Fiehn, W Timothy Garvey, John W Newman, Kerry H Lok, Charles L Hoppel, and Sean H Adams. Plasma metabolomic profiles reflective of glucose homeostasis in non-diabetic and type 2 diabetic obese African-American women. *PloS one*, 5(12): e15234, January 2010. ISSN 1932-6203. doi: 10.1371/journal.pone.0015234. URL http://www.pubmedcentral.nih.gov/articlerender.fcgi?artid=3000813&tool=pmcentrez&rendertype=abstract.

[81] Thomas J TJ Wang, Martin G MG Larson, RS Ramachandran S Vasan, Susan Cheng, Eugene P Rhee, Elizabeth McCabe, Gregory D Lewis, Caroline S Fox, Paul F Jacques, Céline Fernandez, Christopher J O'Donnell, Stephen a Carr, Vamsi K Mootha, Jose C Florez, Amanda

Souza, Olle Melander, Clary B Clish, and Robert E Gerszten. Metabolite profiles and the risk of developing diabetes. *Nature medicine*, 17(4):448–53, April 2011. ISSN 1546-170X. doi: 10.1038/nm.2307. URL http://www.pubmedcentral.nih.gov/articlerender.fcgi?artid=3126616&tool=pmcentrez&rendertype=abstracthttp://www.nature.com/nm/journal/v17/n4/abs/nm.2307.html.

[82] Cristina Menni, Eric Fauman, Idil Erte, John R B Perry, Gabi Kastenmüller, So-Youn Shin, Ann-Kristin Petersen, Craig Hyde, Maria Psatha, Kirsten J Ward, Wei Yuan, Mike Milburn, Colin N A Palmer, Timothy M Frayling, Jeff Trimmer, Jordana T Bell, Christian Gieger, Rob Mohney, Mary Julia Brosnan, Karsten Suhre, Nicole Soranzo, and Tim D Spector. Biomarkers for type 2 diabetes and impaired fasting glucose using a non-targeted metabolomics approach. *Diabetes*, pages db13–0570–, July 2013. ISSN 1939-327X. doi: 10.2337/db13-0570. URL http://diabetes.diabetesjournals.org/content/early/2013/07/17/db13-0570.abstract?sid=5f95a364-db80-4701-80ef-24f447402afe.

[83] Xinjie Zhao, Jens Fritsche, Jiangshan Wang, Jing Chen, Kilian Rittig, Philippe Schmitt-Kopplin, Andreas Fritsche, Hans-Ulrich Häring, Erwin D Schleicher, Guowang Xu, and Rainer Lehmann. Metabonomic fingerprints of fasting plasma and spot urine reveal human pre-diabetic metabolic traits. *Metabolomics : Official journal of the Metabolomic Society*, 6(3): 362–374, September 2010. ISSN 1573-3882. doi: 10.1007/s11306-010-0203-1. URL http://www.pubmedcentral.nih.gov/articlerender.fcgi?artid=2899018&tool=pmcentrez&rendertype=abstract.

[84] Rui Wang-Sattler, Zhonghao Yu, Christian Herder, Ana C Messias, Anna Floegel, Ying He, Katharina Heim, Monica Campillos, Christina Holzapfel, Barbara Thorand, Harald Grallert, Tao Xu, Erik Bader, Cornelia Huth, Kirstin Mittelstrass, Angela Döring, Christa Meisinger, Christian Gieger, Cornelia Prehn, Werner Roemisch-Margl, Maren Carstensen, Lu Xie, Hisami Yamanaka-Okumura, Guihong Xing, Uta Ceglarek, Joachim Thiery, Guido Giani, Heiko Lickert, Xu Lin, Yixue Li, Heiner Boeing, Hans-Georg Joost, Martin Hrabé de Angelis, Wolfgang Rathmann, Karsten Suhre, Hol-

ger Prokisch, Annette Peters, Thomas Meitinger, Michael Roden, H-Erich Wichmann, Tobias Pischon, Jerzy Adamski, and Thomas Illig. Novel biomarkers for pre-diabetes identified by metabolomics. *Molecular systems biology*, 8(615):615, September 2012. ISSN 1744-4292. doi: 10.1038/msb.2012.43. URL http://www.pubmedcentral.nih.gov/articlerender.fcgi?artid=3472689&tool=pmcentrez&rendertype=abstract.

[85] Christopher B Newgard, Jie An, James R Bain, Michael J Muehlbauer, Robert D Stevens, Lillian F Lien, Andrea M Haqq, Svati H Shah, Michelle Arlotto, Cris a Slentz, James Rochon, Dianne Gallup, Olga Ilkayeva, Brett R Wenner, William S Yancy, Howard Eisenson, Gerald Musante, Richard S Surwit, David S Millington, Mark D Butler, and Laura P Svetkey. A branched-chain amino acid-related metabolic signature that differentiates obese and lean humans and contributes to insulin resistance. *Cell metabolism*, 9(4):311–26, April 2009. ISSN 1932-7420. doi: 10.1016/j.cmet.2009.02.002. URL http://www.pubmedcentral.nih.gov/articlerender.fcgi?artid=3640280&tool=pmcentrez&rendertype=abstracthttp://www.ncbi.nlm.nih.gov/pubmed/19356713.

[86] Carolin Jourdan, Ann-Kristin Petersen, Christian Gieger, Angela Döring, Thomas Illig, Rui Wang-Sattler, Christa Meisinger, Annette Peters, Jerzy Adamski, Cornelia Prehn, Karsten Suhre, Elisabeth Altmaier, Gabi Kastenmüller, Werner Römisch-Margl, Fabian J Theis, Jan Krumsiek, H-Erich Wichmann, and Jakob Linseisen. Body fat free mass is associated with the serum metabolite profile in a population-based study. *PloS one*, 7(6):e40009, January 2012. ISSN 1932-6203. doi: 10.1371/journal.pone.0040009. URL http://dx.plos.org/10.1371/journal.pone.0040009.

[87] S. E. Mccormack, O. Shaham, M. A. Mccarthy, A. A. Deik, T. J. Wang, R. E. Gerszten, C. B. Clish, V. K. Mootha, S. K. Grinspoon, and A. Fleischman. Circulating branched-chain amino acid concentrations are associated with obesity and future insulin resistance in children and adolescents. *Pediatric Obesity*, 8(1):52–61, 2013. ISSN 20476302. doi: 10.1111/j.20I47-6T310.2012.Y00087.x. URL http://www.scopus.com/inward/record.url?eid=2-s2.0-84874800752&partnerID=tZOtx3y1.

[88] Rainer Lehmann, Holger Franken, Sascha Dammeier, Lars Rosenbaum, Konstantinos Kantartzis, Andreas Peter, Andreas Zell, Patrick Adam, Jia Li, Guowang Xu, Alfred Königsrainer, Jürgen Machann, Fritz Schick, Martin Hrabé de Angelis, Matthias Schwab, Harald Staiger, Erwin Schleicher, Amalia Gastaldelli, Andreas Fritsche, Hans-Ulrich Häring, and Norbert Stefan. Circulating lysophosphatidylcholines are markers of a metabolically benign nonalcoholic fatty liver. *Diabetes care*, 36(8):2331–8, August 2013. ISSN 1935-5548. doi: 10.2337/dc12-1760. URL `http://care.diabetesjournals.org/content/36/8/2331.long`.

[89] Md Shahidul Islam and Du Toit Loots. Experimental rodent models of type 2 diabetes: a review. *Methods and findings in experimental and clinical pharmacology*, 31(4):249–61, May 2009. ISSN 0379-0355. doi: 10.1358/mf.2009.31.4.1362513. URL `http://www.ncbi.nlm.nih.gov/pubmed/19557203`.

[90] K P Hummel, M M Dickie, and D L Coleman. Diabetes, a new mutation in the mouse. *Science (New York, N.Y.)*, 153(3740):1127–8, September 1966. ISSN 0036-8075. URL `http://www.ncbi.nlm.nih.gov/pubmed/5918576`.

[91] Y Zhang, R Proenca, M Maffei, M Barone, L Leopold, and J M Friedman. Positional cloning of the mouse obese gene and its human homologue. *Nature*, 372(6505):425–32, December 1994. ISSN 0028-0836. doi: 10.1038/372425a0. URL `http://www.ncbi.nlm.nih.gov/pubmed/7984236`.

[92] H Chen, O Charlat, L A Tartaglia, E A Woolf, X Weng, S J Ellis, N D Lakey, J Culpepper, K J Moore, R E Breitbart, G M Duyk, R I Tepper, and J P Morgenstern. Evidence that the diabetes gene encodes the leptin receptor: identification of a mutation in the leptin receptor gene in db/db mice. *Cell*, 84(3):491–5, February 1996. ISSN 0092-8674. URL `http://www.ncbi.nlm.nih.gov/pubmed/8608603`.

[93] Peter J Havel. Update on adipocyte hormones: regulation of energy balance and carbohydrate/lipid metabolism. *Diabetes*, 53 Suppl 1:S143–51, March 2004. ISSN 0012-1797. URL `http://www.ncbi.nlm.nih.gov/pubmed/14749280`.

[94] Kang Uk Yun, Chang Seon Ryu, Ji-Yoon Lee, Jung-Ran Noh, Chul-Ho Lee, Hyun-Sun Lee, Jong Soon Kang, Song Kyu Park, Bong-Hee Kim, and Sang Kyum Kim. Hepatic metabolism of sulfur amino acids in db/db mice. *Food and chemical toxicology : an international journal published for the British Industrial Biological Research Association*, 53:180–6, March 2013. ISSN 1873-6351. doi: 10.1016/j.fct.2012.11.046. URL `http://www.ncbi.nlm.nih.gov/pubmed/23220616`.

[95] Jung Han Kim, Taryn P Stewart, Weidong Zhang, Hyoung Yon Kim, Patsy M Nishina, and Jürgen K Naggert. Type 2 diabetes mouse model TallyHo carries an obesity gene on chromosome 6 that exaggerates dietary obesity. *Physiological genomics*, 22(2):171–81, July 2005. ISSN 1531-2267. doi: 10.1152/physiolgenomics.00197.2004. URL `http://www.ncbi.nlm.nih.gov/pubmed/15870394`.

[96] Edward H Leiter. Selecting the "right" mouse model for metabolic syndrome and type 2 diabetes research. *Methods in molecular biology (Clifton, N.J.)*, 560:1–17, January 2009. ISSN 1940-6029. doi: 10.1007/978-1-59745-448-3_1. URL `http://www.ncbi.nlm.nih.gov/pubmed/19504239`.

[97] Hyun-Jin Kim, Jin Hee Kim, Siwon Noh, Haeng Jeon Hur, Mi Jeong Sung, Jin-Taek Hwang, Jae Ho Park, Hye Jeong Yang, Myung-Sunny Kim, Dae Young Kwon, and Suk Hoo Yoon. Metabolomic analysis of livers and serum from high-fat diet induced obese mice. *Journal of proteome research*, 10(2):722–31, February 2011. ISSN 1535-3907. doi: 10.1021/pr100892r. URL `http://www.ncbi.nlm.nih.gov/pubmed/21047143`.

[98] Anatole Ghazalpour, Brian Bennett, Vladislav a Petyuk, Luz Orozco, Raffi Hagopian, Imran N Mungrue, Charles R Farber, Janet Sinsheimer, Hyun M Kang, Nicholas Furlotte, Christopher C Park, Ping-Zi Wen, Heather Brewer, Karl Weitz, David G Camp, Calvin Pan, Roumyana Yordanova, Isaac Neuhaus, Charles Tilford, Nathan Siemers, Peter Gargalovic, Eleazar Eskin, Todd Kirchgessner, Desmond J Smith, Richard D Smith, and Aldons J Lusis. Comparative analysis of proteome and transcriptome variation in mouse. *PLoS genetics*, 7(6):e1001393, June 2011. ISSN 1553-7404. doi: 10.1371/journal.

pgen.1001393. URL http://www.pubmedcentral.nih.gov/articlerender.fcgi?artid=3111477&tool=pmcentrez&rendertype=abstract.

[99] Michael S Simonson, Margaret Tiktin, Sara M Debanne, Mahboob Rahman, Bruce Berger, Donald Hricik, and Faramarz Ismail-Beigi. The renal transcriptome of db/db mice identifies putative urinary biomarker proteins in patients with type 2 diabetes: a pilot study. *American journal of physiology. Renal physiology*, 302(7):F820–9, April 2012. ISSN 1522-1466. doi: 10.1152/ajprenal.00424.2011. URL http://www.pubmedcentral.nih.gov/articlerender.fcgi?artid=3340934&tool=pmcentrez&rendertype=abstract.

[100] Marcel Leist and Thomas Hartung. Inflammatory findings on species extrapolations: humans are definitely no 70-kg mice. *Archives of toxicology*, 87(4):563–7, April 2013. ISSN 1432-0738. doi: 10.1007/s00204-013-1038-0. URL http://www.pubmedcentral.nih.gov/articlerender.fcgi?artid=3604596&tool=pmcentrez&rendertype=abstract.

[101] Chris Church, Sheena Lee, Eleanor A L Bagg, James S McTaggart, Robert Deacon, Thomas Gerken, Angela Lee, Lee Moir, Jasmin Mecinović, Mohamed M Quwailid, Christopher J Schofield, Frances M Ashcroft, and Roger D Cox. A mouse model for the metabolic effects of the human fat mass and obesity associated FTO gene. *PLoS genetics*, 5(8):e1000599, August 2009. ISSN 1553-7404. doi: 10.1371/journal.pgen.1000599. URL http://www.pubmedcentral.nih.gov/articlerender.fcgi?artid=2719869&tool=pmcentrez&rendertype=abstract.

[102] Chris Church, Lee Moir, Fiona McMurray, Christophe Girard, Gareth T Banks, Lydia Teboul, Sara Wells, Jens C Brüning, Patrick M Nolan, Frances M Ashcroft, and Roger D Cox. Overexpression of Fto leads to increased food intake and results in obesity. *Nature genetics*, 42(12):1086–92, December 2010. ISSN 1546-1718. doi: 10.1038/ng.713. URL http://www.pubmedcentral.nih.gov/articlerender.fcgi?artid=3018646&tool=pmcentrez&rendertype=abstract.

[103] N Wijesekara, F F Dai, A B Hardy, P R Giglou, A Bhattacharjee, V Koshkin, F Chimienti, H Y Gaisano, G A Rutter, and M B Wheeler. Beta cell-specific

Znt8 deletion in mice causes marked defects in insulin processing, crystallisation and secretion. *Diabetologia*, 53(8):1656–68, August 2010. ISSN 1432-0428. doi: 10.1007/s00125-010-1733-9. URL http://www.ncbi.nlm.nih.gov/pubmed/20424817.

[104] Roger D Cox and Christopher D Church. Mouse models and the interpretation of human GWAS in type 2 diabetes and obesity. *Disease models & mechanisms*, 4(2):155–64, March 2011. ISSN 1754-8411. doi: 10.1242/dmm.000414. URL http://www.pubmedcentral.nih.gov/articlerender.fcgi?artid=3046087&tool=pmcentrez&rendertype=abstract.

[105] Joshua K Hartshorne and Adena Schachner. Tracking replicability as a method of post-publication open evaluation. *Frontiers in computational neuroscience*, 6:8, January 2012. ISSN 1662-5188. doi: 10.3389/fncom.2012.00008. URL http://www.pubmedcentral.nih.gov/articlerender.fcgi?artid=3293145&tool=pmcentrez&rendertype=abstract.

[106] C Glenn Begley and Lee M Ellis. Drug development: Raise standards for preclinical cancer research. *Nature*, 483(7391):531–3, March 2012. ISSN 1476-4687. doi: 10.1038/483531a. URL http://dx.doi.org/10.1038/483531a.

[107] Leonard P. Freedman, Iain M. Cockburn, and Timothy S. Simcoe. The Economics of Reproducibility in Preclinical Research. *PLOS Biology*, 13 (6):e1002165, June 2015. ISSN 1545-7885. doi: 10.1371/journal.pbio.1002165. URL http://journals.plos.org/plosbiology/article?id=10.1371/journal.pbio.1002165.

[108] Sean Scott, Janice E Kranz, Jeff Cole, John M Lincecum, Kenneth Thompson, Nancy Kelly, Alan Bostrom, Jill Theodoss, Bashar M Al-Nakhala, Fernando G Vieira, Jeyanthi Ramasubbu, and James A Heywood. Design, power, and interpretation of studies in the standard murine model of ALS. *Amyotrophic lateral sclerosis : official publication of the World Federation of Neurology Research Group on Motor Neuron Diseases*, 9(1):4–15, January 2008. ISSN 1471-180X. doi: 10.1080/17482960701856300. URL http://www.ncbi.nlm.nih.gov/pubmed/18273714.

[109] Javier Mestas and Christopher C W Hughes. Of mice and not men: differences between mouse and human immunology. *Journal of immunology (Baltimore, Md. : 1950)*, 172(5):2731–8, March 2004. ISSN 0022-1767. URL http://www.ncbi.nlm.nih.gov/pubmed/14978070.

[110] M Lai, P C Chandrasekera, and N D Barnard. You are what you eat, or are you? The challenges of translating high-fat-fed rodents to human obesity and diabetes. *Nutrition & diabetes*, 4:e135, January 2014. ISSN 2044-4052. doi: 10.1038/nutd.2014.30. URL http://www.ncbi.nlm.nih.gov/pubmed/25198237.

[111] Ulrich Dirnagl. Modeling immunity and inflammation in stroke: can mice be trusted? *Stroke; a journal of cerebral circulation*, 45(9):e177–8, September 2014. ISSN 1524-4628. doi: 10.1161/STROKEAHA.114.005640. URL http://www.ncbi.nlm.nih.gov/pubmed/25061077.

[112] Junhee Seok, H Shaw Warren, Alex G Cuenca, Michael N Mindrinos, Henry V Baker, Weihong Xu, Daniel R Richards, Grace P McDonald-Smith, Hong Gao, Laura Hennessy, Celeste C Finnerty, Cecilia M López, Shari Honari, Ernest E Moore, Joseph P Minei, Joseph Cuschieri, Paul E Bankey, Jeffrey L Johnson, Jason Sperry, Avery B Nathens, Timothy R Billiar, Michael a West, Marc G Jeschke, Matthew B Klein, Richard L Gamelli, Nicole S Gibran, Bernard H Brownstein, Carol Miller-Graziano, Steve E Calvano, Philip H Mason, J Perren Cobb, Laurence G Rahme, Stephen F Lowry, Ronald V Maier, Lyle L Moldawer, David N Herndon, Ronald W Davis, Wenzhong Xiao, and Ronald G Tompkins. Genomic responses in mouse models poorly mimic human inflammatory diseases. *PNAS*, 110(9):3507–12, February 2013. ISSN 1091-6490. doi: 10.1073/pnas.1222878110. URL http://www.pnas.org/content/early/2013/02/07/1222878110http://www.pubmedcentral.nih.gov/articlerender.fcgi?artid=3587220&tool=pmcentrez&rendertype=abstract.

[113] Christina A Harrington, Carsten Rosenow, and Jacques Retief. Monitoring gene expression using DNA microarrays. *Current Opinion in Microbiology*, 3(3):285–291, June 2000. ISSN 13695274. doi: 10.1016/S1369-5274(00)

00091-6. URL http://www.sciencedirect.com/science/article/pii/S1369527400000916.

[114] R J Lipshutz, S P Fodor, T R Gingeras, and D J Lockhart. High density synthetic oligonucleotide arrays. *Nature genetics*, 21(1 Suppl):20–4, January 1999. ISSN 1061-4036. doi: 10.1038/4447. URL http://www.ncbi.nlm.nih.gov/pubmed/9915496.

[115] J K Nicholson, M P O'Flynn, P J Sadler, A F Macleod, S M Juul, and P H Sönksen. Proton-nuclear-magnetic-resonance studies of serum, plasma and urine from fasting normal and diabetic subjects. *The Biochemical journal*, 217(2):365–75, January 1984. ISSN 0264-6021. URL http://www.pubmedcentral.nih.gov/articlerender.fcgi?artid=1153226&tool=pmcentrez&rendertype=abstract.

[116] Jeremy K Nicholson and Ian D Wilson. Opinion: understanding 'global' systems biology: metabonomics and the continuum of metabolism. *Nature reviews. Drug discovery*, 2(8):668–76, August 2003. ISSN 1474-1776. doi: 10.1038/nrd1157. URL http://www.ncbi.nlm.nih.gov/pubmed/12904817.

[117] Eva Maria Lenz and Ian D Wilson. Analytical strategies in metabonomics. *Journal of proteome research*, 6(2):443–58, February 2007. ISSN 1535-3893. doi: 10.1021/pr0605217. URL http://dx.doi.org/10.1021/pr0605217.

[118] Katja Dettmer. Mass spectrometry-based metabolomics. *Mass spectrometry ...*, 26(1):51–78, 2007. ISSN 0277-7037. doi: 10.1002/mas.20108. URL http://www.pubmedcentral.nih.gov/articlerender.fcgi?artid=1904337&tool=pmcentrez&rendertype=abstracthttp://onlinelibrary.wiley.com/doi/10.1002/mas.20108/full.

[119] B Blümich. *Essential NMR for scientists and engineers*. Springer, 2005 edition, 2005. URL http://www.springer.com/chemistry/analytical+chemistry/book/978-3-540-23605-4http://agris.fao.org/agris-search/search.do?recordID=US201300103524.

[120] Gary J Patti, Oscar Yanes, and Gary Siuzdak. Innovation: Metabolomics: the apogee of the omics trilogy. *Nature reviews. Molecular cell biology*, 13

(4):263–9, April 2012. ISSN 1471-0080. doi: 10.1038/nrm3314. URL http://dx.doi.org/10.1038/nrm3314.

[121] James R Bain, Robert D Stevens, Brett R Wenner, Olga Ilkayeva, Deborah M Muoio, and Christopher B Newgard. Metabolomics applied to diabetes research: moving from information to knowledge. *Diabetes*, 58(11):2429–43, November 2009. ISSN 1939-327X. doi: 10.2337/db09-0580. URL http://www.pubmedcentral.nih.gov/articlerender.fcgi?artid=2768174&tool=pmcentrez&rendertype=abstract.

[122] Ron Edgar, Michael Domrachev, and Alex E Lash. Gene Expression Omnibus: NCBI gene expression and hybridization array data repository. *Nucleic acids research*, 30(1):207–10, January 2002. ISSN 1362-4962. URL http://www.pubmedcentral.nih.gov/articlerender.fcgi?artid=99122&tool=pmcentrez&rendertype=abstract.

[123] Xiangqun Zheng-Bradley, Johan Rung, Helen Parkinson, and Alvis Brazma. Large scale comparison of global gene expression patterns in human and mouse. *Genome Biology*, 11(12):R124, January 2010. ISSN 1465-6906. doi: 10.1186/gb-2010-11-12-r124. URL http://www.pubmedcentral.nih.gov/articlerender.fcgi?artid=3046484&tool=pmcentrez&rendertype=abstract.

[124] Eun-Soo Han and Morgen Hickey. Microarray Evaluation of Dietary Restriction. *J. Nutr.*, 135(6):1343–1346, June 2005. URL http://jn.nutrition.org/content/135/6/1343.abstract.

[125] A. Kumar, M.A. Higgins, J.N. Calley, S.M. McAhren, B.W. Halstead, E.R. Dow, H. Gao, and G.H. Searfoss. Abstracting Genes to Gene Ontology Terms Allows Comparison across Multiple Species. In *18th International Conference on Systems Engineering (ICSEng'05)*, pages 320–325. IEEE, 2005. ISBN 0-7695-2359-5. doi: 10.1109/ICSENG.2005.14. URL http://ieeexplore.ieee.org/lpdocs/epic03/wrapper.htm?arnumber=1562872.

[126] Y Tang, A Lu, B J Aronow, and F R Sharp. Blood genomic responses differ after stroke, seizures, hypoglycemia, and hypoxia: blood genomic fingerprints

of disease. *Annals of neurology*, 50(6):699–707, December 2001. ISSN 0364-5134. URL http://www.ncbi.nlm.nih.gov/pubmed/11761467.

[127] Boryana Stamova, Huichun Xu, Glen Jickling, Cheryl Bushnell, Yingfang Tian, Bradley P Ander, Xinhua Zhan, Dazhi Liu, Renee Turner, Peter Adamczyk, Jane C Khoury, Arthur Pancioli, Edward Jauch, Joseph P Broderick, and Frank R Sharp. Gene expression profiling of blood for the prediction of ischemic stroke. *Stroke; a journal of cerebral circulation*, 41(10): 2171–7, October 2010. ISSN 1524-4628. doi: 10.1161/STROKEAHA.110.588335. URL http://www.pubmedcentral.nih.gov/articlerender.fcgi?artid=2987675&tool=pmcentrez&rendertype=abstract.

[128] Theo Hatzipetros, Laurent P Bogdanik, Valerie R Tassinari, Joshua D Kidd, Andy J Moreno, Crystal Davis, Melissa Osborne, Andrew Austin, Fernando G Vieira, Cathleen Lutz, and Steve Perrin. C57BL/6J congenic Prp-TDP43A315T mice develop progressive neurodegeneration in the myenteric plexus of the colon without exhibiting key features of ALS. *Brain research*, 1584:59–72, October 2014. ISSN 1872-6240. doi: 10.1016/j.brainres.2013.10.013. URL http://www.ncbi.nlm.nih.gov/pubmed/24141148.

[129] K. Takao and T. Miyakawa. Genomic responses in mouse models greatly mimic human inflammatory diseases. *Proceedings of the National Academy of Sciences*, pages 1401965111–, August 2014. ISSN 0027-8424. doi: 10.1073/pnas.1401965111. URL http://www.pnas.org/content/early/2014/07/31/1401965111.abstract.

[130] RM M Salek, ML L Maguire, E Bentley, D V Rubtsov, T Hough, M Cheeseman, D Nunez, B C Sweatman, J N Haselden, R D Cox, S C Connor, and J L Griffin. A metabolomic comparison of urinary changes in type 2 diabetes in mouse, rat, and human. *Physiological genomics*, 29(2):99–108, April 2007. ISSN 1531-2267. doi: 10.1152/physiolgenomics.00194.2006. URL http://physiolgenomics.physiology.org/content/29/2/99.shorthttp://www.ncbi.nlm.nih.gov/pubmed/17190852http://europepmc.org/abstract/MED/17190852/reload=0.

[131] Ran Blekhman, George H Perry, Sevini Shahbaz, Oliver Fiehn, Andrew G Clark, and Yoav Gilad. Comparative metabolomics in primates reveals

the effects of diet and gene regulatory variation on metabolic divergence. *Scientific reports*, 4:5809, January 2014. ISSN 2045-2322. doi: 10.1038/srep05809. URL http://www.nature.com/srep/2014/140728/srep05809/full/srep05809.html.

[132] Melanie Kahle, Marion Horsch, Barbara Fridrich, Anett Seelig, Jürgen Schultheiß, Jörn Leonhardt, Martin Irmler, Johannes Beckers, Birgit Rathkolb, Eckhard Wolf, Nicole Franke, Valérie Gailus-Durner, Helmut Fuchs, Martin Hrabě de Angelis, and Susanne Neschen. Phenotypic comparison of common mouse strains developing high-fat diet-induced hepatosteatosis. *Molecular metabolism*, 2(4):435–46, January 2013. ISSN 2212-8778. doi: 10.1016/j.molmet.2013.07.009. URL http://www.pubmedcentral.nih.gov/articlerender.fcgi?artid=3855089&tool=pmcentrez&rendertype=abstract.

[133] Thomas Illig, Christian Gieger, Guangju Zhai, Werner Römisch-Margl, Rui Wang-Sattler, Cornelia Prehn, Elisabeth Altmaier, Gabi Kastenmüller, Bernet S Kato, Hans-Werner Mewes, Thomas Meitinger, Martin Hrabé de Angelis, Florian Kronenberg, Nicole Soranzo, H-Erich Wichmann, Tim D Spector, Jerzy Adamski, and Karsten Suhre. A genome-wide perspective of genetic variation in human metabolism. *Nature genetics*, 42(2):137–141, February 2010. ISSN 1546-1718. doi: 10.1038/ng.507. URL http://www.nature.com/ng/journal/v42/n2/abs/ng.507.htmlhttp://www.ncbi.nlm.nih.gov/pubmed/20037589.

[134] Rafael A Irizarry, Bridget Hobbs, Francois Collin, Yasmin D Beazer-Barclay, Kristen J Antonellis, Uwe Scherf, and Terence P Speed. Exploration, normalization, and summaries of high density oligonucleotide array probe level data. *Biostatistics (Oxford, England)*, 4(2):249–64, April 2003. ISSN 1465-4644. doi: 10.1093/biostatistics/4.2.249. URL http://www.ncbi.nlm.nih.gov/pubmed/12925520.

[135] Audrey Kauffmann and Wolfgang Huber. Microarray data quality control improves the detection of differentially expressed genes. *Genomics*, 95(3):138–42, March 2010. ISSN 1089-8646. doi: 10.1016/j.ygeno.2010.01.003. URL http://www.sciencedirect.com/science/article/pii/S0888754310000042.

[136] Joe H. Ward. Hierarchical Grouping to Optimize an Objective Function. *Journal of the American Statistical Association*, 58(301):236–244, March 1963. ISSN 0162-1459. doi: 10.1080/01621459.1963.10500845. URL http://www.researchgate.net/publication/216301644_Hierarchical_Grouping_to_Optimize_an_Objective_Function.

[137] W Römisch-Margl, C Prehn, and R Bogumil. Procedure for tissue sample preparation and metabolite extraction for high-throughput targeted metabolomics. *Metabolomics*, 2012. URL http://connection.ebscohost.com/c/articles/70325463/procedure-tissue-sample-preparation-metabolite-extraction-high-throughput-ta //link.springer.com/article/10.1007/s11306-011-0293-4.

[138] So-Youn Shin, Eric B Fauman, Ann-Kristin Petersen, Jan Krumsiek, Rita Santos, Jie Huang, Matthias Arnold, Idil Erte, Vincenzo Forgetta, Tsun-Po Yang, Klaudia Walter, Cristina Menni, Lu Chen, Louella Vasquez, Ana M Valdes, Craig L Hyde, Vicky Wang, Daniel Ziemek, Phoebe Roberts, Li Xi, Elin Grundberg, Melanie Waldenberger, J Brent Richards, Robert P Mohney, Michael V Milburn, Sally L John, Jeff Trimmer, Fabian J Theis, John P Overington, Karsten Suhre, M Julia Brosnan, Christian Gieger, Gabi Kastenmüller, Tim D Spector, and Nicole Soranzo. An atlas of genetic influences on human blood metabolites. *Nature genetics*, 46(6):543–50, June 2014. ISSN 1546-1718. doi: 10.1038/ng.2982. URL http://www.nature.com/ng/journal/v46/n6/full/ng.2982.html#supplementary-information.

[139] Gordon K Smyth. Linear models and empirical bayes methods for assessing differential expression in microarray experiments. *Statistical applications in genetics and molecular biology*, 3:Article3, January 2004. ISSN 1544-6115. doi: 10.2202/1544-6115.1027. URL http://www.ncbi.nlm.nih.gov/pubmed/16646809.

[140] Yoav Benjamini and Yosef Hochberg. Controlling the false discovery rate: a practical and powerful approach to multiple testing. *Journal of the Royal Statistical Society. Series B ...*, 1995. URL http://www.jstor.org/discover/10.2307/2346101?uid=3737864&uid=2&uid=4&sid=21103493641297http://www.jstor.org/stable/2346101.

[141] Xinan Yang, Stefan Bentink, Stefanie Scheid, and Rainer Spang. Similarities of ordered gene lists. *Journal of bioinformatics and computational biology*, 4 (3):693–708, June 2006. ISSN 0219-7200. URL http://www.ncbi.nlm.nih.gov/pubmed/16960970.

[142] Seema B Plaisier, Richard Taschereau, Justin A Wong, and Thomas G Graeber. Rank-rank hypergeometric overlap: identification of statistically significant overlap between gene-expression signatures. *Nucleic acids research*, 38 (17):e169, September 2010. ISSN 1362-4962. doi: 10.1093/nar/gkq636. URL http://nar.oxfordjournals.org/content/38/17/e169.

[143] FRANCINE M. GREGOIRE, CYNTHIA M. SMAS, and HEI SOOK SUL. Understanding Adipocyte Differentiation. *Physiol Rev*, 78(3):783–809, July 1998. URL http://physrev.physiology.org/content/78/3/783.

[144] A A Toye, J D Lippiat, P Proks, K Shimomura, L Bentley, A Hugill, V Mijat, M Goldsworthy, L Moir, A Haynes, J Quarterman, H C Freeman, F M Ashcroft, and R D Cox. A genetic and physiological study of impaired glucose homeostasis control in C57BL/6J mice. *Diabetologia*, 48(4):675–86, April 2005. ISSN 0012-186X. doi: 10.1007/s00125-005-1680-z. URL http://www.ncbi.nlm.nih.gov/pubmed/15729571.

[145] Daniel F Vatner, Sachin K Majumdar, Naoki Kumashiro, Max C Petersen, Yasmeen Rahimi, Arijeet K Gattu, Mitchell Bears, João-Paulo G Camporez, Gary W Cline, Michael J Jurczak, Varman T Samuel, and Gerald I Shulman. Insulin-independent regulation of hepatic triglyceride synthesis by fatty acids. *Proceedings of the National Academy of Sciences of the United States of America*, 112(4):1143–8, January 2015. ISSN 1091-6490. doi: 10.1073/pnas.1423952112. URL http://www.pnas.org/content/112/4/1143.

[146] Katalin Monostory and Zdenek Dvorak. Steroid regulation of drug-metabolizing cytochromes P450. *Current drug metabolism*, 12(2):154–72, March 2011. ISSN 1875-5453. URL http://www.ncbi.nlm.nih.gov/pubmed/21395541.

[147] Irina A Kirpich, Leila N Gobejishvili, Marjorie Bon Homme, Sabine Waigel, Matt Cave, Gavin Arteel, Shirish S Barve, Craig J Mc-

Clain, and Ion V Deaciuc. Integrated hepatic transcriptome and proteome analysis of mice with high-fat diet-induced nonalcoholic fatty liver disease. *The Journal of nutritional biochemistry*, 22(1):38–45, January 2011. ISSN 1873-4847. doi: 10.1016/j.jnutbio.2009.11.009. URL http://www.pubmedcentral.nih.gov/articlerender.fcgi?artid=3860361&tool=pmcentrez&rendertype=abstract.

[148] G Pitari, F Malergue, F Martin, J M Philippe, M T Massucci, C Chabret, B Maras, S Duprè, P Naquet, and F Galland. Pantetheinase activity of membrane-bound Vanin-1: lack of free cysteamine in tissues of Vanin-1 deficient mice. *FEBS letters*, 483(2-3):149–54, October 2000. ISSN 0014-5793. URL http://www.ncbi.nlm.nih.gov/pubmed/11042271.

[149] A J Sanyal, C Campbell-Sargent, F Mirshahi, W B Rizzo, M J Contos, R K Sterling, V A Luketic, M L Shiffman, and J N Clore. Nonalcoholic steatohepatitis: association of insulin resistance and mitochondrial abnormalities. *Gastroenterology*, 120(5):1183–92, April 2001. ISSN 0016-5085. doi: 10.1053/gast.2001.23256. URL http://www.ncbi.nlm.nih.gov/pubmed/11266382.

[150] Lauren M Aleksunes and José E Manautou. Emerging role of Nrf2 in protecting against hepatic and gastrointestinal disease. *Toxicologic pathology*, 35(4):459–73, June 2007. ISSN 0192-6233. doi: 10.1080/01926230701311344. URL http://www.ncbi.nlm.nih.gov/pubmed/17562481.

[151] Young Ho Suh, Younyoung Kim, Jeong Hyun Bang, Kyoung Suk Choi, June Woo Lee, Won-Ho Kim, Tae Jeong Oh, Sungwhan An, and Myeong Ho Jung. Analysis of gene expression profiles in insulin-sensitive tissues from pre-diabetic and diabetic Zucker diabetic fatty rats. *Journal of molecular endocrinology*, 34(2):299–315, April 2005. ISSN 0952-5041. doi: 10.1677/jme.1.01679. URL http://www.ncbi.nlm.nih.gov/pubmed/15821098.

[152] Makoto Osabe, Junko Sugatani, Tomoaki Fukuyama, Shin-ichi Ikushiro, Akira Ikari, and Masao Miwa. Expression of hepatic UDP-glucuronosyltransferase 1A1 and 1A6 correlated with increased expression of the nuclear constitutive androstane receptor and peroxisome proliferator-activated receptor alpha in male rats fed a high-fat and high-sucrose diet. *Drug metabolism and disposition: the biological fate of chemicals*, 36(2):294–302, February 2008. ISSN

1521-009X. doi: 10.1124/dmd.107.017731. URL http://www.ncbi.nlm.nih.gov/pubmed/17967931.

[153] Masakazu Hanagama, Hiromasa Inoue, Munechika Kamiya, Kotaro Shinone, and Masayuki Nata. Gene expression on liver toxicity induced by administration of haloperidol in rats with severe fatty liver. *Legal medicine (Tokyo, Japan)*, 10(4):177–84, July 2008. ISSN 1873-4162. doi: 10.1016/j.legalmed.2007.12.006. URL http://www.ncbi.nlm.nih.gov/pubmed/18280196.

[154] January N Baumgardner, Kartik Shankar, Leah Hennings, Thomas M Badger, and Martin J J Ronis. A new model for nonalcoholic steatohepatitis in the rat utilizing total enteral nutrition to overfeed a high-polyunsaturated fat diet. *American journal of physiology. Gastrointestinal and liver physiology*, 294(1):G27–38, January 2008. ISSN 0193-1857. doi: 10.1152/ajpgi.00296.2007. URL http://www.ncbi.nlm.nih.gov/pubmed/17947452.

[155] Natalie de Souza. Model organisms: Mouse models challenged. *Nature Methods*, 10(4):288–288, March 2013. ISSN 1548-7091. doi: 10.1038/nmeth.2429. URL http://dx.doi.org/10.1038/nmeth.2429.

[156] Frank R Sharp and Glen C Jickling. Modeling immunity and inflammation in stroke: differences between rodents and humans? *Stroke; a journal of cerebral circulation*, 45(9):e179–80, September 2014. ISSN 1524-4628. doi: 10.1161/STROKEAHA.114.005639. URL http://www.ncbi.nlm.nih.gov/pubmed/25061082.

[157] Gina Kolata. Mice fall short as test subjects for deadly illnesses, 2013. URL http://www.nytimes.com/2013/02/12/science/testing-of-some-deadly-diseases-on-mice-mislead-report-says.html.

[158] Kimber L Stanhope, Jean Marc Schwarz, Nancy L Keim, Steven C Griffen, Andrew A Bremer, James L Graham, Bonnie Hatcher, Chad L Cox, Artem Dyachenko, Wei Zhang, John P McGahan, Anthony Seibert, Ronald M Krauss, Sally Chiu, Ernst J Schaefer, Masumi Ai, Seiko Otokozawa, Katsuyuki Nakajima, Takamitsu Nakano, Carine Beysen, Marc K Hellerstein, Lars

Berglund, and Peter J Havel. Consuming fructose-sweetened, not glucose-sweetened, beverages increases visceral adiposity and lipids and decreases insulin sensitivity in overweight/obese humans. *The Journal of clinical investigation*, 119(5):1322–34, May 2009. ISSN 1558-8238. doi: 10.1172/JCI37385. URL http://www.jci.org/articles/view/37385.

[159] Luc Tappy and Kim-Anne Lê. Metabolic effects of fructose and the worldwide increase in obesity. *Physiological reviews*, 90(1):23–46, January 2010. ISSN 1522-1210. doi: 10.1152/physrev.00019.2009. URL http://physrev.physiology.org/content/90/1/23.

[160] Varman T Samuel. Fructose induced lipogenesis: from sugar to fat to insulin resistance. *Trends in Endocrinology & Metabolism*, 22(2): 60–5, February 2011. ISSN 1879-3061. doi: 10.1016/j.tem.2010.10.003. URL http://www.ncbi.nlm.nih.gov/pubmed/21067942http://dx.doi.org/10.1016/j.tem.2010.10.003.

[161] Satish C Kalhan, Lining Guo, John Edmison, Srinivasan Dasarathy, Arthur J McCullough, Richard W Hanson, and Mike Milburn. Plasma metabolomic profile in nonalcoholic fatty liver disease. *Metabolism: clinical and experimental*, 60(3):404–13, March 2011. ISSN 1532-8600. doi: 10.1016/j.metabol.2010.03.006. URL http://www.pubmedcentral.nih.gov/articlerender.fcgi?artid=2950914&tool=pmcentrez&rendertype=abstract.

[162] Anna Floegel, Norbert Stefan, Zhonghao Yu, Kristin Mühlenbruch, Dagmar Drogan, Hans-Georg Joost, Andreas Fritsche, Hans-Ulrich Häring, Martin Hrabě de Angelis, Annette Peters, Michael Roden, Cornelia Prehn, Rui Wang-Sattler, Thomas Illig, Matthias B Schulze, Jerzy Adamski, Heiner Boeing, and Tobias Pischon. Identification of serum metabolites associated with risk of type 2 diabetes using a targeted metabolomic approach. *Diabetes*, 62(2): 639–48, February 2013. ISSN 1939-327X. doi: 10.2337/db12-0495. URL http://www.ncbi.nlm.nih.gov/pubmed/23043162.

[163] Enoka P Wijekoon, Craig Skinner, Margaret E Brosnan, and John T Brosnan. Amino acid metabolism in the Zucker diabetic fatty rat: effects of insulin resistance and of type 2 diabetes. *Canadian journal of physiology and pharma-*

cology, 82(7):506–14, July 2004. ISSN 0008-4212. doi: 10.1139/y04-067. URL http://www.ncbi.nlm.nih.gov/pubmed/15389298.

[164] S L Macaulay and R G Larkins. Insulin stimulates turnover of phosphatidylcholine in rat adipocytes. *Molecular and cellular biochemistry*, 136 (1):23–8, July 1994. ISSN 0300-8177. URL http://www.ncbi.nlm.nih.gov/pubmed/7854328.

[165] David E Kelley, Jing He, Elizabeth V Menshikova, and Vladimir B Ritov. Dysfunction of mitochondria in human skeletal muscle in type 2 diabetes. *Diabetes*, 51(10):2944–50, October 2002. ISSN 0012-1797. URL http://www.ncbi.nlm.nih.gov/pubmed/12351431.

[166] Mary Elizabeth Patti, Atul J Butte, Sarah Crunkhorn, Kenneth Cusi, Rachele Berria, Sangeeta Kashyap, Yoshinori Miyazaki, Isaac Kohane, Maura Costello, Robert Saccone, Edwin J Landaker, Allison B Goldfine, Edward Mun, Ralph DeFronzo, Jean Finlayson, C Ronald Kahn, and Lawrence J Mandarino. Coordinated reduction of genes of oxidative metabolism in humans with insulin resistance and diabetes: Potential role of PGC1 and NRF1. *Proceedings of the National Academy of Sciences of the United States of America*, 100(14):8466–71, July 2003. ISSN 0027-8424. doi: 10.1073/pnas.1032913100. URL http://www.pubmedcentral.nih.gov/articlerender.fcgi?artid=166252&tool=pmcentrez&rendertype=abstract.

[167] Vladimir B Ritov, Elizabeth V Menshikova, Jing He, Robert E Ferrell, Bret H Goodpaster, and David E Kelley. Deficiency of subsarcolemmal mitochondria in obesity and type 2 diabetes. *Diabetes*, 54(1):8–14, January 2005. ISSN 0012-1797. URL http://www.ncbi.nlm.nih.gov/pubmed/15616005.

[168] J H HAGEN, J A MOORHOUSE, and J STEINBERG. Effect of insulin on plasma glycerol in man. *Metabolism: clinical and experimental*, 12:346–51, April 1963. ISSN 0026-0495. URL http://www.ncbi.nlm.nih.gov/pubmed/13951883.

[169] L Marai and A Kuksis. Molecular species of lecithins from erythrocytes and plasma of man. *Journal of lipid research*, 10(2):141–52, March 1969. ISSN 0022-2275. URL http://www.ncbi.nlm.nih.gov/pubmed/5782351.

[170] Philipp Wiesner, Katharina Leidl, Alfred Boettcher, Gerd Schmitz, and Gerhard Liebisch. Lipid profiling of FPLC-separated lipoprotein fractions by electrospray ionization tandem mass spectrometry. *Journal of lipid research*, 50 (3):574–85, March 2009. ISSN 0022-2275. doi: 10.1194/jlr.D800028-JLR200. URL http://www.jlr.org/content/50/3/574.long.

[171] Arshag D Mooradian. Dyslipidemia in type 2 diabetes mellitus. *Nature clinical practice. Endocrinology & metabolism*, 5(3):150–9, March 2009. ISSN 1745-8374. doi: 10.1038/ncpendmet1066. URL http://dx.doi.org/10.1038/ncpendmet1066.

[172] Kunihisa Kobayashi, Trudy M. Forte, Susumu Taniguchi, Brian Y. Ishida, Kazuhiro Oka, and Lawrence Chan. The db/db mouse, a model for diabetic dyslipidemia: Molecular characterization and effects of western diet feeding. *Metabolism*, 49(1):22–31, January 2000. ISSN 00260495. doi: 10.1016/S0026-0495(00)90588-2. URL http://www.sciencedirect.com/science/article/pii/S0026049500905882.

[173] a S Udupa, P S Nahar, S H Shah, M J Kshirsagar, and B B Ghongane. Study of comparative effects of antioxidants on insulin sensitivity in type 2 diabetes mellitus. *Journal of clinical and diagnostic research : JCDR*, 6(9): 1469–73, November 2012. ISSN 2249-782X. doi: 10.7860/JCDR/2012/4464.2535. URL http://www.pubmedcentral.nih.gov/articlerender.fcgi?artid=3527772&tool=pmcentrez&rendertype=abstract.

[174] Anand Baburao Jain and Vaishali Anand Jain. Vitamin E, Its Beneficial Role in Diabetes Mellitus (DM) and Its Complications. *Journal of clinical and diagnostic research : JCDR*, 6(10):1624–8, December 2012. ISSN 2249-782X. doi: 10.7860/JCDR/2012/4791.2625. URL http://www.pubmedcentral.nih.gov/articlerender.fcgi?artid=3552190&tool=pmcentrez&rendertype=abstract.

[175] Mukaddes Gulec, Ahmet Gurel, and Ferah Armutcu. Vitamin E protects against oxidative damage caused by formaldehyde in the liver and plasma of rats. *Molecular and cellular biochemistry*, 290(1-2):61–7, October 2006. ISSN 0300-8177. doi: 10.1007/s11010-006-9165-z. URL http://www.ncbi.nlm.nih.gov/pubmed/16937016.

[176] Andreia Madruga de Oliveira, Patrícia Helen Carvalho Rondó, Liania Alves Luzia, Francisco Homero D'Abronzo, and Vanessa Kristine Illison. The effects of lipoic acid and α-tocopherol supplementation on the lipid profile and insulin sensitivity of patients with type 2 diabetes mellitus: a randomized, double-blind, placebo-controlled trial. *Diabetes research and clinical practice*, 92(2): 253–60, May 2011. ISSN 1872-8227. doi: 10.1016/j.diabres.2011.02.010. URL http://www.ncbi.nlm.nih.gov/pubmed/21371770.

[177] Howard D Sesso, Julie E Buring, William G Christen, Tobias Kurth, Charlene Belanger, Jean MacFadyen, Vadim Bubes, JoAnn E Manson, Robert J Glynn, and J Michael Gaziano. Vitamins E and C in the prevention of cardiovascular disease in men: the Physicians' Health Study II randomized controlled trial. *JAMA : the journal of the American Medical Association*, 300(18):2123–33, November 2008. ISSN 1538-3598. doi: 10.1001/jama.2008.600. URL http://www.pubmedcentral.nih.gov/articlerender.fcgi?artid=2586922&tool=pmcentrez&rendertype=abstract.

[178] Marian J Muis, Ronald P Stolk, Hans M G Princen, P S Van Dam, L D Dikkeschei, Diederick E Grobbee, and Henk J G Bilo. alpha-Tocopherol levels in plasma in new-onset, insulin-dependent diabetes mellitus. *European journal of internal medicine*, 15(6):371–374, January 2004. ISSN 1879-0828. doi: 10.1016/j.ejim.2004.04.018. URL http://www.ncbi.nlm.nih.gov/pubmed/15522571.

[179] A Romero-Corral, V K Somers, J Sierra-Johnson, R J Thomas, M L Collazo-Clavell, J Korinek, T G Allison, J A Batsis, F H Sert-Kuniyoshi, and F Lopez-Jimenez. Accuracy of body mass index in diagnosing obesity in the adult general population. *International journal of obesity (2005)*, 32(6):959–66, June 2008. ISSN 1476-5497. doi: 10.1038/ijo.2008.11. URL http://www.pubmedcentral.nih.gov/articlerender.fcgi?artid=2877506&tool=pmcentrez&rendertype=abstract.

[180] G R Steenge, J Lambourne, A Casey, I A Macdonald, and P L Greenhaff. Stimulatory effect of insulin on creatine accumulation in human skeletal muscle. *The American journal of physiology*, 275(6 Pt 1):E974–9, December 1998. ISSN 0002-9513. URL http://www.ncbi.nlm.nih.gov/pubmed/9843739.

List of Figures

List of Tables

List of Abbreviations

A1c	Glycated Hemoglobin
ACCORD	Action to Control Cardiovascular Risk in Diabetes
BCAA	Branched Chain Amino Acid
BHBA	3-hydroxybutyrate
BPA	Bisphenol A
BMI	Body Mass Index
B6N	C57BL/6NTac
B6J	C57BL/6J
cDNA	coding DNA
CI	Chemical Ionization
C3H	C3Heb/FeJ
CYP	Cytochrome P450
db/db	BKS.Cg-Dock7m+/+ Leprdb/J
wt	Dock7m+/+
DNA	DeoxyriboNucleic Acid
DPP	Diabetes Prevention Programm
ESI	Electron Spray Ionization
FDR	False Discovery Rate
FPR	False Positive Rate
FWER	Family Wise Error Rate
GC	Gas Chromatography
GFR	Glomerular Filtration Rate
GST	Glutathione S-Transferase
GWAS	Genome Wide Association Study

HDL	High Density Lipoprotein
HFD	High Fat Diet
IDF	International Diabetes Federation
IFG	Impaired Fasting Glucose
IGT	Impaired Glucose Tolerance
KORA	Cooperative Health Research in the Region of Augsburg
LC	Liquid Chromatography
LDL	Low Density Lipoprotein
LFD	Low Fat Diet
AHEAD	Look Action for Health and Diabetes
IDF	International Diabetes Foundation
lh	lean healthy
MS	Mass Spectrometry
MODY	Maturity-Onset Diabetes of the Young
mRNA	messenger RNA
MWAS	Metabolome Wide Association Study
NAFLD	Non-Alcoholic Fatty-Liver Disease
NAFLD	Nicht-alkoholische Fettleber
NASH	Non-Alcoholic Steatohepatitis
NEFA	Nonesterified fatty acid
NGS	Next Generation Sequencing
NMR	Nuclear Magnetic Resonance spetroscopy
Nnt	Nicotine amide-Nucleotide Transhydrogenase
NZO	New Zealand Obese
od	obese diabetic
oh	obese healthy
OGTT	Oral Glucose Tolerance Test
ORIGIN	Outcome Reduction With Initial Glargine Intervention
pAUC	Partial Area Under the Curve
PC	Phosphatidylcholine
PPAR	Peroxisome Proliferator-Activated receptor
QC	Quality Control
RMA	Robust Multichip Average
RNA	RiboNucleic Acid

ROC	Receiver Operating Characteristic
RRHO	Rank-Rank Hypergeometric Overlap
SGLT-2	Sodium Dependent Glucose Transporter 2
SNP	Single Nucleotide Polymorphism
T1DM	Type 1 Diabetes Mellitus
T2DM	Type 2 Diabetes Mellitus
T2DM	Typ 2 Diabetes Mellitus
TALLYHO	TALLYHO/JngJ
TAG	Triacylglycerol
TODAY	Treatment Options for type 2 Diabetes in Adolescents and Youth
TPR	True Positive Rate
UKPDS	United Kingdom Prospective Diabetes Study
VLDL	Very Low Density Lipoprotein
VNN1	Vanin-1
WHO	World Health Organization
ZDF	Zucker Diabetic Fatty
129	129P2/OlaHsd